1st Session

ON THE BEHAVIOR OF A HEAVY STEEL COLUMN

Negussie Tebedge
Postdoctoral
Research Associate
of Civil Engineering

Wai-Fah Chen
Associate Professor
of Civil Engineering

Lambert Tall
Professor
of Civil Engineering
and Director, Division
for Fatigue and Fracture

Fritz Engineering Laboratory
Lehigh University
Bethlehem, Pennsylvania
U.S.A.

ABSTRACT

This report presents a theoretical and experimental investigation of the behavior and the strength of a heavy shape column built up from oxygen-cut plates. The theoretical part of the analysis includes two-dimensional in-plane column investigations by the tangent modulus concept and by the load-deflection approach, and a three-dimensional biaxial bending column analysis. The effects of residual stress, yield strength variations over the cross section, and initial out-of-straightness about the two principal axes, are considered in the theoretical analysis.

To obtain experimental data on the behavior and the strength of heavy built-up columns, a complete experimental investigation was conducted on one particular shape--H23x681, ASTM 36 steel. The experimental part includes the measurement of the yield strength levels and residual stresses over the cross section, a stub column test, and a full-size column test. The column tests were conducted at the National Bureau of Standards, Gaithersburg, Maryland in their 12-million pound testing machine.

Failure of the column was observed in biaxial bending with excessive bending about the major axis. The results of the column test and the theoretical prediction based on a three-dimensional biaxial bending column analysis are compared and good agreement is observed. The need for the biaxial bending analysis for centrally loaded heavy columns built up from flame cut plates is attributed to the particular pattern of residual stress distribution as well as to the initial out-of-straightness about the two principal axes which are inherent in such columns.

1. INTRODUCTION

At present, the design of heavy shape columns does not differ from that of small and medium-size shapes. Very little information is available on the strength and behavior of heavy columns, yet they are used extensively, for instance, in high-rise buildings, in major bridges, and in off-shore structures. The major problems associated with the design of heavy columns are the lack of data on residual stresses, yield strength variation over the cross section, and initial geometric imperfections of the columns.

The AISC column formula [1] is based on the CRC basic strength formula [2] which is developed from studies of small and medium-size shapes. Data for heavy column shapes have not been included in the strength formulas. Consequently, there exists a need for design rules that are applicable to heavy shape columns.

An extensive research program is currently underway at Lehigh University on residual stresses in heavy welded plates and shapes. A significant portion of the experimental phase--on the measurement of residual stresses in heavy shapes--has been reported in Refs. 3 and 4. Using these results, the theoretical strength of heavy columns built up from flame-cut plates can be predicted, and have shown an increase in strength when compared with lighter welded members and their rolled counterparts [3]. However, there are no full-size heavy column test results presently available to give experimental verifications.

This report presents a comprehensive experimental investigation performed on one particular shape--H23x681, ASTM A36 steel--whose slenderness ratio is within the range normally encountered in practice for such members. Failure of the column was observed in biaxial bending with excessive bending about the major axis. The results of the column test and the theoretical prediction based on the analysis of biaxially loaded columns are compared and good agreement is observed. The need for the biaxial bending analysis for centrally loaded heavy columns built up from flame-cut plates is attributed to the particular pattern of residual stress distribution as well as the initial out-of-straightness about both axes.

2. SCOPE OF TEST PROGRAM

Specimen

Heavy shapes are available in different steel grades and cross sectional forms. Rolled shapes are presently available to W14x730, the so-called "jumbo" shape. When the strength of the available rolled shape is insufficient for a particular application, the column may be strengthened by welding additional plates to it. Alternatively, and perhaps more conveniently, a heavy shape can be fabricated by welding together component plates; for instance, three plates can form an H-shape and four plates a box-shape. Heavy tubular columns, used extensively in offshore structures, are usually prepared from single plates. The residual stresses in such shapes are built up as a consequence of a superposition of residual stresses developed in the various phases of manufacturing and fabrication.

Herein, a comprehensive experimental investigation for one particular heavy welded shape, H23x681, is presented. It is the heaviest shape ever tested in column tests. The tests were performed in the newly installed 12-million pound capacity testing machine at the National Bureau of Standards, Gaithersburg, Maryland.

Fabrication

The test specimen was fabricated according to AWS specifications [5] by steel fabricators following the normal practices and procedures using automatic oxygen-cutting and submerged arc-welding equipment. The component plates were first obtained by oxygen-cutting from larger base metal plates of ASTM A36 steel. The H23x681 shape was welded using two tandem electrodes. Thus, it was possible to deposit the fillet welds simultaneously in one pass. After the first flange and web were joined together, the T-shape was turned over and the other flange was welded to form the final H-shape. A summary of the pertinent welding data is given in Table 1. A more detailed account of the fabrication of the H23x681 shape is given in Ref. [3]

Table 1 WELDING DATA FOR FABRICATION OF TEST SPECIMEN

	Type	Voltage (ohm)	Current (amp)	Speed (in/min)
1st Flange	DC	26	700	15
	AC	31	530	15
2nd Flange	DC	26	710	18
	AC	30	530	18

Preparation of Test Specimen

Figure 1 shows the layout for the preparation of the test specimens to carry out the supplementary tests and a full-size column test. The test pro-

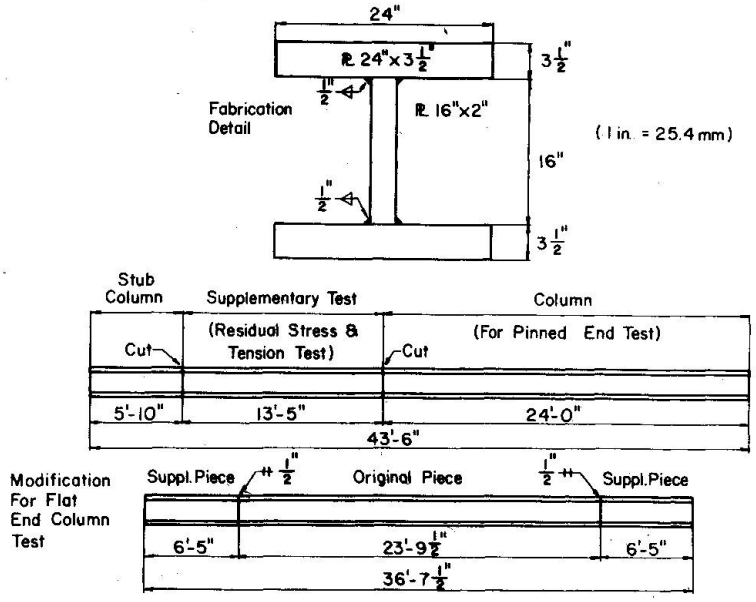

Fig. 1 Schematic Layout of Test Specimens

gram consists of: 1) Tension coupon tests; 2) Residual stress measurement; 3) Stub column test; 4) Full-size column test.

The column specimen was originally prepared to be tested under a pinned-end condition. At a later stage, it was decided to test the column under the flat-end condition to simulate fixed-end conditions. This change was made due to the limitations of the capacity of the available end-fixtures, and the considerable expense involved in preparing high-capacity end-fixtures. To maintain the same order of magnitude of slenderness ratio originally intended, the column was made longer by welding to it specimens at the two ends. The details of this modification are shown in Fig. 1.

3. SUPPLEMENTARY TESTS

Supplementary tests were conducted to determine the basic properties of specimens which are required to evaluate the theoretical column strengths. The following supplementary tests were performed:

Tension Coupon Tests

A total of twenty-four 2-inch gage length (ASTM A570) specimens were tested: fourteen from the flange and ten from the web. The specimens were cut at four different locations on the shape and five or seven specimens (from the web and flange, respectively) were taken across the thickness of each location (Fig. 2a). Results of the static yield strength defined by the stress at 0.005 strain are summarized in Fig. 2c. The recorded yield strength varies between 29.5 ksi (203.4 N/mm^2) and 33.7 ksi (232.4 N/mm^2) for the flange, and between 30.7 ksi (211.7 N/mm^2) and 34.8 ksi (239.9

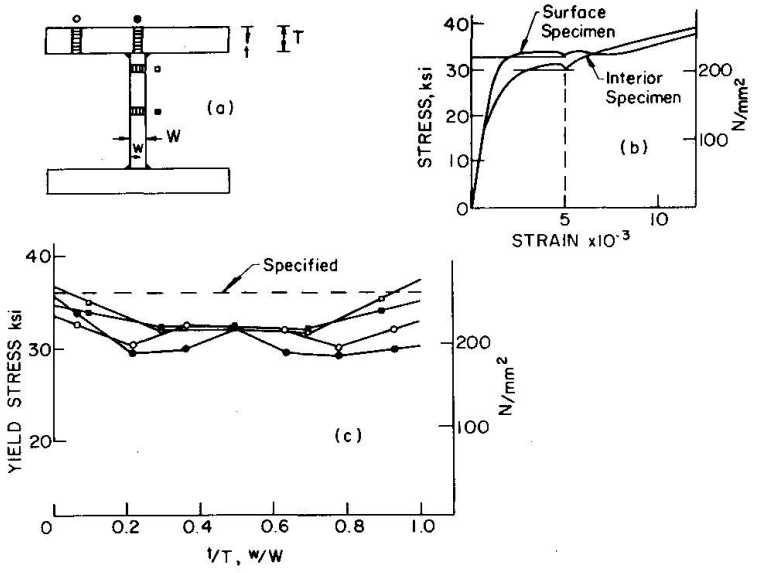

Fig. 2 Variation of Yield Strength for the H23x681

N/mm^2) for the web. The average yield strengths are 31.0 ksi (223.7 N/mm^2) and 32.5 ksi (224.1 N/mm^2) for the flange and web, respectively. It was observed that the interior specimens had a lower yield strength and a gradual transition from the elastic to the strain hardening range, while the surface specimens exhibited a higher yield strength and a "flat" yield plateau and a marked onset of strain hardening usually observed in ASTM A36 tensile coupons (Fig. 2b) [6].

Residual Stress Measurement

The procedure used for the residual stress measurement was the sectioning method, involving longitudinal saw cuts across the width and through the thickness of the component plates. A detailed description of the sectioning method is given in Ref. [7].

The variation of residual stresses through the thickness was measured by employing the "slicing" technique. After the first set of saw cuts are performed (complete sectioning), additional gage points were laid along the

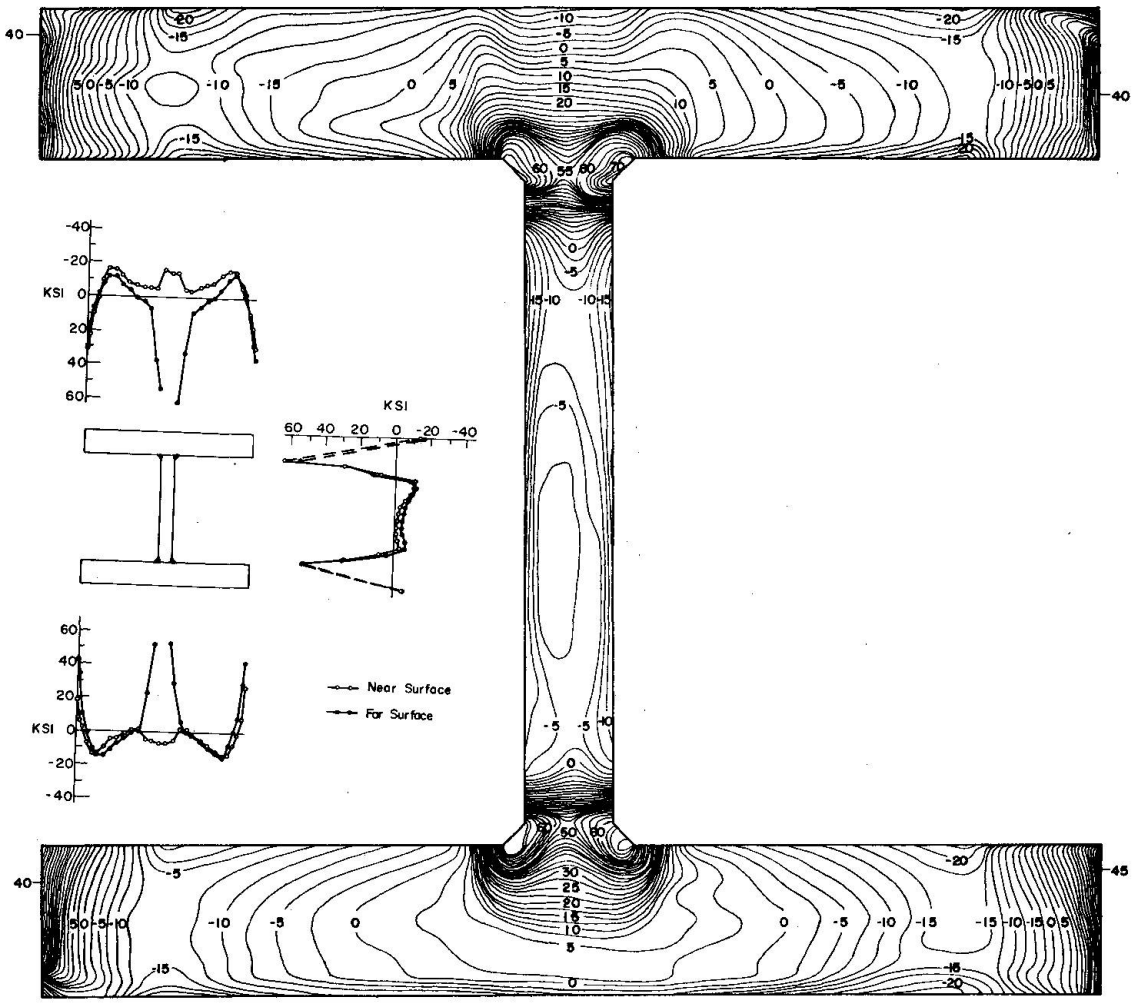

Fig. 3 Two-Dimensional Variation of Residual Stress in the H23x681 Shape

sides of the elements. New readings were then taken, followed by sawing the elements into strips across the thickness (slicing). The results for the H23x681 shape are shown in Fig. 3 where the residual stress distribution in ksi is represented in the form of an isostress diagram, that is, contour lines for constant stress [3].

Stub Column Test

The purpose of a stub column test is to determine the average stress-strain curve for the entire cross section, including the effects of residual stress and yield strength variation over the cross section. The most important data furnished by this curve is the tangent modulus. Hence, a smooth curve must be established above the proportional limit by taking test points at closer intervals.

The length of the stub column was selected such that it is sufficiently long to retain the original residual stress in the column but short enough to prevent any premature failure occurring before the yield load of the section is obtained. For the H23x681 shape considered, a length of 5 ft 10 in (1.78 m) was selected. The procedure used in testing the stub column is described in detail in Ref. [8].

After the specimen was aligned such that the deviation in strain did not exceed 5 percent of the average value, the specimen was loaded continuously with only one stop made at the yield plateau to determine the static yield strength level. A strain rate corresponding to a stress rate of 1.0 ksi/min (6.9 N/mm^2/min) was used throughout the test after it was established in the elastic range. The average stress-strain curve obtained from this test is shown in Fig. 4. The proportional limit, the elastic modulus, and the tangent modulus are the important data furnished by this curve.

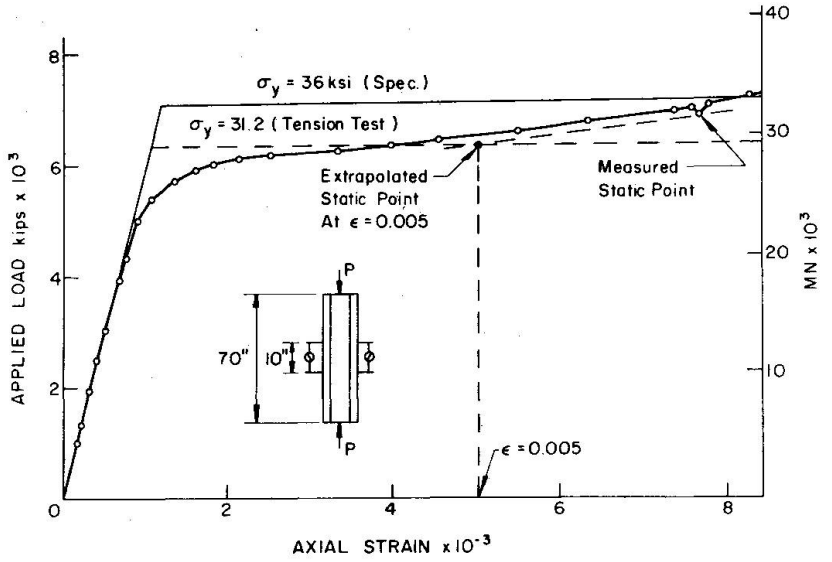

Fig. 4 Stub Column Test Result

Using the yield strength level criteria defined by the stress at 0.005 in/in strain [8], the static yield stress was found to be 31.3 ksi (216 N/mm^2), which indicates a close correlation to the weighted average yield stress determined by tensile coupons, 31.2 ksi (215 N/mm^2). The measured yield strength of the specimen was below the specified value of 36.0 ksi (248.2 N/mm^2).

4. COLUMN TEST

Pinned end conditions are frequently used in column tests, and, it is necessary to provide end fixtures for such a condition. For heavy columns, this condition introduces practical difficulties and considerable expense. Flat end conditions are, in comparison, easy to perform.

Theoretically, the effective length of a column tested in the fixed-end condition in one-half that of a pinned-end column. However, in testing columns under fixed-end conditions, there is a problem in determining the degree of end fixity since complete fixity cannot be attained in reality, since in effect, the column is usually tested in the flat-end condition. The amount of end fixity and, thus, the effective length of the column is not a constant but a function of the applied load. This effective length can be determined accurately by locating the positions of inflection points in the column test.

Column Testing

Prior to testing the column, initial measurements were taken of the geometric characteristics of the column specimen; these include the cross-sectional area and the initial out-of-straightness. Cross-sectional measurements were taken at five locations, at the ends, and at the quarter points

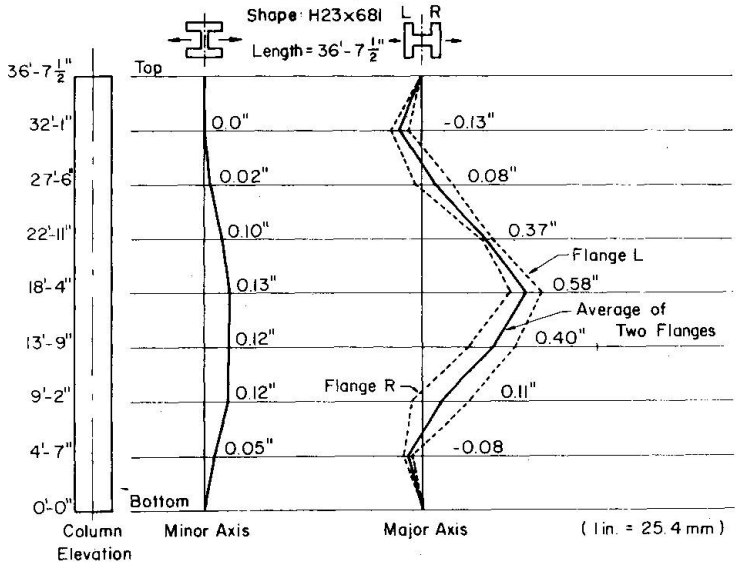

Fig. 5 Initial Out-of-Straightness of the Column Specimen

of the column length. The initial out-of-straightness of the column was measured at nine-levels, each spaced at one-eighth of the column length. Measurements were taken in the two principal axes and are shown schematically in Fig. 5. The maximum out-of-straightness was 0.58 inch (14.9 mm) at the column midheight about the major axis. The initial out-of-straightness of the column was symmetric for the major axis and unsymmetric for the minor axis (Fig. 5).

The column testing procedure described in Ref. 9 is then followed. The alignment of the column was performed geometrically by matching the end plate centers to the centers of the flanges at each support--the reference point was located at the midpoint of the line connecting the two centers of the flanges. The end plates were centered with reference to the centerline of the machine.

The instrumentation for the column test consists of potentiometers attached at quarter points to measure lateral deflections, electric resistance strain gages at characteristic points to measure strain and curvature variations along the column length, electrical rotation gages at the cross-head to measure end rotations about the two axes, and a dial gage to measure the overall shortening. The test set-up is shown in Fig. 6 under the 12-million-pound hydraulic testing machine.

The load was applied continuously at a rate of 1 ksi/min (6.9 N/mm^2/min) and all measurements were instantly recorded automatically at one minute intervals. The maximum "static" load was recorded as 6140 kips (27,300 MN) or 0.98 P_y by maintaining the cross-head movement until the load was stabilized. The loading was terminated when the midheight deflection was approximately seven inches, (180 mm). The specimen at the end of test is shown in Fig. 6.

Test Results

The measured load versus midheight deflection curves are shown by the small circles in Fig. 7 for the case of minor axis bending and in Fig. 8 for the case of major axis bending. The values shown at zero-load level correspond to the midheight initial out-of-straightness of the column. Also shown in these figures are the theoretical curves derived from the two dimensional in-plane column analysis as well as the three dimensional biaxial bending column analysis. A detailed discussion on these theoretical predictions is given later.

A substantial deviation of the measured curve from the linear behavior is seen to initiate approximately at the load P = 5400 kips (24,000 MN) or 0.865 P_y. Beyond this load, the curve starts to bend very rapidly and this rate of bending falls steadily as the axial load increases. When the lateral deflection for the minor axis reaches the value approximately 0.8 inch (20 mm), the value of minor deflection becomes practically a constant until the end of the test (Fig. 8). The column finally failed with excessive bending about the major axis. Unloading of the column did not occur in the loading range of the test.

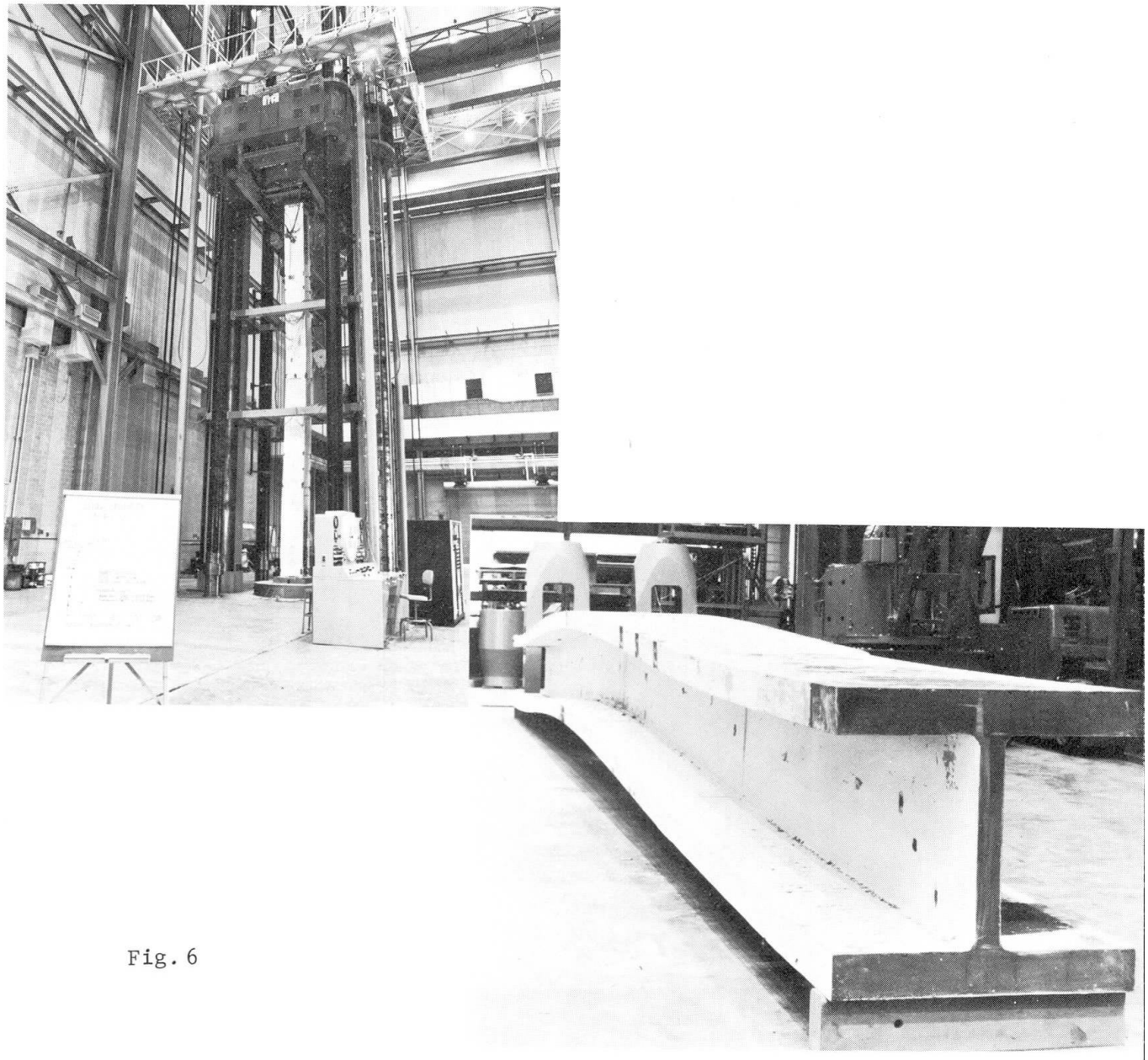

Fig. 6

a) Column Test Under the 12-Million Capacity Testing Machine
b) The Column Specimen at the End of Test

Rotation of the cross-head was measured using two electrical rotation gages oriented along the minor and major axes of the column cross section. Figure 9 shows the rotation measured at different load levels. A sharp

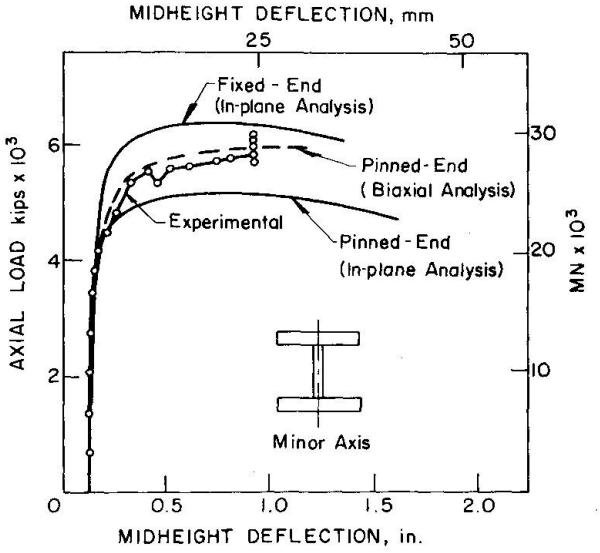

Fig. 7 Midheight Lateral Deflection About the Minor Axis

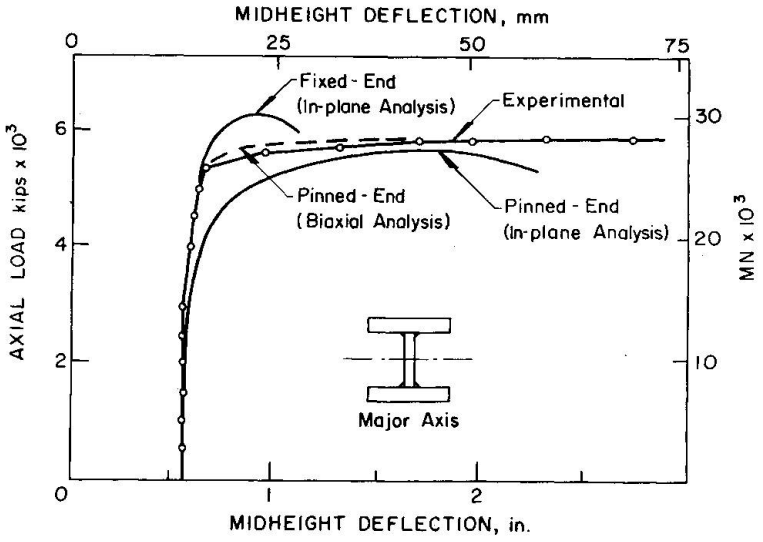

Fig. 8 Midheight Lateral Deflection About the Major Axis

deviation of the major axis rotation is observed at the initial stages of loading after which a fixed-end condition was maintained until the load reached 5500 kips (24,500 MN) or 0.880 P_y. The cause for the initial deviation is believed to be due to the adjustments of the cross-head. It is of interest to note that the shape of the load-rotation curves are very similar to that of the load-midheight deflection curves shown in Figs. 7 and 8. The two sets of curves are seen to start to bend very rapidly almost at the same load level.

The overall shortening of the column was obtained by measuring the cross-head movement using a dial gage. The load versus overall shortening curve is shown in Fig. 10. Similar to that of the load-rotation curves shown in Fig. 9, a deviation is also observed at the initial stages of the loading. The additional factor causing this deviation may be attributed to the deformation of the copper plates inserted between the end plates and the specimen. The stiffness of the column beyond the value of axial load P = 2000 kips (8900 MN) agrees very closely to the theoretical stiffness which is predicted by the formula AE/L where the value of AE is obtained from the stub column test.

Strain readings were recorded at selected points along the column lengths using electric resistant strain gages. Figure 11 shows the strain measurements at the column midheight for different load levels. Bernoulli's hypothesis on the linear strain distribution over the cross section is seen to be rather good up to the initiation and subsequent yield plastification of the cross section. However, when the cross section has been substantially plastified, a linear strain distribution assumption for the heavy shape column section may not be justified.

5. THEORETICAL ANALYSIS

The strength of an axially loaded column may be determined either by its bifurcation load or by its maximum load. For a perfectly straight column with concentric load application, the column remains straight under increasing load until the tangent modulus load is reached. Real columns, however, show an initial out-of-straightness, unsymmetric distributions in material properties, and residual stresses. This geometrical and material imperfection, along with the fact that the load can not be applied axially along the center line of the column, will cause the column to deflect immediately upon loading. Thus, all columns must be treated as beam-columns (deflection problem), not as straight columns (eigenvalue problem, tangent-modulus method).

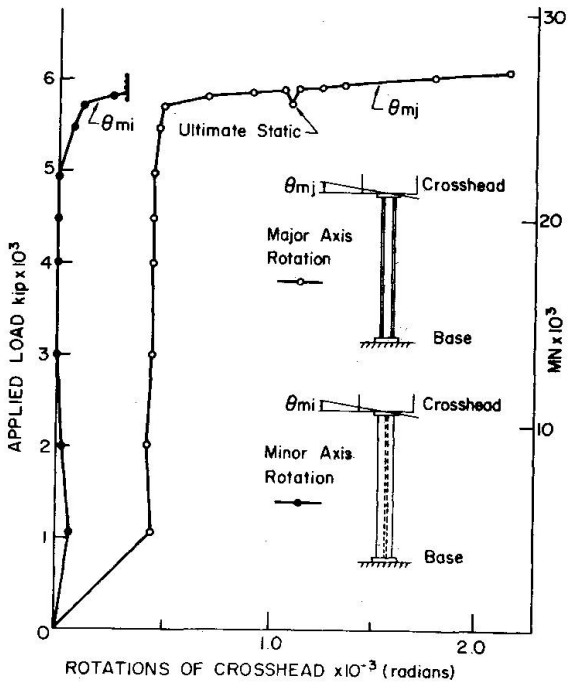

Fig. 9 End-Rotations of the Column at the Cross Head

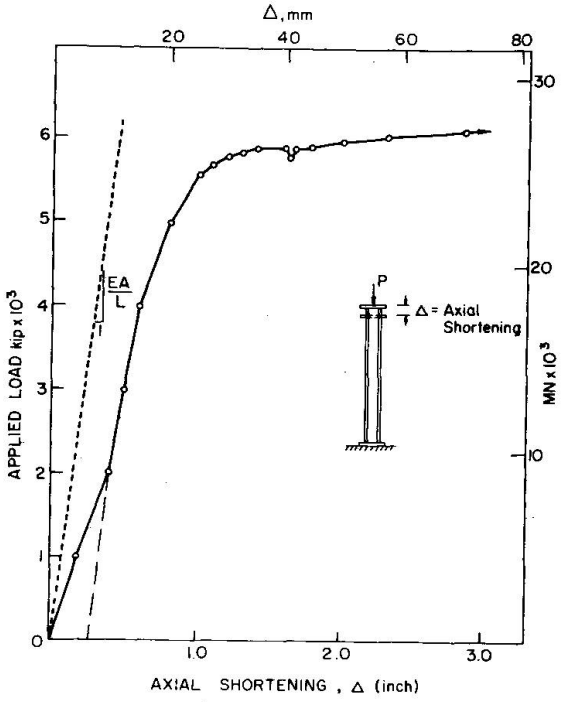

Fig. 10 Overall Shortening of Column

Several methods of solution exist to determine the behavior of such columns. However, in determining the behavior of heavy shape columns, the major problems are: (1) the variation in yield strength and residual stresses through the thickness of the component plates, and (2) the initial out-of-straightness in the two principal axes directions. The theoretical analysis presented herein considers both the two-dimensional in-plane column analysis and three-dimensional biaxial bending column analysis.

In-Plane Column Analysis--Tangent Modulus Load

The strength of a centrally loaded column based on the tangent modulus concept may be written in the form

$$P_T = \frac{\pi^2 E}{L^2} \int_A \left(\frac{E_T}{E}\right) y^2 \, dA \qquad (1)$$

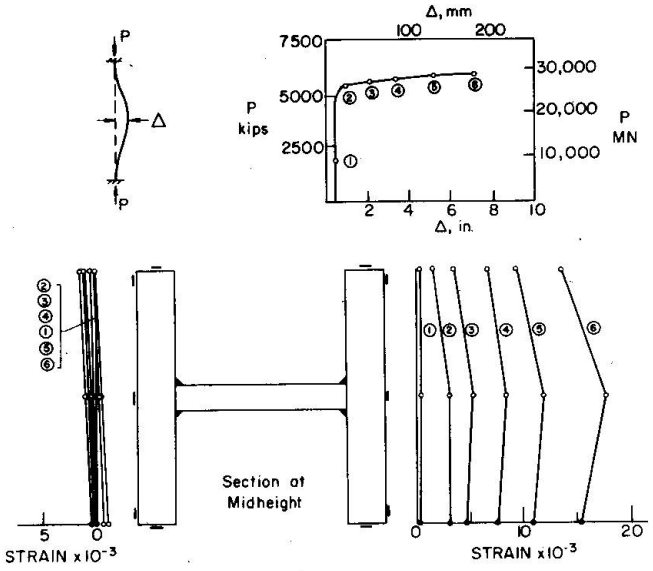

Fig. 11 Strain Variations at Midheight of Column

where P_T = tangent modulus load, E = elastic modulus, A = total cross sectional area, L = effective length of the column and E_T = effective tangent modulus of the shape. The tangent modulus load can be computed based on either measured residual stresses or the stress-strain relationship of a stub column test [10]. The stub column approach is adopted herein for the theoretical predictions. Figure 12 shows the tangent modulus load curves with bending permitted about the minor and major axes of the column.

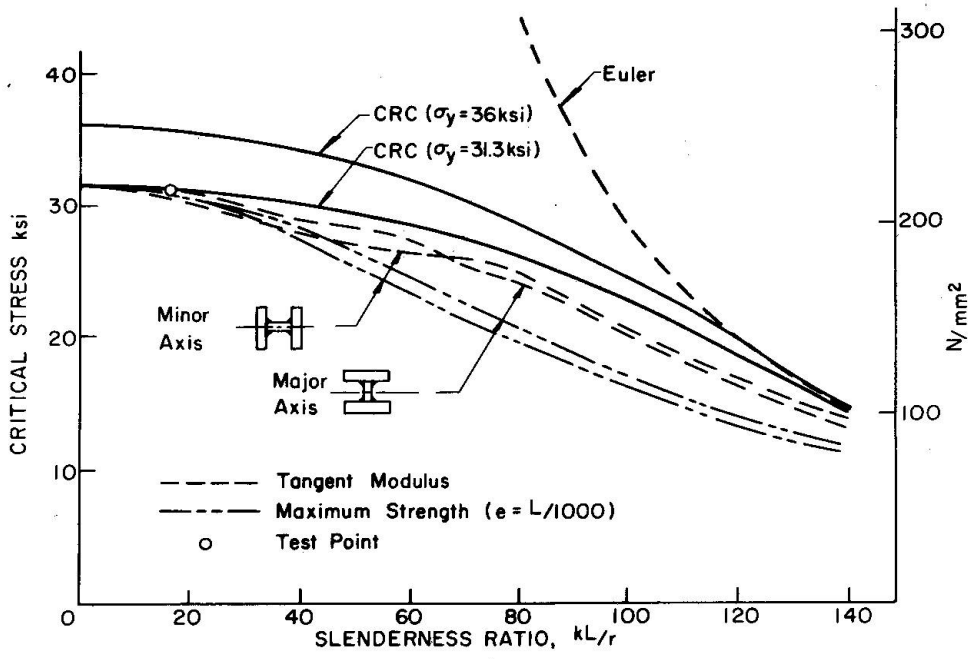

Fig. 12 Column Strength Curves

In-Plane Column Analysis--Maximum Load

The calculations become more involved for maximum strength predictions even though the underlying basic concepts are rather simple. The method adopted herein is based on the assumption that the initial as well as the deflected shape under increasing load can be described by a half-sine wave. The equilibrium condition at the midheight cross section may be written in the form

$$\Delta P_{int} = \int_A E_t \, \Delta\epsilon \, dA = \frac{1}{\delta_m} \int_A E_t \, \Delta\epsilon y \, dA = \frac{1}{\delta_m} \Delta M_{int} \tag{2}$$

where ϵ is the strain distribution in the cross section. By assuming linear strain distribution, Eq. 2 can be solved by using a numerical increments iterative procedure. The maximum load, under which the column assumes a state of neutral equilibrium, is then determined when the rate of resisting internal moment of the column approaches zero.

The in-plane behavior of the column was determined using a computer program (CDC 6400 Digital Computer) developed at Lehigh University [11]. The program computes the load-deflection relationship for a column with sinusoidal initial out-of-straightness. It also handles residual and yield strength variation through the cross section but constant through the thickness of the component plates.

In calculating the load-deflection curves for the H23x681 column the measured yield strength, residual stress variations, and initial out-of-straightness were used. The flanges and the web were subdivided into 50 and 30 segments, respectively. The average measured residual stress and yield strength values were used as the input data. Since the degree of end fixity during the test was unknown the two extreme end conditions were used in the analysis: pinned-end and fixed-end. Thus, the load-deflection curves obtained correspond to the upper and lower bound solutions to the problem. The calculated deflection curves are shown in Fig. 7 for the case of minor axis bending and in Fig. 8 for the case of major axis bending. In both figures the test results are seen to be bound between the two bounds. In Fig. 12 the maximum load column curves are shown. The curves are seen to be below the CRC basic column curve since the specimen had a yield strength lower than the specified value.

Biaxial Bending Column Analysis--Maximum Load

Several analytical procedures are available for the determination of the load deformation behavior of an isolated, initially imperfect column under biaxial bending [12]. Herein, the tangent stiffness method to the solution of the heavy shape column is adopted for the theoretical analysis [13]. The method is based on the analytical development of the linear relationship between the infinitesimal changes of the generalized forces $\{\delta f\}$ and displacements $\{\delta\Delta\}$. The derivation is based on the assumption that the initial as well as the deflected shape under increasing load can be described by a half-sine wave. It has the simple form

$$\{\delta f\} = [Q] \{\delta\Delta\} \tag{4}$$

The matrix $[Q]$ is defined as the tangent stiffness matrix as it represents the tangent of the force-deformation curve as well as the stiffness of the cross section. In this procedure the load is applied as a sequence of

sufficiently small increments so that during the application of each increment the column is assumed to behave linearly. Thus, the nonlinear behavior is determined by solving a sequence of linearized equations

$$\{\delta\Delta\} = [Q]^{-1} \{\delta f\} \tag{5}$$

An improved solution may be obtained by starting with an initial estimate of the displacement solution. This solution is then backsubstituted into the equations and the procedure is repeated until an accepted convergence or a prescribed tolerance is obtained. The iterational scheme is similar to the Newton-Raphson method, thus, the solution will generally converge within a few cycles even for larger load increments.

The load-deflection curves for the H23x681 column based on biaxial bending column analysis was performed using a computer program developed also at Lehigh University 14 . The program computes the relationship between the applied load and the three generalized displacements: lateral deflections in the two principal axes and twist of the cross section. The program can handle residual stress and yield strength variations throughout the cross section including the variations through the thickness of the component plates.

In the computation both the flanges and the web were divided equally into 30 segments through the width and 5 segments through the thickness. The average residual stress and yield strength (Figs. 2 and 4) at each segment was used as the input data. The calculated deflection curves are also shown in Figs. 7 and 8. It can be seen that the theoretical curves predicted by the biaxial bending column analysis are in good agreement with the results.

The effective length of the column was determined by plotting the curvature variation along the column length for different load levels. The curvature at each location is determined from the strain gage readings mounted at various levels and at opposite sides of the specimen. The curvature curves are shown in Fig. 13 for the minor axis bending and in Fig. 14 for the case of the major axis bending. It is noted that the point of inflection, that is, zero curvature points are not fixed but rather change with

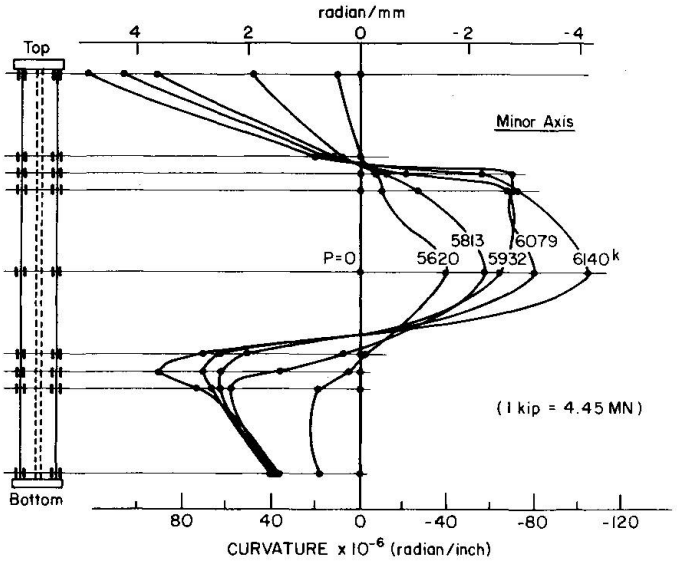

Fig. 13 Measured Curvature Curves about the Minor Axis

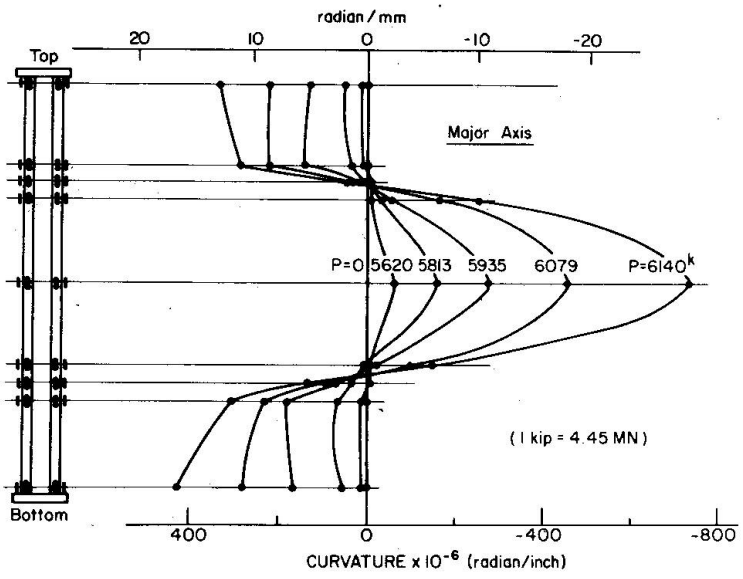

Fig. 14 Measured Curvature Curves about the Major Axis

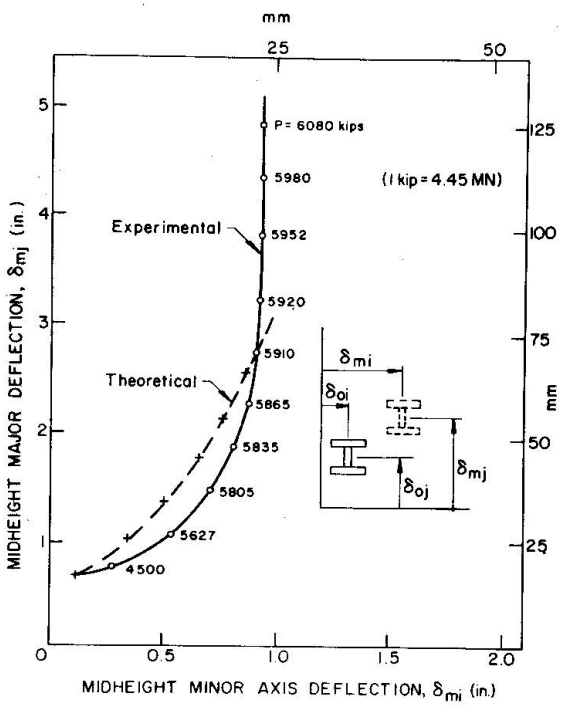

Fig. 15 Comparison of Experimental and Theoretical Load-Deflection Curves (Biaxial Analysis)

load for the case of minor axis bending and seem stationary for the major axis bending. The effective lengths determined from the experiment (Figs. 13 and 14) were used in the biaxial bending analysis of the column. The load versus the deflections in the two principal axes are compared in Fig. 15 and good agreement is observed.

6. SUMMARY AND CONCLUSIONS

This paper contains a theoretical and experimental analysis of the behavior and the strength of a heavy shape column built up from flame-cut plates. The theoretical part of the analysis includes two-dimensional in-plane column analyses by tangent modulus concept and by a load-deflection approach, and a three-dimensional biaxial bending column analysis. The effects of residual stress, yield strength variations over the cross section and initial out-of-straightness in the two principal axes are considered in the theoretical analysis. Comprehensive experimental investigation was performed to determine the strength and behavior of one particular heavy built-up shape--H23x681, ASTM A36 steel. The experiment includes: (i) measurements of yield stress levels in the cross section; (ii) measurements of residual stress distribution in the cross section; (iii) a stub column test; and (iv) a full-size column test.

Failure of the column was observed in biaxial bending with excessive bending about the major axis. The results of the column test and the theoretical prediction based on a recently developed three-dimensional biaxial bending column analysis are compared and good agreement is observed.

Based on this study the following conclusions may be stated:

1. The two-dimensional in-plane column analysis considering the geometric and material imperfection of the column can predict the maximum strength of the heavy shape columns with good accuracy; however, the method may give a false representation of the load deflection behavior of heavy shape columns.

2. Because of the particular pattern and variation in residual stress distribution in the cross section as well as the initial out-of-straightness along the two principal axes for the heavy shape columns, the three-dimensional biaxial bending column analysis is needed in order to predict accurately the load-deflection behavior of such columns.

3. The strengths of heavy shape columns built up from flame-cut plates are found to be higher than those of lighter welded whapes as well as their rolled counterparts.

4. Bernoulli's hypothesis on the linear strain distribution over the cross section of heavy shapes is found to be good up to the initiation of yielding and including the subsequent plastification of the cross section. However, when the cross section has been substantially plastified, the assumption of linear strain distribution may not be justified.

5. The AISC column formula or the CRC strength formula may be used to predict the maximum strength of a heavy column shape built-up from oxygen-cut plates of ASTM A36 steel.

7. ACKNOWLEDGMENTS

This investigation was conducted at Fritz Engineering Laboratory (L. S. Beedle, Director), Lehigh University, Bethlehem, Pennsylvania. The American Iron and Steel Institute, the American Institute of Steel Construction, the Column Research Council and the National Science Foundation (Grant GK 28049XI) jointly sponsored the study.

The guidance of Task Group 1 of the Column Research Council, under the chairmanship of John A. Gilligan, is gratefully acknowledged.

Thanks are due to R. L. Bloss and A. F. Kirstein of the National Bureau of Standards for their assistance in testing the columns in the 12-million-pound capacity testing machine. The assistance of Reidar Bjorhovde during the testing and also in reducing the experimental data is sincerely appreciated.

Thanks are also due to Mrs. Sharon Balogh for the preparation of the drawings and to Miss Shirley Matlock for her care in typing the manuscript.

8. REFERENCES

1. American Institute of Steel Construction
   SPECIFICATION FOR THE DESIGN, FABRICATION AND ERECTION OF STRUCTURAL STEEL FOR BUILDING, AISC, New York, February 1963.

2. CRC - Column Research Council
   GUIDE TO DESIGN CRITERIA FOR METAL COMPRESSION MEMBERS, 2nd ed., B. G. Johnston, Ed., John Wiley and Sons, Inc., New York, 1966.

3. Alpsten, G. A. and Tall, L.
   RESIDUAL STRESSES IN HEAVY WELDED SHAPES, The Welding Journal, Vol. 49, March 1970.

4. Bjorhovde, R., Brozzetti, J., Alpsten, G. A. and Tall, L.
   RESIDUAL STRESSES IN THICK WELDED PLATES, The Welding Journal, Vol. 51, August 1972.

5. American Welding Society
   CODE FOR WELDING IN BUILDING CONSTRUCTION, AWS D1.0-66, New York, 1966.

6. Tall, L. and Alpsten, G. A.
   ON THE SCATTER IN YIELD STRENGTH AND RESIDUAL STRESSES IN STEEL MEMBERS, Symp. on Concepts of Safety of Structures and Methods of Design, IABSE, London, 1969.

7. Tebedge, N., Alpsten, G. A. and Tall, L.
   MEASUREMENT OF RESIDUAL STRESSES--A COMPARATIVE STUDY OF METHODS, Proceedings, Joint British Committee for Stress Analysis Conference on "The Recording and Interpretation of Engineering Measurements", Institute of Marine Engineers, London, April 1972.

8. Tall, L.
   STUB COLUMN TEST PROCEDURE, Document C-282-61, Class C Document, International Institute of Welding, Oslo, June 1962; also CRC Tech. Memo No. 3, "Column Research Council Guide", 2nd ed., edited by B. G. Johnston, Wiley, 1966.

9. Tebedge, N. and Tall, L.
   PROCEDURE FOR TESTING CENTRALLY-LOADED COLUMNS, Fritz Engineering Laboratory Report No. 351.6, December 1971; also, CRC Tech. Memo No. 4, "Column Research Council Guide", 3rd ed. (to be published), edited by B. G. Johnston.

10. Yu, C. K. and Tall, L.
    SIGNIFICANCE AND APPLICATION OF STUB COLUMN TEST RESULTS, Journal of the Structural Division, ASCE, Vol. 97, ST7, July 1971.

11. Beer, G. and Tall, L.
    THE STRENGTH OF HEAVY WELDED BOX COLUMNS, Fritz Engineering Laboratory Report No. 337.27, December 1970.

12. Chen, W. F. and Santathadaporn, S.
    REVIEW OF COLUMN BEHAVIOR UNDER BIAXIAL LOADING, Journal of the Structural Division, Proc. ASCE, Vol. 94, No. ST12, December 1968.

13. Santathadaporn, S. and When, W. F.
    ANALYSIS OF BIAXIALLY LOADED STEEL H-COLUMNS, Journal of the Structural Division, ASCE, Vol. 99, No. ST3, March 1973.

14. Santathadaporn, S. and Chen, W. F.
    ANALYSIS OF BIAXIALLY LOADED COLUMNS, Fritz Engineering Laboratory Report No. 331.12, September 1970.

RESIDUAL STRESSES IN HOT ROLLED MEMBERS

B. W. Young
Lecturer in Structural Engineering
School of Applied Sciences
University of Sussex
Brighton, England

ABSTRACT

The distribution of residual stress in I-sections due to uneven cooling after hot-rolling has been examined. A survey covering a large number of previous measurements has been made in order to establish typical patterns for subsequent inelastic buckling strength calculations. Measured residual stresses in some commonly used British UB and UC sections are in good agreement with these results. When compared with the results of the general survey, American residual stress assumptions are seen to be unrealistic both as to magnitude and distribution.

Patterns of residual stress for different I-section geometries have been selected which are about the worst likely to be encountered in British rolled sections. Buckling strength calculations for I-sections can therefore be based with confidence on residual stress distributions which are representative of the real situation.

1. INTRODUCTION

Residual or "locked-in" stresses have a significant effect on the brittle fracture, fatigue, stress corrosion and buckling strength of structural steel sections. In recent work at Cambridge and Sussex attention has been confined to their particular effect on buckling.

A combination of applied and residual stresses will promote inelastic behaviour in a member cross-section at levels of applied stress less than yield. Since plastic material which does not subsequently unload elastically can make no contribution to resist bending, a knowledge of the effective cross-section stiffness under load is essential for buckling calculations. When buckling is not a consideration, the fully plastic load carrying capacity is not impaired, but deformations will be greater than in a corresponding initially stress free member.

Longitudinal residual stresses arise from uneven heating or cooling of the cross-section during the manufacturing process. Such stresses are thus encountered in hot-rolled sections as well as those fabricated by welding and flame-cutting. Attention here will be restricted to residual stresses in I-sections induced by hot-rolling.

A hot-rolled I-section starts life as an ingot at a temperature of about 1250°C. During the rolling process the section shape is formed. By the time the cooling bed is reached, the average temperature will be down to 600°C to 900°C depending on the section's thickness.

During the final stages of rolling, the flange toes and the centre of the web which are the more exposed parts of the section, have cooled more than the shrouded web to flange junction. The contraction in the cooler material is resisted in the hotter regions where compressive plastic flow takes place at a low value of yield stress associated with the high temperature. The cooler material has now extended in relation to the hotter core and as this latter region contracts on cooling to ambient temperature, a reversal in stress takes place. The material which cools first is now in residual compression, whilst the region which cooled last is in residual tension. The longitudinal stresses must give rise to a system of forces in the cross-section which is in equilibrium.

Considerations of member strength have prompted the investigation of residual stresses by both direct measurement and analysis. References to residual stress measurement are numerous and will be given in connexion with a survey of results

in a later section. Alpsten (1) has recently developed a sophisticated computer analysis to predict residual stresses in hot-rolled steel sections of different geometries. Although the analysis is theoretically sound, in practice the many variations in rolling technique can produce quite different residual stress patterns in identical sections. This tendency is aptly illustrated by M. J. Baker's work at Imperial College (2). It therefore appears that the most satisfactory way of arriving at an estimate of residual stresses in structural sections is by making a study of published results and thereby inferring typical stress patterns for various section geometries.

The magnitude of residual stresses is largely independent of material properties (3,1) and can therefore be considered as a function of section geometry for identical cooling conditions. If the residual stresses are expressed as a proportion of the yield stress their significance is seen to reduce as the material yield stress increases.

We are concerned here only with residual stresses in thin sections, that is to say, those sections for which the stress variation through the thickness can be ignored. Attention at Lehigh University (1,4) has recently turned to thick sections where large variations in residual stress can occur through the thickness. Residual stresses increase in severity for geometrically similar shapes as the size of the section increases.

2. MANUFACTURE OF HOT-ROLLED SECTIONS

The processes involved in the manufacture of hot-rolled sections are generally well known. Techniques however, tend to vary slightly from country to country and details of British practice are given in Ref. 5. In particular, British mills cool sections spaced well apart with the web vertical. In American mills it appears that sections are close packed on the cooling bed. This may account for the fact that webs of American sections end up with tensile residual stresses (3) while the more exposed webs of British sections are in compression.

As far as residual stresses are concerned an important part of the manufacturing process is cold straightening. This acts beneficially as a form of mechanical stress relief (6). The amount of redistribution of residual stress during roller straightening depends on the operator's setting of the rollers. It can easily happen that no change in the original cooling residual stress pattern is made. Gagging operates only on a short length of the member. To straighten the whole length, it is necessary to pass the member through the gag-press several times. It is possible that after leaving the press, portions of

the length may still contain the original stresses. Alpsten (1) reports undisturbed cooling residual stress patterns in nominally straightened sections. The present measurements (Section 3) confirm this. Basing member strength calculations on the full cooling residual stress pattern rather than the more favourable pattern produced during cold straightening is thus a sensible precaution.

3. PRESENT RESIDUAL STRESS MEASUREMENTS

A large proportion of the work on residual stresses and their measurement has been carried out in the United States. As a result, information is biased towards American sections and rolling practice.

To obtain further information on residual stresses in typical British sections a small programme of measurements was undertaken at Cambridge. As a secondary investigation the effect of cold straightening was examined by making residual stress measurements on two lengths of the same bar, one length having been cold straightened and the other left untouched.

Residual stresses will be relieved completely by cutting the bar longitudinally into thin strips. Extensometer readings made before and after cutting will determine the strain relaxation in the strip and hence the original magnitude of residual stress. This 'sectioning' method as it is called provides the most useful means of measuring residual stresses. With thick members, sectioning may be followed by 'slicing' to obtain the stress variation through the thickness (4).

When long gauge length extensometers are used, an automatic averaging of the stresses is obtained. A 250 mm gauge length has been used at Lehigh University (3). A 200 mm gauge length Demec extensometer was used for the present tests. Measurements made by Jez-Gala (7) at Cambridge using a 20 mm gauge length were unsatisfactory because only local values of residual stress were measured. A similar criticism can be levelled at other well-known methods of measurement such as trepanning, hole drilling and X-ray diffraction.

The present residual stress measurements were carried out on seven lengths of five commonly used Universal Column and Beam sections. Five lengths were not cold straightened (NCS) and two lengths were (CS). The section sizes are shown in Table I. All material was to BS 4360 Grade 43A (σ_y = 250 MN m^{-2}) and was supplied by courtesy of the British Steel Corporation's Lackenby and Cargo Fleet Iron Works, Middlesbrough.

TABLE I PRESENT RESIDUAL STRESS MEASUREMENTS

No.	SECTION	$\frac{Bt}{DT}$	RESIDUAL STRESS: MN m^{-2}		
			σ_f	σ_{fw}	σ_w
1	6x6x14.7 lb - NCS[a]	0.89	+122	-100	+110
2	8x8x31 lb - NCS[b]	0.67	+122	- 90	+100
3	8x8x31 lb - CS[b]	0.67	+ 10	- 75	+120
4	10x5¾x21 lb - NCS[a]	0.41	+ 55	-125	+260
5	12x6½x31 lb - NCS[a]	0.31	+ 38	-150	+340
6	16x7x36 lb - NCS[b]	0.31	+ 68	-144	+220
7	16x7x36 lb - CS[b]	0.31	+ 45	-133	+216

Source: a) Cargo Fleet Iron Works, b) Lackenby Works

The sectioning method was used to determine the residual stress distribution. A number of specimens parallel to the longitudinal axis were selected from both web and flange. Preparation of each specimen consisted of drilling a pair of 1 mm diameter holes, 1 mm deep and 200 mm apart. The change in strain on a 200 mm gauge length was determined by comparing Demec extensometer readings before and after sectioning. Each specimen after cutting was 12 mm wide and some 220 mm long. Readings were made on both faces of each specimen except for that at the centre of each flange where a reading could only be made on the outside face. The number of specimens per section ranged from thirteen for the 6 in x 6 in x 15.7 lb section to nineteen for the 16 in x 7 in x 36 lb section.

The measured residual stresses are plotted in Figures 1a to g. The simple theoretical distribution, flange toes and web in compression and web to flange junction in tension is confirmed. Severe cold straightening is seen to have redistributed flange stresses for the 8 in x 8 in x 31 lb (CS) section although the web is largely unaffected. Cold straightening by rotorising in the 16 in x 7 in x 36 lb section has had no effect. Peak residual stress values from Figure 1 appear in Table I, where σ_f, σ_{fw}, and σ_w are respectively the stresses at flange toes, flange to web junction and centre of web. Compressive stresses are positive.

Tensile tests were made on two coupons cut from each section, one coupon coming from a flange and one from the web. The non-

waisted coupons were pulled in a 100 kN Instron machine. The strain rate at yield was maintained at $8.3 \times 10^{-6} s^{-1}$ which was as close to the zero strain rate condition which could be attained without stopping the machine altogether. Tensile yield stress values appear in Table II below together with the mill test results.

TABLE II TENSILE COUPON TESTS

SPEC. No.	POSITION	σ_y MN m^{-2}	σ_y (MILL TEST) MN m^{-2}
1	Flange	291	-
	Web	310	386
2	Flange	296	-
	Web	303	345
3	Flange	300	-
	Web	332	334
4	Flange	273	-
	Web	366	352
5	Flange	256	-
	Web	338	357
6	Flange	273	-
	Web	340	357
7	Flange	281	-
	Web	335	341

4. PREVIOUS RESIDUAL STRESS MEASUREMENTS

The theoretical work by Alpsten (1) has shown that the magnitude and disposition of residual stresses in hot-rolled sections are governed mainly by section geometry and cooling conditions. Whilst the first of these parameters is well behaved, the second may vary considerably from mill to mill. A survey of published residual stress measurements shows a wide variation of residual stresses in geometrically similar shapes. The results of this survey are given in Table III. Many of the results shown in the Table are averaged from several tests. In general the material was ordinary structural mild steel having a yield stress in the region of 250 MN m^{-2}. A few results are included for high strength steel to BS 4360: Grade 55, (σ_y = 450 MN m^{-2}).

It is difficult to describe the geometry of an I-section in a single parameter, but Ketter (8) has suggested the non-dimensional grouping Bt/DT. B and D are the breadth and depth of

TABLE III RESIDUAL STRESS MEASUREMENTS

SECTION	$\frac{Bt}{DT}$	ORIGIN	REF.	RESIDUAL STRESSES: $MN\,m^{-2}$ σ_f	σ_{fw}	σ_w	SECTION	$\frac{Bt}{DT}$	ORIGIN	REF.	RESIDUAL STRESSES: $MN\,m^{-2}$ σ_f	σ_{fw}	σ_w
12x6½x27 lb	0.31	Aust.	9	- 34	-117	+207	8x4 RSJ	0.28	Aust.	11	0	- 70	+168
12x6½x27 lb	0.32	Japan	"	- 7	-117	+155	12x5x25 lb	0.27	G.B.	12	+ 42	-135	+148
16x7x50 lb	0.26	Aust.	"	- 7	-158	+103	8 WF 31	0.67	U.S.A.	13	+ 85	- 35	- 58
16x7x50 lb	0.20	Japan	"	0	-165	+172	8 WF 31	0.67	"	"	+ 78	- 8	-105
10x10x49 lb	0.53	Aust.	"	-	-	+ 90	8 WF 31	0.67	"	"	+ 80	- 28	- 33
10x10x49 lb	0.61	Japan	"	0	- 55	+103	8 WF 31	0.67	"	"	+102	- 62	+ 25
27x10x102 lb	0.24	Aust.	"	+ 35	-124	+160	IAP 150	0.34	Belg.	14	+ 45	-115	+100
27x10x102 lb	0.22	G.B.	"	0	-193	+262	IPE 200	0.34	"	"	+ 25	- 90	+230
12x6½x31 lb	0.32	Aust.	10	+ 17	-172	+307	DIE 20	0.68	"	"	+130	- 48	+ 30
16x7x50 lb	0.26	"	"	+ 15	-188	+250	DIR 20	0.60	"	"	+ 70	+ 8	- 60
16x7x50 lb	0.27	"	"	+ 13	-152	+230	DIE 20	0.68	"	15	+128	- 95	+ 42
10x10x89 lb	0.60	"	"	+117	-110	+138	6x6x20 lb	0.68	G.B.	7	+ 80	- 75	+ 82
12x12x190 lb	0.53	"	"	+122	- 98	+147	8x8x31 lb	0.66	"	"	+ 77	- 75	+ 93
27x10x102 lb	0.23	"	"	0	-193	+276	10x10x49 lb	0.61	"	"	+138	-138	+138
12 WF 50	0.37	U.S.A.	8	+ 37	- 72	+120	12x12x92 lb	0.61	"	"	+120	-102	+110
12 WF 65	0.64	"	"	+135	-105	+110	8 WF 67	0.57	U.S.A.	1	+ 82	- 70	+ 38
14 WF 426	0.55	"	"	+155	- 90	- 98	10x4½ RSJ	0.27	Aust.	16	+ 25	-200	+142
4 WF 13	0.80	"	"	+ 98	- 22	- 67	8x4 RSJ	0.35	"	"	+ 18	-160	+215
8 WF 24	0.50	"	"	+ 75	+ 22	-127	6x5 RSJ	0.66	"	"	+ 53	- 70	+ 98
8 WF 31	0.67	"	"	+112	- 37	+ 22	*6x6x20 lb	0.68	G.B.	17	+ 10	- 30	+ 54
8 WF 67	0.57	"	"	+ 60	+ 37	-112	*8x8x58 lb	0.60	"	"	+ 10	- 19	+ 25
14 WF 43	0.33	"	"	+ 67	-145	+190	*8x5½x17 lb	0.50	"	"	+ 5	- 31	+ 70
36 WF 150	0.22	"	"	+ 52	- 82	+ 60	*12x4x19 lb	0.23	"	"	- 30	-102	+140
6 M 15.5	0.89	"	"	+112	- 75	+ 15	12x5x32 lb (A)	0.25	"	2	0	- 92	+118
12 J 14	0.20	"	"	+ 30	-	-	" (B)	"	"	"	0	-155	+147
4 WF 13	0.80	"	11	+ 90	- 30	- 30	" (C)	"	"	"	0	-145	+147
8 WF 31	0.67	"	"	+ 90	- 37	+ 37	18x7½x66 lb (A)	0.24	"	"	0	- 38	+ 42
12 WF 65	0.64	"	"	+ 82	- 82	+ 98	" (B)	"	"	"	+ 25	-182	+180
14 WF 426	0.55	"	"	+112	- 30	- 60	" (C)	"	"	"	0	-115	+100

*High Yield Steel (Grade 55)

the section and T and t are respectively the flange and web thicknesses. It would be wrong to attach too much authority to this simple parameter, but it does have the virtue of separating I-sections into Universal Column and Beam shapes. Values of Bt/DT are included in Tables I and III.

To examine the trend in residual stress magnitudes with section geometry, the values of residual stresses in Table III together with the results of the present measurements given in Table I are plotted against Bt/DT in Figure 2a, b, and c.

Typical patterns of residual stress found for the tests reported in Table III were parabolic in both flange and web (Figure 3(a)). Certain American results for column sections showed a tendency towards a bilinear stress distribution in the flange accompanied by a tensile uniform stress level in the web (Figure 3(b)). The present measurements on column shapes also showed this type of flange distribution but the web stresses were found to be predominantly compressive with a parabolic distribution (Figure 1a and b).

The bilinear distribution of stress in the flange implies a discontinuity over the junction with the web which is unnatural in view of the continuously varying conditions which produce these stresses in the first place. It therefore seems more reasonable to assume a rounding of this sharp corner giving the residual stresses in the flange more of a parabolic distribution. All beam shapes included in Tables I and III had residual stress patterns which conformed with Figure 3(a).

The present residual stress measurements are shown as open circles on Figure 2. They agree well with values from the general survey (plotted as solid circles).

5. ADOPTION OF CHARACTERISTIC RESIDUAL STRESS PATTERNS FOR HOT-ROLLED UNIVERSAL SECTIONS

To simplify the subsequent treatment of residual stresses in column and beam shapes a parabolic distribution in both flange and web is assumed as in Figure 3(a). The magnitudes of the peak stresses are deduced from the plots in Figure 2. A simple calculation to balance longitudinal forces in the cross-section will show the effect of the ratio of web to flange area on the residual stress values in a particular cross-section.

Taking a pessimistic view of the possible residual stresses in a column section ($A_W = 0.3A_F$) we obtain

σ_f = + 125 MN m^{-2} from Figure 2(a)

σ_{fw} = - 100 MN m^{-2} from Figure 2(b)

and σ_w = + 175 MN m^{-2} by balance of longitudinal forces

where A_w is the web area (= dt)

A_F is the total flange area (= 2BT)

σ_f is the stress at the flange toes

σ_{fw} is the stress at the web to flange junction

and σ_w is the stress at the centre of the web.

Characteristic residual stress patterns for beam sections having A_w equal to 0.75 A_F and 1.2 A_F are also deduced in this way. Use is made here of the empirical observation that as the ratio A_w/A_F increases, σ_f decreases and σ_{fw} increases. This change is assumed to take place linearly, with σ_f for very deep beams (A_w/A_F = 1.2) being zero.

The principle influence of residual stresses on the inelastic buckling length of I-sections will be felt in the flanges. It is essential therefore to take representative values here. The peak web stresses calculated from the balance of residual forces are of secondary importance and may not always agree with typical figures plotted in Figure 2(c). This result is a consequence of assuming the simple parabolic stress distribution in both web and flange.

Although, in general, residual stresses do not depend on the yield stress, it is possible for yielding to occur in the webs of a few deep beams (see the Wyalla results (9,10)). This situation will result in a departure from the assumption of a parabolic web distribution. The consequent redistribution of residual stresses in the section is thus now affected by the magnitude of the material yield stress. Reference to flange stresses as the characteristic parameters will avoid the need to pay particular attention to this effect.

The peak residual stresses assumed in later buckling calculations for the column section and two beam sections are shown in Table IV. The overall distribution is assumed to be parabolic as shown in Figure 3(a). Included in Table IV are the stress values for column shapes that American workers have been using for many years. The stress pattern is that of Figure 3(b). Simple formulae for peak residual stresses appear under Table IV.

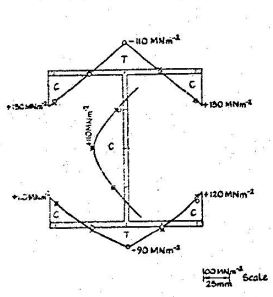

1(a)

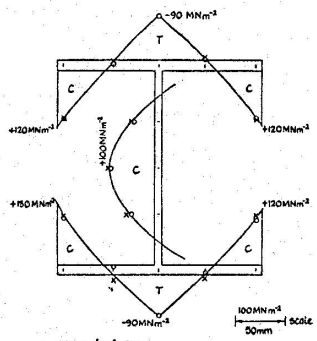

1(b)

Figures 1(a) to 1(g) - Present measurements of residual stress in British UC and UB sections

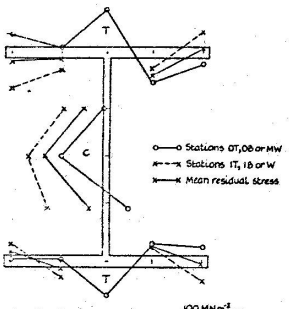

1(c)

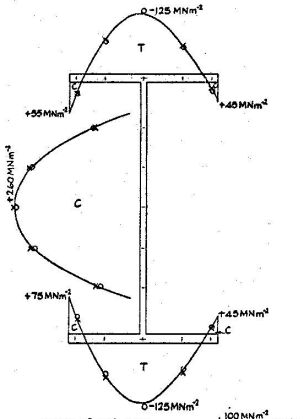

1(d)

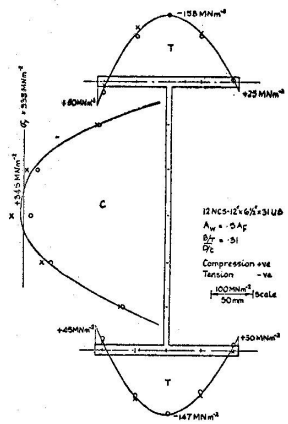

1(e)

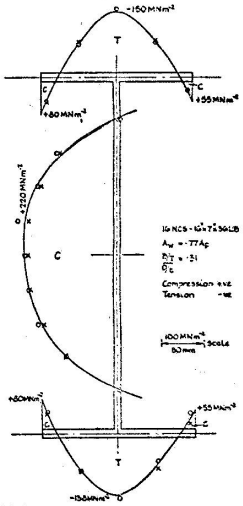

1(f)

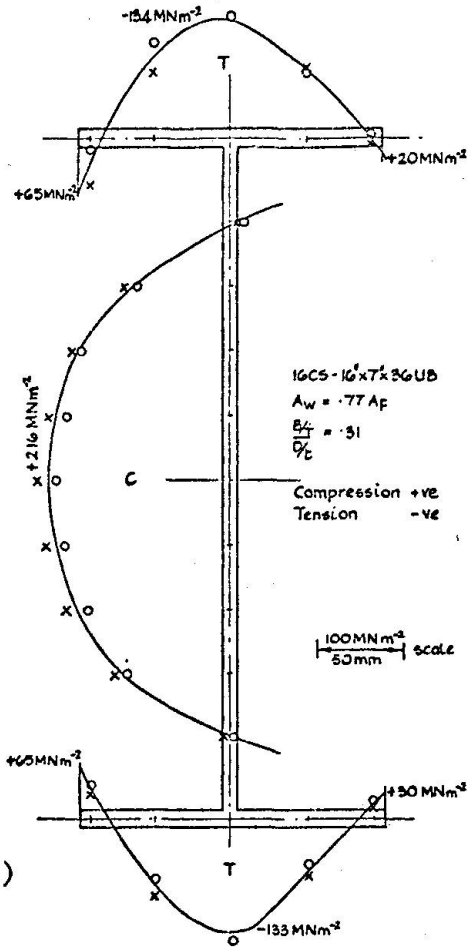

1(g)

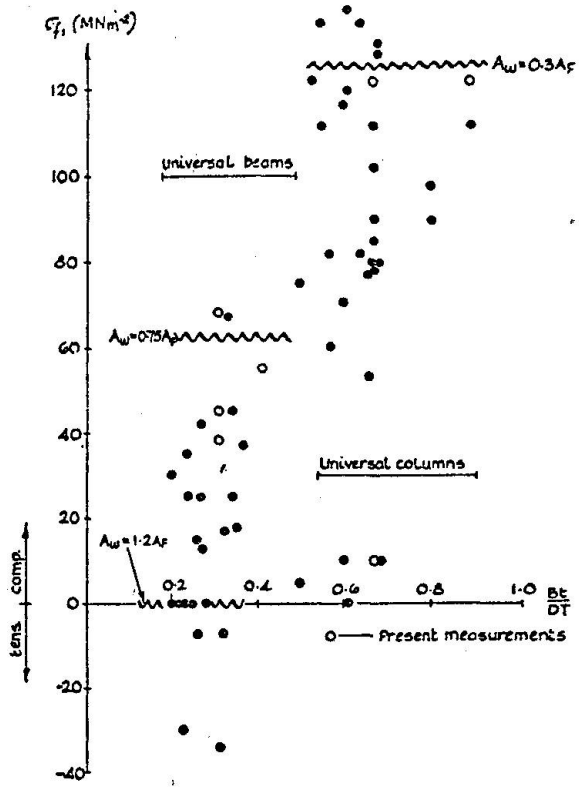

Figure 2(a) Residual stress measurements in I-sections: at the flange toes

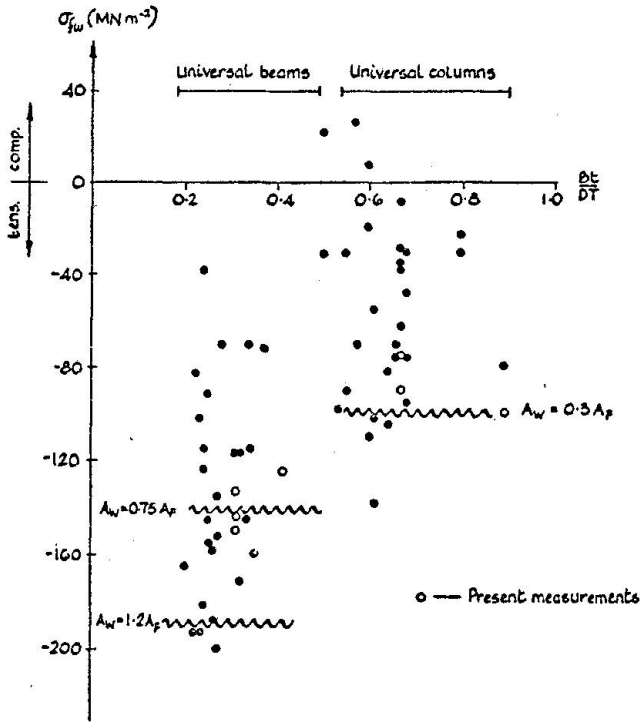

Figure 2(b) Residual stress measurements in I-sections: at the web to flange junction

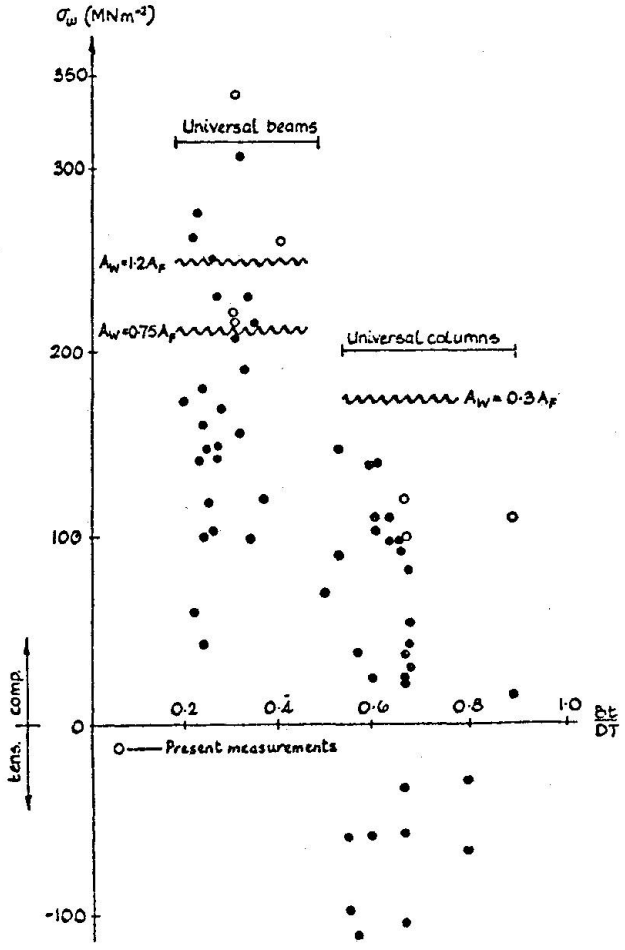

Figure 2(c) Residual stress measurements in I-sections: at the web centre

TABLE IV

SECTION	$\frac{A_W}{A_F}$	σ_f MN m^{-2}	σ_{fw} MN m^{-2}	σ_w MN m^{-2}
COLUMN	0.3	+125	-100	+175
BEAMS	0.75	+ 62	-144	+212
	1.2	0	-188	+250
COLUMN (U.S.A.)	0.3	+ 75	- 50	- 50

Approximate formulae adopted for peak residual stresses in hot-rolled Universal sections:

$$\sigma_f = 165 \left(1 - \frac{A_W}{1.2A_F}\right) \quad \text{MN m}^{-2}$$

$$\sigma_{fw} = -100 \left(0.7 + \frac{A_W}{A_F}\right) \quad " \quad "$$

$$\sigma_w = 100 \left(1.5 + \frac{A_W}{1.2A_F}\right) \quad " \quad "$$

A parabolic stress distribution is assumed in both flanges and web.

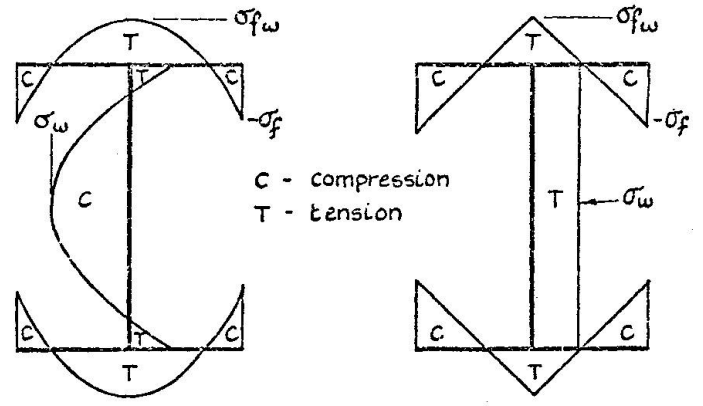

Figure 3. Comparison of assumed residual stress patterns

Acknowledgements

The author wishes to thank the Construction Industry Research and Information Association (CIRIA) for the financial support of this work and the British Steel Corporation (Northern and Tubes Group) for donating sections for residual stress measurement. The latter organization also provided generous hospitality and invaluable information during a visit to Lackenby Works in November 1969.

Notation

A_F	total flange area (=2BT)
A_w	web area (=dt)
B	flange width
d	web depth
T	flange thickness
t	web thickness
σ_f	residual stress at flange toe
σ_{fw}	residual stress at web/flange junction
σ_w	peak residual stress in web
σ_y	yield stress

References

1. Alpsten, G. A.
"Thermal residual stresses in hot-rolled steel members"
Fritz. Lab. Rep. No. 337.3 Dec. 1968

2. Baker, M. J.
"Variations in material properties and flexural behaviour of certain UB's"
Imperial College, London. Report: Jan. 1969

3. Beedle, L. S. and Tall, L.
"Basic column strength"
Trans.A.S.C.E. V.127 Pt II 1962 p.138

4. Alpsten, G. A. and Tall, L.
"Residual stresses in heavy welded shapes"
Fritz. Lab. Rep. No. 337.12 Jan. 1969

5. Young, B. W.
"Steel column design"
Ph.D. Thesis, Cambridge 1971

6. Lay, M. G. and Ward, R.
"Residual stresses in steel sections"
Steel Const. V.3 No. 3 1969

7. Jez-Gala, C.
"Residual stresses in rolled I-sections"
Proc. I.C.E., V.23 Nov. 1962 p.361

8. Ketter, R. L.
"The influence of residual stresses on the strength of structural members"
Weld. Res. Coun. Bull. No. 44 Nov. 1958

9. Ward, R. F.
"Comparison of BHP manufactured universal sections with competitors"
BHP Co. Ltd. Rep. No. QR20 Apr. 1967

10. Ward, R. F.
"Internal stresses and notch ductility determination of Group 1 commissioned universal sections"
BHP Co. Ltd. Rep. No. QR14 Nov. 1966

11. Tall, L.
"Recent developments in the study of column behaviour"
J. Inst. Engrs. Aust. V.36 No.12 Dec. 1964

12. Dibley, J. and Sowter, J. S.
"Tests on laterally unsupported beams of steel to BS 15"
BISRA Open Rep. No. FE/E/31/67

13. Huber, A. W. and Beedle, L. S.
"Residual stress and the compressive strength of steel"
Weld. Res. Supp. V. 33 Dec. 1954 p.589s

14. Mas, E. and Massonet, Ch.
"Belgium's part in ... European column research"
Acier-Stahl-Steel Sept. 1966 p.385

15. Massonet, Ch.
"The problem of buckling with steel struts"
Acier-Stahl-Steel Oct. 1966 p.453

16. O'Conner, C.
"Residual stresses and their influence on structural design"
J. Inst. Engrs. Aust. V.27 No. 12 Dec. 1955 p.313

17. Dibley, J.
"Lateral-torsional buckling of I-sections in Grade 55 steel"
BISRA Rep. No. PE/E/42/68 1968

RESIDUAL STRESSES, YIELD STRESS, AND COLUMN STRENGTH OF HOT-ROLLED AND ROLLER-STRAIGHTENED STEEL SHAPES

Göran A. Alpsten
Tech. Dr , Associate Director
Swedish Institute of Steel Construction
Stockholm, Sweden

ABSTRACT

An investigation of mechanical properties, residual stresses, and column strength of roller-straightened ("rotorized") steel shapes is reviewed briefly. Rotorizing small to medium-size wide-flange members is used in the production line routine at modern structural steel mills, yet most previous investigations of column strength have been concerned with as-rolled members only.

The investigation, being both experimental and theoretical, included a comparison of residual stresses, mechanical properties, and column strength of four lots of HE 200 A shapes, all taken from the same heat but rotorized in various ways. The experimental program included chemical analysis, determination of grain size, tensile specimen tests, as well as stub column and full-length column tests. A theoretical analysis was carried out to study the formation of residual stresses in the manufacturing process, including both the thermal stresses due to cooling, and the stresses due to rotorizing which superimpose upon the cooling stresses. The maximum ("ultimate") column strength in plane buckling was studied theoretically, taking into account the effects of non-symmetrical residual stresses, variable yield strength, initial out-of-straightness, and eccentricities.

In addition to the systematic experiments on HE 200 A shapes, several residual-stress measurements and tensile specimen tests were made on various hot-rolled steel shapes taken from local material suppliers, that is, in the as-delivered condition. Some of these specimens probably were gag-straightened, while others were rotorized.

The investigation showed that the maximum column strength may be increased by about 20 percent due to a suitable rotorizing procedure. It is suggested that the improved column strength of rotorized rolled members be considered in the scheme for assigning proper column curves if multiple column-curve systems are adopted.

1. INTRODUCTION

To fulfill the straightness requirements of hot-rolled shapes, most members have to be straightened after rolling and cooling in the mill. The straightening is performed in a roller-straightening ("rotorizing") machine in the production line routine at modern structural steel mills for small to medium-size wide-flange shapes. In rotorizing, the member is deflected back and forth between a number of rollers adjusted in such a manner as to cause plastic deformations in the member, see Fig. 1. For other members, the straightening may be carried out in a gag press. In gagging the member is placed on two supports and loading is applied locally -- the process may be repeated several times along the member to produce a sufficiently straight member.

While practically all delivered wide-flange members thus have been straightened, most research in the past on column buckling of wide-flange shapes has been focused on as-rolled members. Since there was no complete assurance that a delivered member had been straightened, the thermal residual stresses in the as-rolled member were considered, assuming this to be on the safe side.

The fact that residual stresses in a member are affected by an applied bending moment has been known for over 100 years. Wöhler, in his famous investigations of the fatigue strength of railroad car axles, discussed in 1860 residual stresses resulting from a bending which produces plastic deformations [1]. His assumed theoretical model for the formation of residual stresses after bending is essentially the same as used in more recent theoretical investigations of the effect of straightening [2, 3, 4, 5]. Several observations of residual stresses as measured in straightened members have been published in the literature, see for instance Refs. 2 through 9.

However, there appeared to be a need for a truly experimental study to investigate the effects of the straightening process on residual stresses, mechanical properties, and column strength. ("Experiment" is used here as defined in the behavioral sciences, that is, as opposed to an "observation".) This paper is a brief review of some results of such an experimental program, with additional theoretical studies of the formation of residual stresses as well as of the column strength. The paper is based upon three progress reports in Swedish [10, 11, 12]. In addition to the systematic experimental study, several supplemental residual stress measurements and tensile specimen tests were made on various hot-rolled steel shapes taken from local material suppliers, that is, in the as-delivered conditions [10, 13, 14]. While no account is available as to the detailed straightening procedure used for these supplemental test members, yield lines indicate that some of the members were probably gag-straightened and others rotorized.

A specific objective of the study reported here was to find out whether different column curves should be used for as-rolled as compared to rotorized members, if a multiple column curve system is adopted. Since rotorized columns

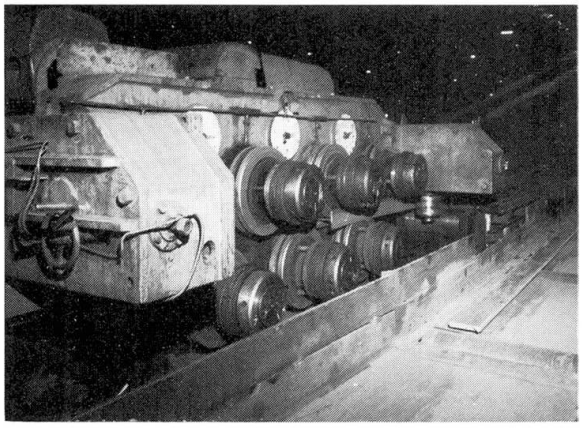

(a)

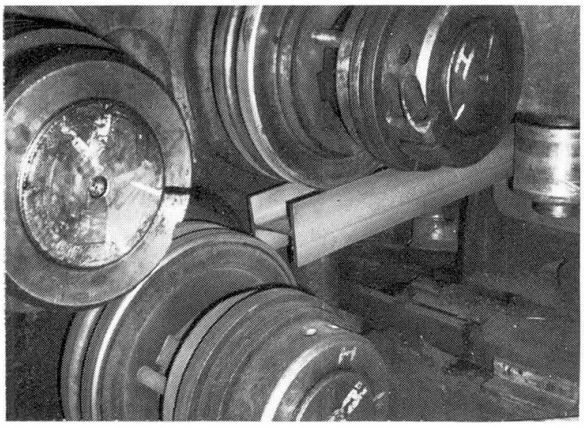

(b)

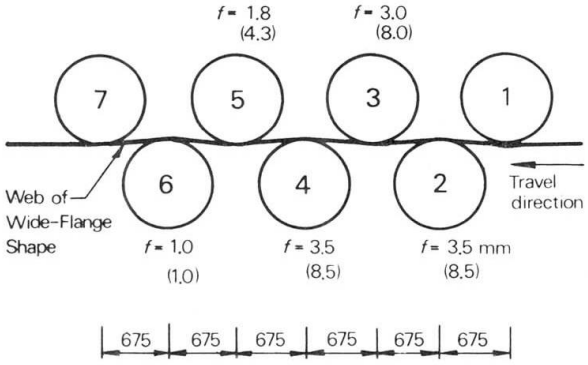

(c)

Fig. 1 Rotorizing. (a) Wide-flange shape HE 200 A entering the machine. The rollers above the beam are fixed, those below adjustable. (b) Detail at entering rollers. (c) Dimensions and deflections used in the experiments on HE 200 A shapes. Deflections in brackets are for modified rotorizing, see sec. 2.1.

constitute a large share of the total bulk of columns used in structures, the economical benefit from including the favorable effect of a controlled rotorizing should be substantial.

Stress data in the paper are given in the unit kp/mm^2, as used in the original reports. (1 kp/mm^2 = 9.81 MN/m^2 = 1.42 ksi.)

2. SYSTEMATIC EXPERIMENTS ON HE 200 A

2.1 Test Material

The systematic study was performed on a wide-flange shape type HE 200 A, corresponding roughly to a W 8x31. The test members were manufactured bythe Norrbottens Järnverk steel mills at Luleå, Sweden. The steel grade was SIS 1412, a semi-killed steel of IIW Quality B with a specified minimum lower yield stress of 26 kp/mm^2, a nominal tensile strength of 44 to 52 kp/mm^2, and a specified elongation of minimum 23 percent. All test material was taken from the same heat.

The test members were manufactured according to standard practice, except that they were subjected to three different controlled rotorizing procedures. One lot was rotorized in the normal production line, and one was taken twice through the rotorizing machine, using the same roller positions as in the normal production. Another member was straightened with modified adjustments of the rollers, the deflections of the member being approx. 2.5 times larger than in the normal production. The actual deflections at the various rollers are shown in Fig. 1 c. Finally, one lot of material was left as-rolled, that is, without any straightening, and serving as a reference to the rotorized material. In the following, these treatments will be referred to as "as-rolled", "normal rotorizing", "twice rotorizing", and "modified rotorizing". They represent gradually larger energy put into the member being rotorized. This is reflected also in the appearance of the mill scale of the flanges, see Fig. 2. The as-rolled member shown in Fig. 2 displays an undamaged mill scale whereas the number and extension of yield lines in the mill scale of the others is larger the more severely the member was rotorized.

All particulars relevant to the manufacture of test members were recorded and a detailed description may be found in Ref. 11.

Results of chemical analysis at 22 locations over four sections of the specimens and the chemical requirements are summarized in Table I. It may be noted that the variations in chemical contents are very small between the mill test analysis and the check analysis, over each section measured, and between the four sections measured. Thus the material may be considered homogeneous and differences in mechanical properties between the various sections, representing members subjected to different rotorizing procedures, must be attributed to other reasons than variations in chemical analysis.

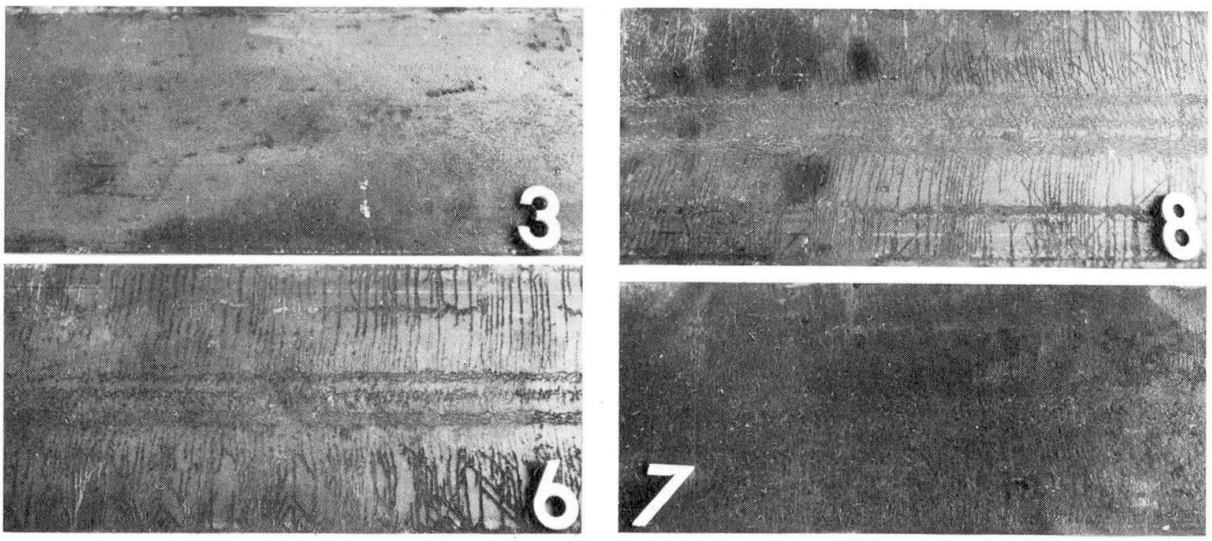

Fig. 2 Mill scale on flange outer surfaces of HE 200 A shapes. As-rolled ("3"), normal rotorizing ("6"), twice rotorizing ("8"), and modified rotorizing ("7").

The grain size was measured at various locations over the cross section of the HE 200 A test shape. The results were as could be expected from the cooling process. The flange tips and the thinner web, cooling faster than the juncture region between flanges and web, had an average grain size of approx. 16 μ, as compared to approx. 30 μ at the junctures.

Table II gives a summary of the test program on HE 200 A designed to determine mechanical properties, residual stresses, and column strength. The results will be discussed in the subsequent sections.

Table I Chemical analysis of test material, HE 200 A. Percent values given (see Fig. 2 for section codes)

Test	C	Si	Mn	P	S	N
Mill test analysis	0,16	0,06	0,94	0,023	0,030	0,006
Check analysis						
Sec. 3	0,16±0,01	0,06±0,00	0,97±0,03	0,022±0,002	0,026±0,003	0,009±0,001
Sec. 6	0,15±0,01	0,08±0,01	0,97±0,01	0,021±0,003	0,027±0,004	0,009±0,001
Sec. 7	0,16±0,01	0,07±0,01	0,99±0,01	0,023±0,001	0,029±0,002	0,008±0,001
Sec. 8	0,17±0,01	0,07±0,00	1,00±0,02	0,024±0,002	0,029±0,003	0,010±0,001
Average	0,16±0,02	0,07±0,02	0,98±0,05	0,023±0,004	0,027±0,005	0,009±0,002
SIS Spec. (SIS 1412)	max. 0,20	approx. 0,05	approx. 0,5-1,1	max. 0,05	max. 0,05	max. 0,009

Table II Summary of mechanical tests on HE 200 A

Roller-straightening procedure	No. of tensile specimens	No. of residual-stress sections	No. of stub columns	No. of columns $\frac{L}{r} = 60$	No. of columns $\frac{L}{r} = 90$
As-rolled (A)	13	1	2		4
Normal rotorizing (N)	13	1	2	1	4
Twice rotorizing (T)	13	1	2		1
Modified rotorizing (M)	13	1	1		1
Total	52	4	7	1	10

2.2 Tensile-Specimen Tests

A total of 52 tensile-specimen tests were made on HE 200 A shapes, representing various locations over the cross section of the four test groups. The results are summarized in Fig. 3. All specimens were flat, and tested at a strain rate corresponding to max. 1 kp/mm^2-s in the elastic range. The lower yield stress R_{eL}, as defined by ISO [15], the tensile strength R_m, both in kp/mm^2, and the elongation A_5 in percent are given.

The variation of lower yield stress in the as-rolled member is compatible with the measured variation of grain size, that is, the flange tips and the web displays a yield stress which is about 9 percent higher than in the interior of the flange. This is a result of the cooling behavior since no systematic differences could be detected in the chemical contents, see Table I. Similar results were obtained for the rotorized members. This is consistent with previous results obtained on as-rolled members [16].

For the rotorized members there is a tendency of increasing yield stress and decreasing elongation values with increasing rotorizing work. This may be observed in Table III which gives different average values of the individual data values from Fig. 3. Thus, the lower yield stress of the member exposed to modified rotorizing is about 7 percent above that of the as-rolled member. The reduction in elongation is much greater than could be predicted from the strains occuring at straightening, probably because of strain aging. Thus, the ductility requirements will pose a limit to the straightening work that can be used in practice.

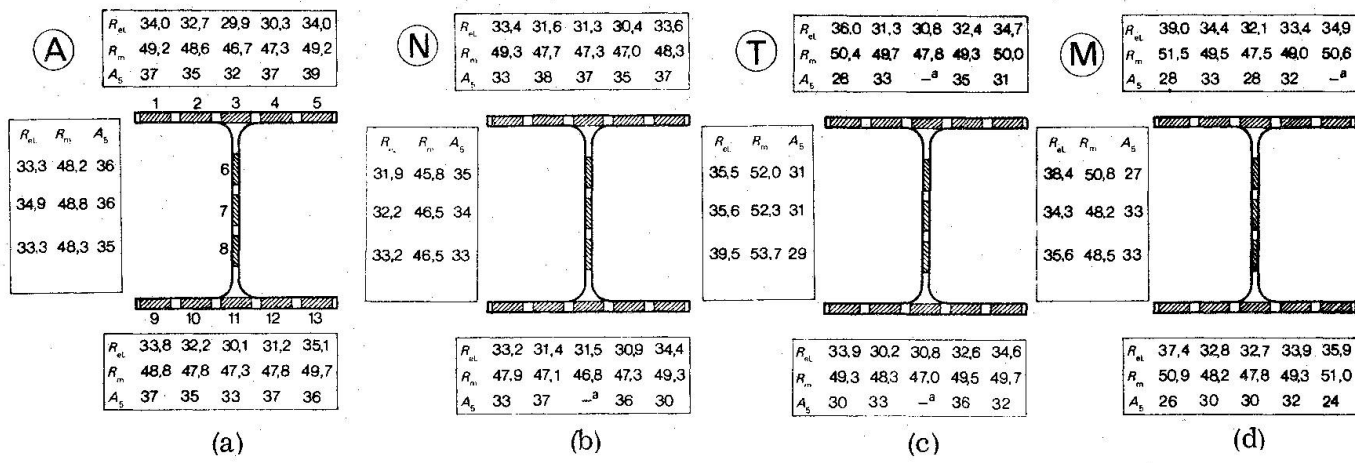

Fig. 3 Results of 52 tensile-specimen tests on HE 200 A shapes being (a) as-rolled and subjected to (b) normal rotorizing, (c) twice rotorizing, and (d) modified rotorizing. The symbol "a" denotes fracture outside gage length.

Table III Average values of tensile-specimen data of Fig. 3. Values given are average of all specimens at each section ("total"), of specimens at flange tips, and of specimens in remaining cross section ("interior")

Roller-straightening procedure	Lower yield stress R_{eL}, kp/mm^2				Tensile strength R_m, kp/mm^2			Elongation A_5, percent		
	Total	Relative to A	Flange tips	Interior	Total	Flange tips	Interior	Total	Flange tips	Interior
As-rolled (A)	32.7	1.00	34.2	32.0	48.3	49.2	47.8	36	37	35
Normal rotorizing (N)	32.2	0.98	34.4	31.6	47.4	48.7	46.9	35	33	36
Twice rotorizing (T)	33.7	1.03	34.8	33.2	49.9	49.8	50.0	32	30	33
Modified rotorizing (M)	35.0	1.07	36.8	34.2	49.4	51.0	47.6	30	26	31

No indications of detrimental Bauschinger effects could be observed in the test results. The yield stress at the flange tips of both sides of the cross section is always higher than in the interior of the flanges.

Strain-hardening properties were not recorded for this series of tensile specimen tests on HE 200 A shapes. Such properties were measured in several specimens from two cold-straightened sections of HE 200 B [10]. It is difficult to compare these results with previous strain-hardening data on as-rolled members because many different definitions have been used in the literature [17]. It is, however, interesting to note that the material, including that from the flange tips, exhibits the usual behavior with an upper yield point and a marked yield plateau. The length of the yield plateau, as measured by the strain ϵ_{sh} at onset of strain-hardening, is approx. 19 ϵ_y (where ϵ_y = strain at first yield) for specimens taken from the flange tips affected most by the cold-straightening, and approx. 15 ϵ_y for specimens from the remaining cross section. These observations do not support the mechanical model used in the literature for representing the material behavior in loading and unloading to yield [18, 19]. According to that model, the yield plateau would occur only in material that is virginal (no yielding) in a particular strain direction.

Furthermore, the strain-hardening data from cold-straightened HE 200 B sections indicated no significant difference between the strain-hardening modulus E_{st} of the flange tips and that of the remaining cross section. Thus, the reduction of E_{st} due to roller-straightening to between 10 and 28 percent of E_{st} of the virgin material, as anticipated in studies of the effect of rotorizing on the inelastic behavior of beams [18], appears much exaggerated judging from the present data. The average strain-hardening modulus, defined as the secant to the stress-strain curve at strains ϵ_{sh} and 4 percent, is about 300 kp/mm^2 or E/70. Measured over the strain range ϵ_{sh} to (ϵ_{sh} + 0.002), the average E_{sh} value obtained for the HE 200B shape is 590 kp/mm^2 or E/36. This is within the range of E/45 to E/35 reported in the literature for as-rolled structural carbon steels [18,20, and others]. The experimental scatter obtained with the latter definition of E_{st} is so large that there would be no point in comparing values at different locations over the cross section etc.

2.3 Residual-Stress Measurements

Longitudinal residual stresses were measured using a sectioning method. The released strains were recorded with a mechanical extensometer of 165 mm gage length. The total number of measured points, each consisting of two gage marks, was 98 for each cross section. The accuracy in the measured stress was estimated to ± 1 kp/mm^2 [10]. This includes the thermal and mechanical effects of carefully cold-sawing the cross section into strips. Localized residual stresses at cold-sawn surfaces were measured by X-ray diffraction technique for the purpose of estimating this source of error [10].

Figures 4, 5, 6, and 7 show the measured residual-stress distributions in the as-rolled HE 200 A member, and those subjected to normal rotorizing, twice rotorizing, and modified rotorizing, respectively. All residual-stress diagrams are plotted with tension towards the cross section. Open points are measured values at the near surface, solid points at the far surface.

The residual stresses in the as-rolled member, Fig. 4, are distributed with -12 kp/mm^2 in compression at flange tips and -14 kp/mm^2 at the web center. The compressive stresses are balanced by tension in the remainder of the cross section. This stress distribution is typical for the thermal stresses resulting from a free cooling [4]. The residual stresses obtained on both sides of each sectional element are very close, the difference being less than 3 kp/mm^2. The stress at the outside of the flanges is generally about 2 kp/mm^2 below the corresponding inside stress (sign included). While this does not reveal the true through-thickness variation, the fact that the two sides follow each other closely is a good indication of the accuracy of the measurements.

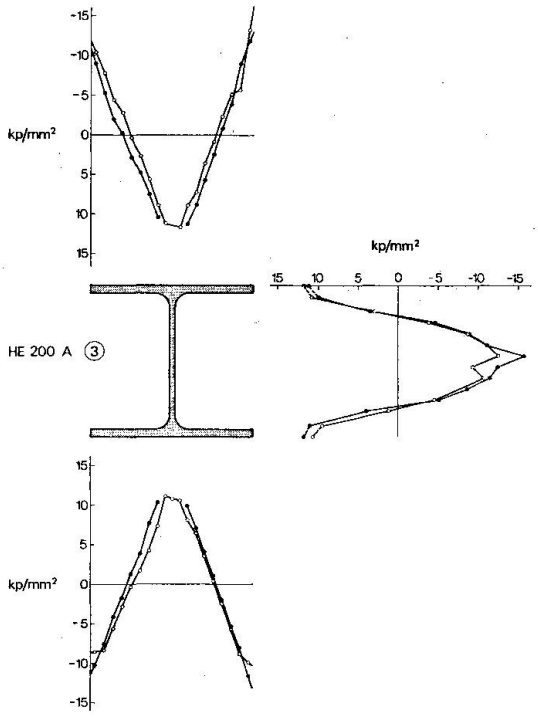

Fig. 4 Residual stresses in an as-rolled HE 200 A shape

Fig. 5 Residual stresses in an HE 200 A shape rotorized in normal production

The member rotorized in the production exhibits a completely different distribution, Fig. 5. Although there is still a tendency of compression towards the flange tips and tension in the flange centers, the distribution is more irregular and the stresses are much smaller. There is a large variation across the flanges, the difference being

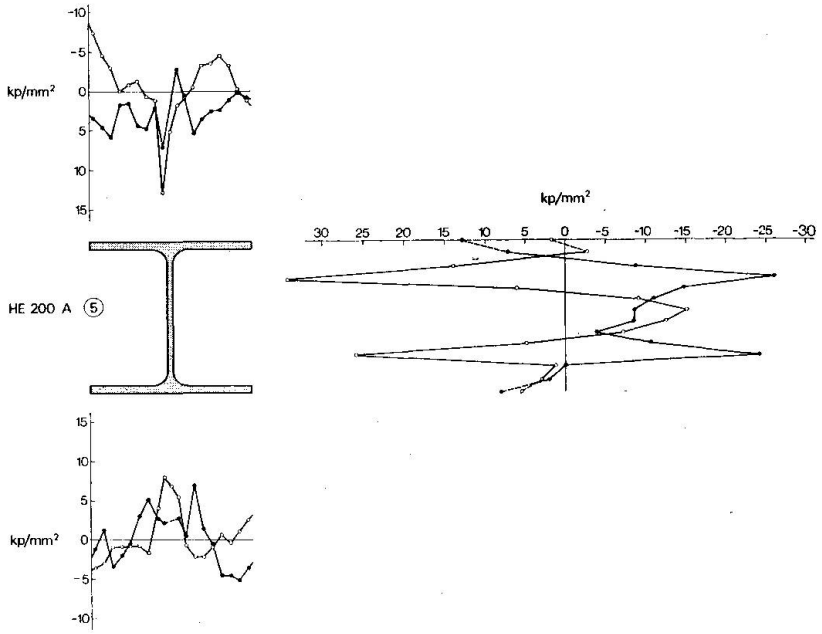

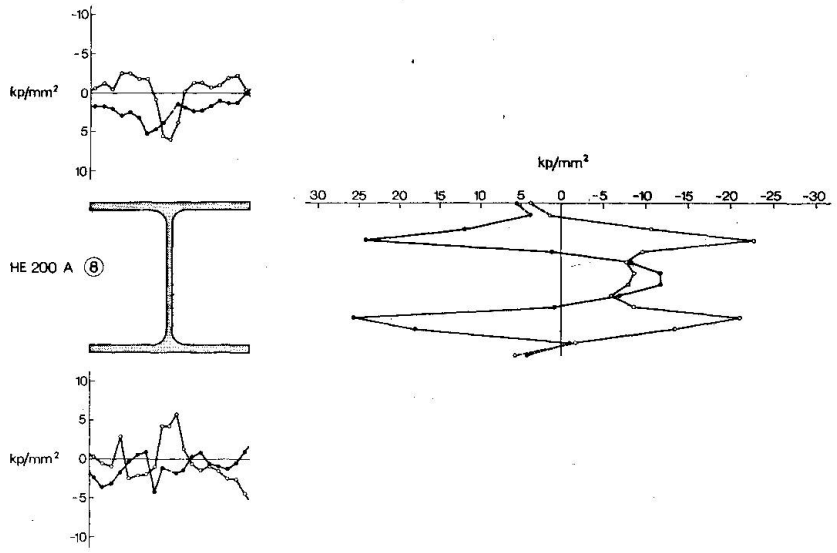

Fig. 6 Residual stresses in an HE 200 A shape rotorized twice

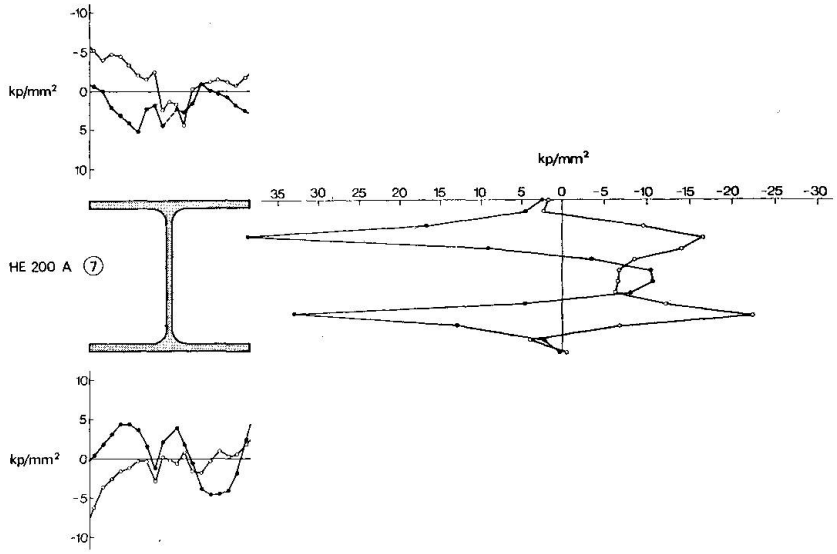

Fig. 7 Residual stresses in an HE 200 A shape rotorized using a modified procedure with larger deflections than in normal production

up to 10 kp/mm^2. This variation is still larger in the web, where differences of up to 60 kp/mm^2 were obtained locally, near the fillets at the flange-web junctures. These stress peaks at yield level result from the local load effects under the rollers in the rotorizing machine.

The residual-stress distribution in the member rotorized twice, Fig. 6, resembles that of Fig. 5. The residual stresses in the flanges have been further smoothened out. The stress in all measured flange points falls between -5 and +6 kp/mm^2. A similar distribution was obtained in the member which was rotorized using larger deformations, see Fig. 7. The stress peaks in the web are at approx. 36 kp/mm^2, to be compared with the recorded lower yield stress of 37 kp/mm^2, see Fig. 3.

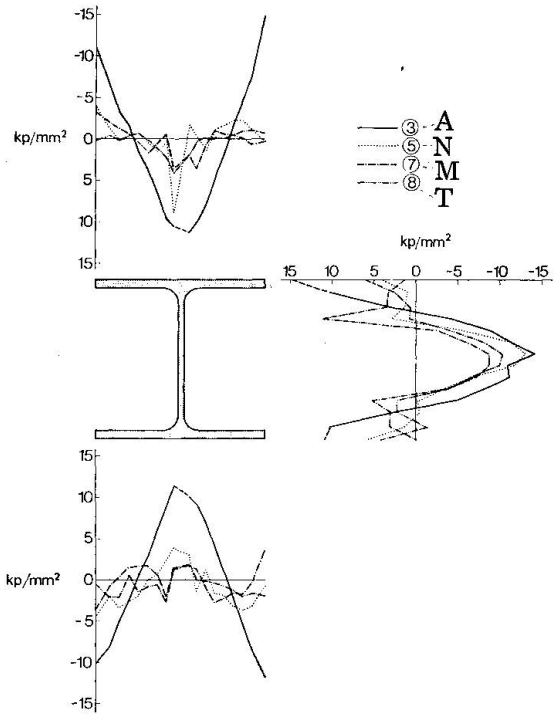

Fig. 8 Residual stresses in HE 200 A shapes. Average stresses across thickness

It is interesting to note that, although the rotorizing procedures used are drastically different, the residual-stress distributions at large in the three rotorized members, Figs. 5 through 7, are quite similar. This is even more evident if average stresses over the thickness are considered as in Fig. 8. When compared with the residual stresses in the flanges of the as-rolled member, the rotorized flange stresses are almost negligible. The average stresses in the web are less affected by the rotorizing as may be seen in Fig. 8. This is because the web is close to the neutral axis in minor axis bending.

2.4 Column Tests

The extent of the experimental program for testing rotorized HE 200 A columns is shown in Table II. A total of 18 columns were tested, of which seven were stub columns, one was a full-length column with a slenderness ratio of 60, and ten were full-length columns with a slenderness ratio of 90. The purpose of the stub columns was to determine the overall material strength in compression. The slenderness ratio of 90 for most columns was chosen to allow comparisons with previous column-test results [21].

All columns were tested in a universal testing machine of 400 Mp capacity. The columns were fully instrumented. The column testing followed the procedure suggested in Ref. 22. Both "statical" and "dynamical" recordings were taken. The details relevant to the columns tests are given in Ref. 11.

Figure 9 shows stress-strain curves from the stub columns. An average curve was drawn when more than one stub column was tested for each rotorizing procedure. The values given in Fig. 9 are the "static" yield stress level at 0.5 percent strain.

It may be noted that local buckling started on the yield plateau at approx. 0.7 percent strain with some variation. The actual b/t ratio of the flanges is 21 (nominally 20). In one stub column, buckling started even before the yield stress was reached. Thus, the maximum stress attained in the stub columns is not much higher than the yield stress. Table IV summarizes the test results of the stub columns. The yield stress level is increased by 14 percent for a modified rotorizing as compared to the as-rolled member. This is about twice as much as obtained in the tensile specimen tests, see Table III. When comparing the tensile specimen properties in Fig. 3 and Table III with the yield properties in compression in Table IV, it should be kept in mind that the latter are "static" values obtained at a negligible strain rate (see also Fig. 9) whereas the tensile specimens were tested at a strain rate of the order of 1 kp/mm^2-s (see Sec. 2.2).

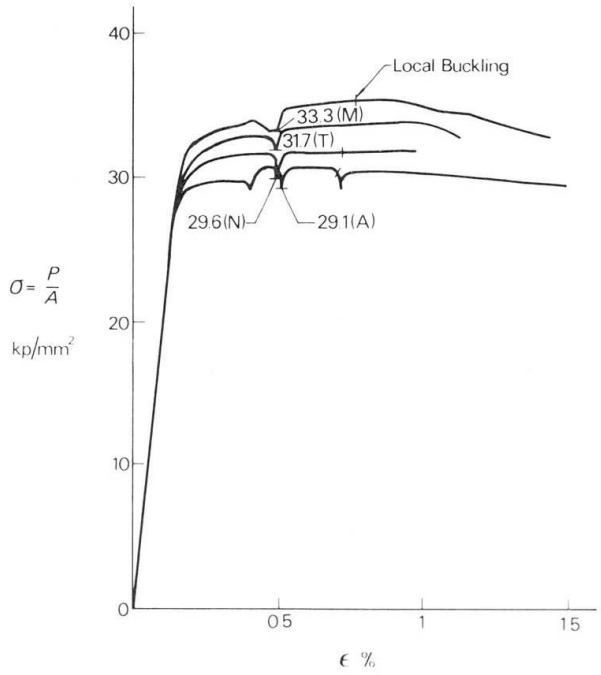

Fig. 9 Stress-strain curves from stub columns. Curves and values shown are average for stub columns with same rotorizing procedure

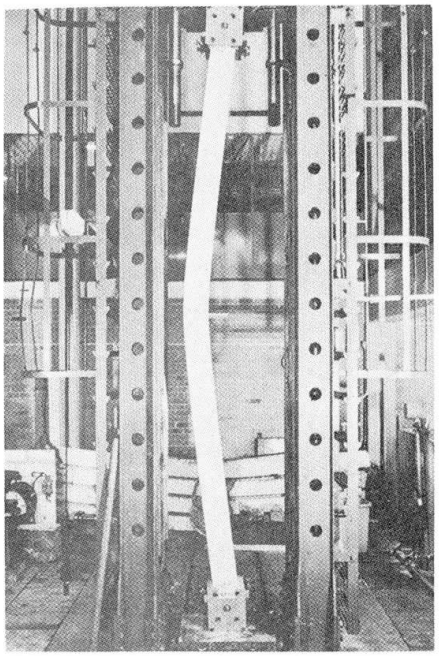

Fig. 10 Column with slenderness ratio of 90 in testing machine

Table IV Stub-column test results (average where more than one stub column was tested)

Roller-straightening procedure	Static yield stress level		Maximum stress	
	kp/mm^2	Relative to A	kp/mm^2	Relative to A
As-rolled (A)	29.1	1.00	31.2	1.00
Normal rotorizing (N)	29.6	1.02	31.9	1.02
Twice rotorizing (T)	31.7	1.09	33.8	1.08
Modified rotorizing (M)	33.3	1.14	35.3	1.13

For a perfectly concentric loading of a stub column with constant strain over the cross section and along the column, the difference between the yield stress level and the proportional limit of the stress-strain curve should equal the maximum compressive residual stress in the column. There appears to be no such correlation between the maximum compressive stresses in Figs. 4 to 7 and the stress-strain curves of Fig. 9. The reason for this is that it was not possible to maintain a perfectly concentric loading, probably because of the thin cross-sectional elements and the effect of early onset of local buckling.

The full-length columns were tested with pinned-end conditions and end rotations permitted about the minor axis. Twisting of the ends was prevented by friction in the cylindrical bearings. Figure 10 shows a column in the testing machine at a late stage of buckling. All columns failed in plane buckling about the minor axis. No appreciable cross-sectional rotation was observed in the test columns, in spite of the fact that residual stresses in the rotorized members were non-symmetrical and, for some columns, the initial deflection of the two flanges were in opposite directions.

A summary of the column test results for slenderness ratio 90 is given in Fig. 11. The static maximum stress obtained is plotted against the equivalent initial deflection of the column. This corresponds to the maximum deflection of a sine curve equivalent with the actual initial deflection. It may be noted in Fig. 11 that the rotorizing results in a 10 to 15 percent increase in column strength for this slenderness ratio. There appears to be no large difference between the normal rotorizing and the member rotorized twice or by a modified procedure. Since only one column each was tested for these latter groups, and because the initial deflection of the column with modified straightening was much larger than for all other columns, no definite conclusions may be drawn as to the effectiveness of various rotorizing procedures. It should also be borne in mind that all columns were of one slenderness ratio only. Further discussion will follow below in connection with theoretical column strength predictions.

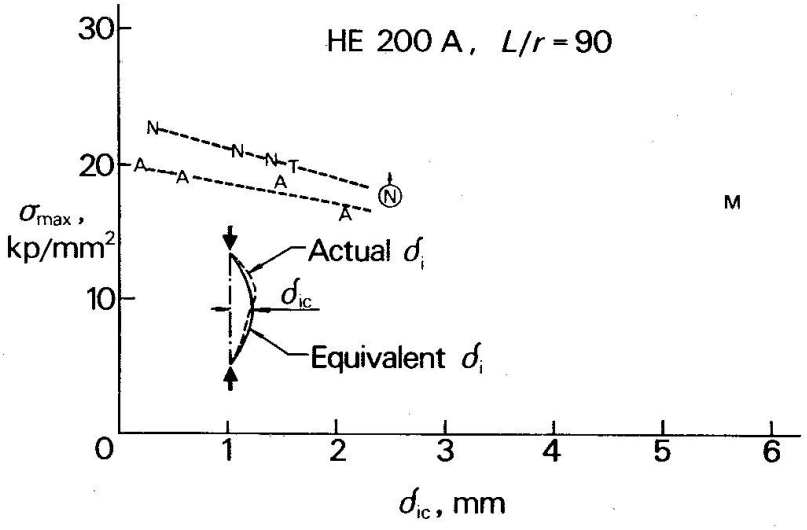

Fig. 11 Summary of test results for columns with slenderness ratio of 90

3. THEORETICAL PREDICTIONS OF RESIDUAL STRESSES AND COLUMN STRENGTH OF ROTORIZED HE 200 A

3.1 Predicted residual stresses in as-rolled HE 200 A

The thermal residual stress distribution in as-rolled shapes may be predicted using a theoretical model to represent the temperature and thermal strain history during cooling on the cooling bed in the steel mill. The simulation model has been described in detail elsewhere [4, 23, 24]. The numerical analysis was performed in a computer.

A calculated thermal-stress distribution is given in Fig. 12. The distribution is to be compared with the measured distribution in Fig. 4. The difference in stress level at the flange-web junctures is due to the effect of the fillet areas not included in the theoretical calculations. For the HE 200 A shape as much as 5 percent of the total cross-sectional area is located in these fillet areas. The residual-stress distribution representing the inside of the flanges is about 2 kp/mm^2 below that of the outside, as was obtained also in the measurements, Fig. 4.

3.2 Predicted residual stresses in rotorized HE 200 A

The mechanical behavior in rotorizing H-shapes was simulated theoretically. A specific purpose was to allow a better understanding of the process and the possible effects of different variables. Furthermore, the calculations were intended to facilitate the interpretation of experimental measurements.

The member was treated as a continuous beam loaded and supported by the straightening rollers, as shown schematically in Fig. 13. Each concentrated load shown in Fig. 13 is actually two concentrated loads closely spaced in such a manner as to achieve a constant moment over the contact surface of each roller. A more detailed account of the calculations is given in Ref. 12.

Several assumptions were made in the simulations:

- Only minor axis bending was considered. Although the principal straightening action is about the minor axis, only small moments need be applied about the major axis to achieve a definite straightening effect because the cross section yielding for minor axis bending produces only slight resistance to major axis bending.

- Plane sections are assumed to remain plane during deformation in the elastic as well as the elastic-plastic region. In actual rotorizing the local loads at rollers will cause deviations from the assumed action. Furthermore, large strains and deformations due to initiated local buckling of compressed flanges may give similar effects.

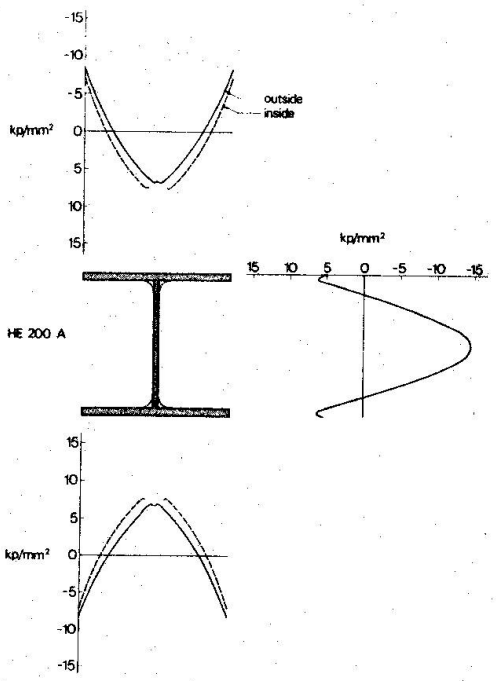

Fig. 12 Thermal residual stresses in as-rolled HE 200 A as calculated from the cooling behavior

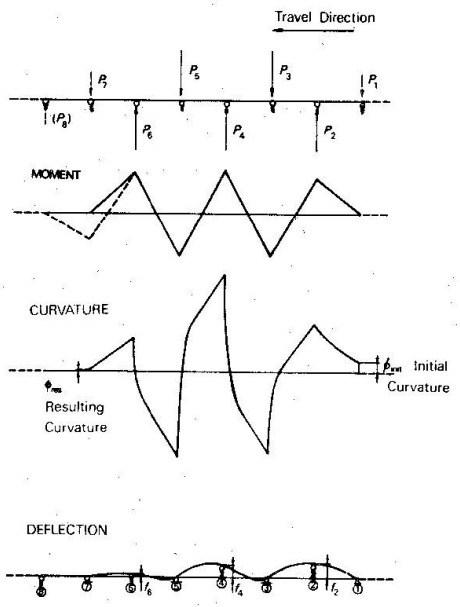

Fig. 13 Calculation of moments, curvatures and deflections in a rotorizing procedure (schematic)

- Only longitudinal stresses are considered. Transverse stresses are, however, created by the concentrated loads from the rollers, and they affect in reality the yield conditions at the sections under the rollers.

- Effect of shear deformations are neglected.

- The material behavior is represented by a mechanical model shown in Fig. 14, as used previously in the literature [18,19]. It was noted above that the tensile-test results did not support some implications resulting from this model. For this reason the Bauschinger effect was neglected in the simulations, that is, R^{*}_{eL} was assumed equal to R_{eL}. The stress-strain relationship in the strain-hardening range was assumed to follow the well-known Ramberg-Osgood equation

$$\epsilon - \epsilon_{sh} = \frac{\sigma - R_{eL}}{E_{sh}} + K \left(\frac{\sigma - R_{eL}}{E_{sh}} \right)^{m}$$

The following coefficients were used, and assumed constant over the cross section:

$E = 21\,000$ kp/mm^2 $\qquad$ $\epsilon_{sh} = 1{,}4$ %

$R_{eL} = (R_{eH}=)\ 32.7$ kp/mm^2 $\qquad$ $K = 21$

$E_{sh} = 600$ kp/mm^2 $\qquad$ $m = 2$

The number of numerical operations involved in the calculations is tremendous, in spite of the simplifying assumptions noted above. The structure is highly statically

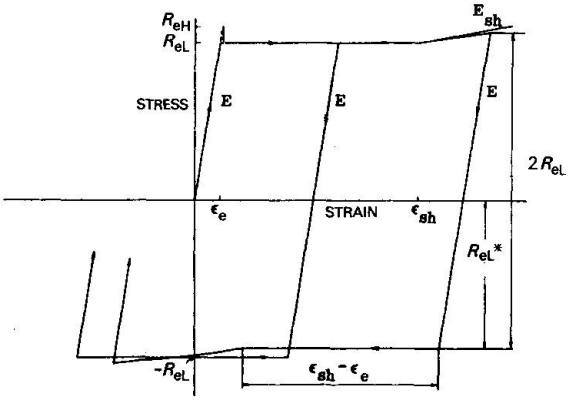

Fig. 14 Stress-strain relationship for yielding and strain-hardening alternating in tension and compression

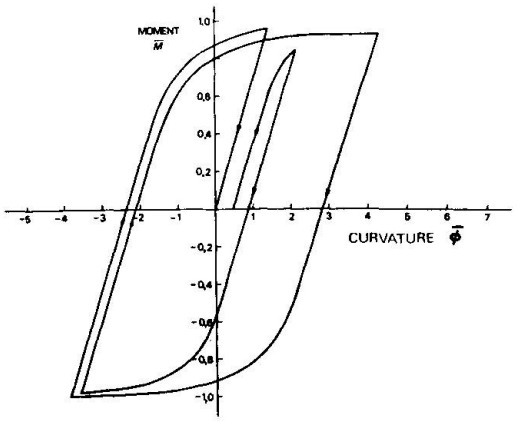

Fig. 15 Typical moment-curvature history as calculated for a simulated rotorizing

indeterminate and the moment-curvature relationship at each point is affected by the complete loading history at previous positions. Since loads are controlled by deflections, this means that all variables are highly interrelated in a complicated way. The problem was solved by an iteration procedure in a computer. Because of all assumptions involved, the simulations must be regarded as qualitative only.

A typical simulated moment-curvature history for a particular cross section moving through the rotorizing machine is shown in Fig. 15. The initial residual stresses were those obtained in measurements on the as-rolled HE 200 A, see Fig. 4. The initial curvature was about 0.5 ϕ_y, where ϕ_y is the curvature which corresponds to attainment of the yield strain ($= R_e/E$) at the extreme fibers. This curvature is of the order of 10 times larger than allowed in mill tolerances on straightness.

Three different rotorizing procedures were simulated. These correspond to three levels of rotorizing work termed a "weak", a "normal", and a "heavy" rotorizing. The deflected curves from the simulations are shown in Fig. 16. The weak and the normal rotorizing do not produce any strain-hardening. In the heavy rotorizing, the maximum strain was approx. 2.3 percent. From a comparison with Fig. 1 c it is noted that the "normal" and the "heavy" simulated rotorizing relate to the "normal" and the "modified" rotorizing in the experimental study.

Figure 17 shows residual-stress distributions resulting from the three simulated rotorizing procedures. It may be noted that all flange distributions in rotorized members are similar in nature, but quite different from that of the as-rolled

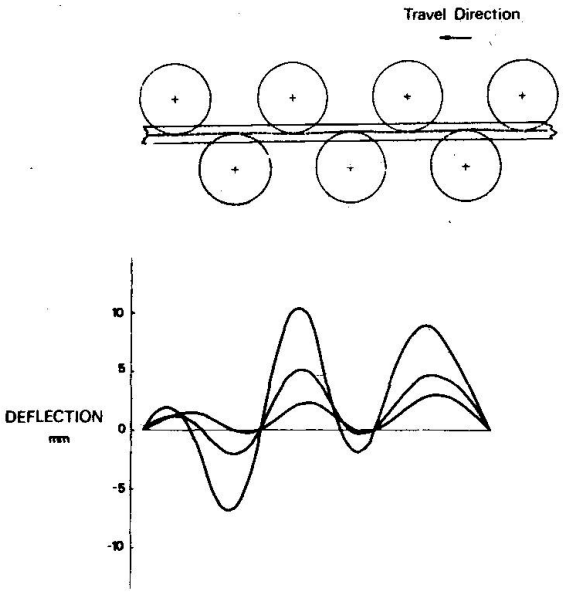

Fig. 16 Deflected curves in simulated rotorizing

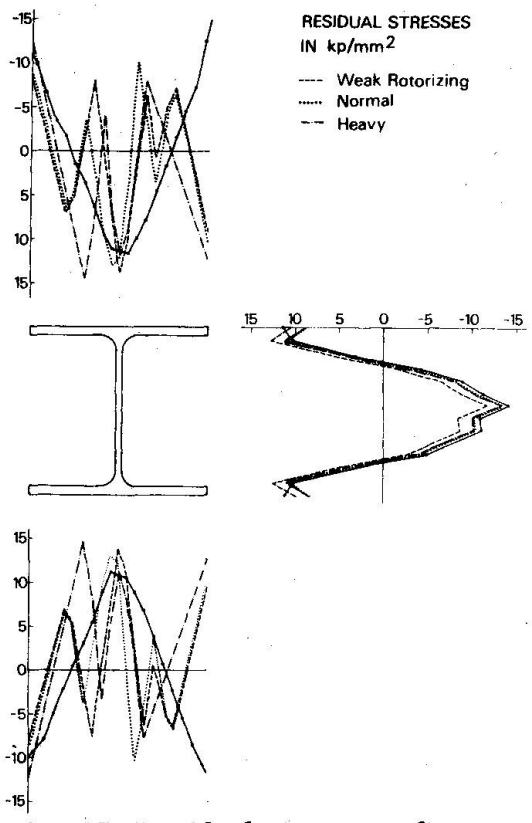

Fig. 17 Residual stresses after simulated rotorizing at three levels as shown in Fig. 16

member. The rotorizing has almost no effect on the distribution of average residual stresses in the web. All this was noted from the experimental results also, see Fig. 8. The magnitude of the stress peaks in the flanges of the members subjected to simulated rotorizing is, however, larger than encountered in the experimental results. Thus, the actual rotorizing is more efficient in breaking down the thermal residual stresses than theoretical simulations based upon beam action of the rotorized member. A better agreement between test and theory might be achieved by superimposing the local effects under the rollers, including transverse stresses.

No increase in yield stress could be expected from the simulated rotorizing of "weak" and "normal" magnitude since no strain-hardening occured. The maximum strain of 2.3 percent in the "heavy" simulated rotorizing corresponds to an increase of 4.7 kp/mm^2 in the yield stress of the extreme fiber. At the location of tensile test specimens in the outer flanges, see Fig. 3, the increase in yield stress is between 2 and 3 kp/mm^2. These results are all in agreement with the experimental results: no increase in yield stress of the normally rotorized member was observed, whereas the yield stress increased by 2.6 kp/mm^2 at the outer flange specimens for modified rotorizing. The simulated data may explain partially why the stub column subjected to a modified rotorizing had a larger incrase in yield stress than the average of tension specimens -- these did not represent the flange tips with the highest increase from the simulated rotorizing. (The reduced gage section of the tension specimens is smaller than the gross sections indicated in Fig. 3).

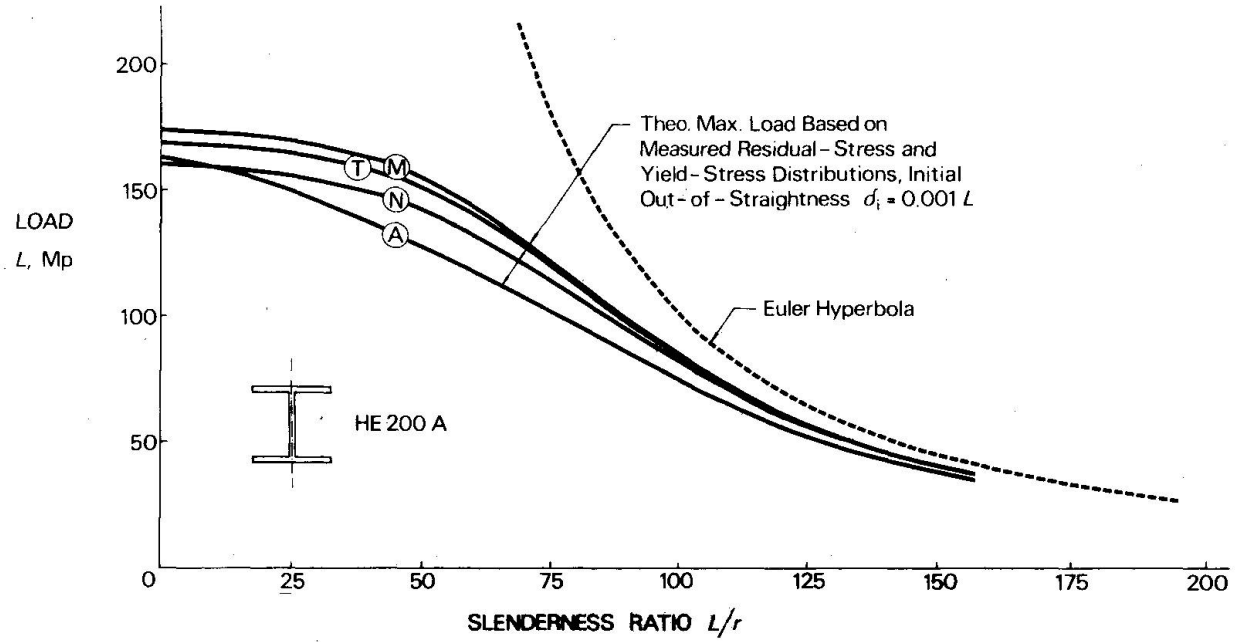

Fig. 18 Maximum strength curves from simulated column tests including measured residual stresses, yield stresses from tension-specimen tests, and initial deflection of 0.001 L

The simulated rotorizing can not explain why the mechanical properties of the interior of the section are affected as shown in Table III, nor can it explain the marked effects on the tensile strength and the elongation values -- the reduction in elongation due to different rotorizing procedures, being up to 9 percent in the flange tips for modified rotorizing, is several times larger than expected from the assumed mechanical model for material behavior. A better correspondence in some respects may be obtained by including the local loading effects.

3.3 Predicted column strength of rotorized HE 200 A

The mechanical behavior of rotorized columns was simulated using a maximum ("ultimate") strength approach. The numerical method used will be described elsewhere [25], but is similar in principle to other methods available in the literature [26]. A tangent modulus approach could not be used since the tangent modulus load is not defined for non-symmetrical residual stresses. The computer program includes the effects of non-symmetrical residual stresses, variable yield stress, irregular out-of-straightness, and end eccentricities. Plane buckling was considered, as was also encountered in the column tests (see Sec. 2.4).

Figure 18 shows maximum strength curves for simulated column tests about the minor axis of members subjected to the four rotorizing procedures of the experimental study. The curves were based on measured residual stresses, yield stress data from the tension-specimen tests (the stub-column data were not available when the simulations were made), measured cross-sectional dimensions (the actual area was about 5 percent less than the nominal area), and an assumed initial sine

curvature with a mid-height deflection of 0.001 L. The actual initial out-of-straightness was not used here because the intention was to separate the effects of residual stresses and yield stress on column strength.

From a comparison of the curves in Fig. 18 it may be noted that the rotorizing increases the simulated column strength by 10 to over 20 percent in the important range of slenderness ratios of 40 to 100. The increase for the larger slenderness ratios in this range is primarily due to the redistributed residual stresses, whereas the effect at lower slenderness ratios is primarily due to the magnitude of yield stress. At $\frac{L}{r}$ equal to 90 the predicted increase in column strength is between 10 and 14 percent, depending upon the rotorizing procedure. This increase, and the rotorized column curves being very close in this slenderness range, are in agreement with the experimental column test results as summarized in Fig. 11.

4. CONCLUSIONS AND SUMMARY

From the systematic experimental study of HE 200 A columns and observations of residual stresses and mechanical properties in sveral other cold-straightened members, as described in several reports [10 through 14] and summarized in this paper, the following conclusions may be drawn.

1. Residual stresses in the flanges of wide-flange shapes are completely redistributed by a rotorizing procedure. Theoretical simulations indicate that only small plastic deformations in the rotorizing are necessary to achieve this end. It appears that a "heavier" rotorizing, with larger deflections of the member, will improve the residual-stress distribution further, however this effect is only marginal. The effect of rotorizing on residual stresses in the flanges appears more favorable than predicted by theory. This is probably due to local loading effects under the straightening rollers.

2. Rotorizing may affect the tensile properties by increasing the yield stress and the tensile strength and reducing the ductility (measured as elongation). Theoretical simulations indicate that a fairly heavy rotorizing is necessary to produce definite strain-hardening effects. The experiments show that, indeed, a heavy rotorizing produces an increased yield stress of 7 percent, but the effect is obtained over a much wider area than predicted from simulations. This is probably due to local loading effects under the straightening rollers.

3. The strain-hardening properties measured in some cold-straightened shapes are not much different from those reported in the literature for as-rolled material. The commonly accepted mechanical model for material behavior would predict the yield plateau to be reduced or wiped out completely by the cold-straightening, depending upon the maximum strain in the straightening process. For sufficiently large strains produced in the straightening, that is, strains larger than ϵ_{st}, also the strain-hardening modulus would be reduced. The measured data contradict this altogether -- the flange tips being mostly affected by the straightening moments show in fact a somewhat longer yield plateau

and about the same strain-hardening modulus as the interior of the flange. The measured behavior could be the result of strain-aging effects. More data would be necessary to draw any general conclusions regarding the strain-hardening properties of rotorized members.

4. Stub column tests on HE 200 A shapes indicate that the improvement in compressive yield strength due to a rotorizing operation is even greater than obtained in the tensile specimen tests. The improvement in static yield stress level is 2, 9, and 14 percent for the normal rotorizing, twice rotorizing, and modified rotorizing, respectively. Due to a large width-over-thickness ratio of the HE 200 A test specimens ($\frac{b}{t} = 21$), the stub columns start to buckle locally at relatively small strains and the maximum stress exceeds the static yield stress by less than 10 percent.

5. All full-length columns tested fail in plane buckling about the minor axis. (The end fixtures used permit end rotations about the minor, but not the major axis.) The column tests for slenderness ratio 90 show that rotorizing increases the maximum column strength by 10 to 15 percent. Theoretical simulations based upon measured residual stresses and mechanical properties support this result. From the simulations it is clear that even greater improvements are obtained at lower slenderness ratios -- well over 20 percent increase in column strength for slenderness ratios in the range 40 to 70 may be obtained from a suitable rotorizing procedure.

The column tests were performed on only one shape, the HE 200 A. However, the important variables affected by the rotorizing, that is, the residual-stress and the yield-stress distributions, have been studied in supplemental tests on several other shapes in the research program [4, 10, 12, 13, 14]. These supplemental tests were performed on as-delivered members taken from local material suppliers. Further results of residual-stress measurements are available in the literature [2, 3, 5, 6, 7, 8, 9]. All these measurements show clearly that rotorizing efficiently redistributes the unfavorable thermal residual stresses of as-rolled shapes.

Since rotorizing is used to straighten all small to medium-size shapes in the production line at modern steel mills, exploiting the favorable effects on column strength does not need any new equipment or any new operations. The necessary extra control of the rotorizing effects at the mill would require only a visual inspection of the yield line pattern on the flanges.

The theoretical and experimental research described in the paper may also be used to optimize the rotorizing operation. Today the rotorizing appears to be a subjective trial-and-error process guided only by the experience of the personnel involved in the operation.

It is suggested that the improved column strength of rotorized rolled members be considered in the scheme for assigning proper column curves if a multiple column curve system be adopted. Since rolled and rotorized columns constitute a large share of the total number of columns used in structures, the economical benefit from including this effect should prove substantial.

5. REFERENCES

1. A. Wöhler: "Versuche zur Ermittlung der auf die Eisenbahnwagen-Achsen einwirkenden Kräfte und der Widerstandfähigkeit der Wagen-Achsen". Zeitschrift für das Bauwesen 10, 1860, p. 583.

2. A.W. Huber: "The influence of residual stress on the instability of columns". Ph.D. Diss., Lehigh University, 1956.

3. A. Nitta & B. Thürlimann: "Ultimate strength of high-yield strength constructional-alloy circular columns - Effect of cold-straightening". IABSE Publications 22, Zürich 1962, pp. 265 to 288.

4. G. Alpsten: "Egenspänningar i varmvalsade stålprofiler" ("Residual stresses in hot-rolled steel profiles"). Dissertation, Institution of Structural Engineering and Bridge Building, Royal Institute of Technology, Stockholm, June 1967.

5. F. Frey: "Effet du dressage à froid des profilés laminés en double té sur leur force portance". IABSE Publications 29-II, Zürich 1969, pp. 101 to 123.

6. C.H. Yang, L.S. Beedle & B.G. Johnston: "Residual stress and the yield strength of steel beams". Welding Journal 31, 1952,pp. 205-s to 229-s.

7. J.A. Yura: "The strength of braced multi-story steel frames". Report No. 273.28, Fritz Engineering Laboratory, Lehigh University, Sept. 1965.

8. P.F. Adams, M.G. Lay & T.V. Galambos: "Experiments on high strength steel members". Welding Research Council, Bulletin No. 110, Nov. 1965.

9. J. Brozzetti, G.A. Alpsten & L. Tall: "Residual stresses in a heavy rolled shape 14WF730". Report No. 337.10, Fritz Engineering Laboratory, Lehigh University, Febr. 1970.

10. G.A. Alpsten: "Egenspänningar och materialhållfasthet i kallriktade bredflänsprofiler" ("Residual stresses and mechanical properties of cold-straightened H-shapes"). Jernkontorets Annaler, Stockholm 154, Aug. 1970.

11. O. Ersvik & G.A. Alpsten: "Experimentell undersökning av knäckhållfastheten hos bredflänsprofiler HE 200 A riktade på olika sätt" ("Experimental investigation of the column strength of wide-flange shapes HE 200 A roller-straightened in different ways"). Report 19:3, Swedish Institute of Steel Construction, Stockholm, Dec. 1970.

12. G.A. Alpsten: "Egenspänningar och töjhärdningseffekter i kallriktade bredflänsprofiler" ("Residual stresses and strain-hardening properties of cold-straightened wide-flange shapes"). Paper presented at the Scandinavian Research Conference on Steel Construction, August 1970. Published in Report R39:1971, National Swedish Council for Building Research, Stockholm, pp. 25:1 to 25:18.

13. G.A. Alpsten & G. Appeltofft: "Egenspänningar i några tunnväggiga svetsade och valsade I-balkar" ("Residual stresses in some welded and rolled light I-beams"). Report 35:3, Swedish Institute of Steel Construction, Stockholm, Dec. 1972.

14. G.A. Alpsten: "Egenspänningar i ramstångsprofil till järnvägsbromateriel 3" ("Residual stresses in the chord member of railroad bridge matériel"). Report A:FA 6130:15, Försvarets Materielverk, Stockholm, In Preparation.

15. ISO: "Steel - Tensile testing". Draft International Standard ISO/Dis 82, 1972.

16. L.S. Beedle & L. Tall: "Basic column strength". Proc. ASCE 86, 1960, pp. 139 to 173.

17. G.A. Alpsten: "Variations in mechanical and cross-sectional properties of steel". Proc., state-of-art report 9:1, International Conference on the Planning and Design of Tall Buildings, Lehigh University, Aug. 1972.

18. P.F. Adams & T.V. Galambos: "Material considerations in plastic design". IABSE Publications 29-II, 1969, pp. 1 to 18.

19. M.G. Lay: "Effect of large alternating strains on steel beams". Discussion, Journal of the Structural Division, ASCE 91, ST4, Aug. 1965, pp. 248 to 251.

20. G. Haaijer: "Plate buckling in the strain-hardening range". Proc. ASCE, Paper No. 1212, EM2, April 1957.

21. E. Mas & C. Massonnet: "Belgium´s part in the experimental research on the buckling of axially loaded mild-steel members conducted by the CECM". Acier-Stahl-Steel, No. 9, Sept.1966.

22. N. Tebedge, P. Marek, and L. Tall: "Column testing procedure". Report No. 351.1, Fritz Engineering Laboratory, Lehigh University, June 1969.

23. G.A. Alpsten: "Thermal residual stresses in hot-rolled steel members". Report No. 337.3, Fritz Engineering Laboratory, Lehigh University, Dec. 1968. (To be published in the Welding Journal.)

24. G.A. Alpsten: "Prediction of thermal residual stresses in hot-rolled plates and shapes of structural steel". Final Report, 9th IABSE Congress, Amsterdam, May 1972, pp. 3 to 13.

25. G.A. Alpsten: Theoretical simulation of the behavior and maximum strength of actual steel columns". (In preparation.)

26. R.H. Batterman & B.G. Johnston: "Behavior and maximum strength of metal columns. Journal of the Structural Division, Proc. ASCE 93, ST2, April 1967, pp. 205 to 230.

WELDING PARAMETERS, THICK PLATES, AND COLUMN STRENGTH

J. Brozzetti
Research Engineer
Centre Technique Industriel
de la Construction Métallique
Puteaux, France

G.A. Alpsten
Associate Director
Swedish Institute of
Steel Construction
Stockholm, Sweden

L. Tall
Professor of Civil Engineering
Fritz Engineering Laboratory
Lehigh University
Bethlehem, Pennsylvania
U.S.A.

ABSTRACT

As a part of an overall research program on experimental investigation of residual stresses in thick welded plates, sponsored jointly by the National Science Foundation and the Column Research Council, a particular attention was paid to the influence of varying the welding parameters on plates, each representing in fact a component plate of a built-up shape.

The welding parameters included were the speed of welding, the number of passes, the voltage of the welding current and the temperature of post or pre-heating. One plate was annealed after welding to compare the effects of this type of treatment.

After having observed the differences in magnitude and distribution of residual stresses, conclusions are drawn with respect to the effect of various welding parameters on the theoretical column strength of a simulated section 24 H 428 built-up with those welded plates.

This work described herein has been carried out at the Fritz Engineering Laboratory, Lehigh University, Bethlehem, U.S.A.

THIS PAPER HAS BEEN PUBLISHED IN THE

WELDING JOURNAL, Vol. 50, August 1971,

published by the AMERICAN WELDING SOCIETY,

New York, New York, U.S.A.

BUCKLING STRENGTH AND DESIGN GUIDE OF WELDED, LINEARLY TAPERED COLUMNS

George C. Lee
Professor and Acting Chairman
Department of Civil Engineering
State University of New York at Buffalo
Buffalo, U.S.A.

ABSTRACT

This paper presents the results of both experimental and analytical research regarding the buckling strength and design guide for centrally loaded tapered columns. The columns considered are H-shaped sections with a linear variation in the cross-sectional depth and are fabricated by welding only on one side of the web.

The specific contents of this paper are :

1) Analytical elastic buckling solutions of tapered columns.

2) Residual stresses measured in tapered column specimens welded from both sheared and flame cut plate elements.

3) Analytical inelastic buckling solutions of tapered columns by considering the residual stresses.

4) Formulation of design guide including effective length factors for centrally loaded tapered columns.

1. INTRODUCTION

The results presented in this paper are a part of a comprehensive research program on the behavior of tapered structural members sponsored by the Naval Facilities Engineering Command, American Institute of Steel Construction, American Iron and Steel Institute, the Metal Building Manufacturer's Association, and the State Univeristy of New York at Buffalo. The study has primarily been concerned with linear, web tapered I-shapes as illustrated in Figure 1.

At first the research program was devoted to residual stress measurements in welded tapered I-shapes (Lee and Ketter, 1972). Next, an extensive analytical program was launched to determine the elastic stability (axial, lateral, and lateral-torsioned buckling) loads for such members in order to develop design recommendations (Lee et al, 1972). The philosophy of these recommendations was not to develop "new" formulas but to determine modification factors to the current American Institute of Steel Construction specifications. As a consequence, the proposed design formulas for inelastic behavior were based on Johnson's parabola and not on any analytical or experimental* data for tapered members.

Thus it is imperative to investigate the analytical behavior of inelastic columns. This paper describes the buckling strength of axial loaded tapered columns with emphasis on inelastic behavior.

2. RESIDUAL STRESSES IN FABRICATED TAPERED SHAPES

Since residual stresses have a profound effect on non-slender columns, it is necessary to discuss the results presented by Lee and Ketter. The program was divided into two series, Figure 2. Series A dealt with 20 fabricated sections from shear cut plates. Series B was broadened to include shear cut and flame cut plates, some of which were welded together to form 20 fabricated sections. By determining the residual stresses in the plates prior to welding and after welding, the effect of the welding process can be evaluated. In both series the flange to web weld was on one side only by an automatic welding process. The members were fabricated such that one flange was horizontal and the other was sloping in the longitudinal direction. The residual stresses were determined using the section method with an 8-inch gauge length. Measurements were recorded at four equally spaced panels along the length of the members (the first and last panels were 18 inches from their respective ends). In Series A the web sections in each panel were measured parallel to the horizontal flange. In Series B they were measured along a radius originating at the point of intersection of the two flanges, i.e. along an arc from the horizontal flange to the sloping flange. In Figure 3, representative residual stress measurements are illustrated. The shear cut and flame cut patterns are alike in three ways : (1) the respective patterns are similar to welded prismatic I-shapes, (2) they are unsymmetrical about the weak axis due to the one-side welding procedure, and (3) the flange pattern is independent of the depth of the member while the web has a variation with depth. The effect of the two cutting procedures appears only at the flange tips ; for the shear cut plates the flange tips are in compression and for the flame cut plates the tips are in tension. Comparing the unwelded plates with the fabricated member in Series B, the effect of welding increases the stress at the tips for shear cut plates and decreases the stress at the tips for flame cut plates. Also the effect of one-side welding causes the flanges to bow laterally.

---

* Concurrently with the analytical program, experiments were performed on tapered members to determine their bending strength (Prawel et al). The 15 beams tested do not supply positive proof for the inelastic bending formula (although all beams had greater strength than the design formulas predicted.) The author does not know of any published information regarding inelastic tapered column tests.

Two typical residual stress patterns derived from average values of all measurements (Figure 4). The distinguishing feature between residual stresses in tapered and prismatic members is reflected in the assumed patterns by allowing the value of stress in the central portion of the web to vary with the depth of the member. Both patterns are doubly-symmetric with tension yield stress at the flange-web connection and one-half compressive yield stress in the flange. The difference between the two patterns is the tension stress at the flange tips in the flame cut pattern.

3. BUCKLING STRENGTH

The elastic buckling strength of tapered columns was investigated using the Rayleigh-Ritz procedure. A ten term power series was assumed for the displacements and using the principle of virtual displacements, a homogeneous set of equations were derived. The non-trivial solution to these equations yielded the elastic axial buckling load. Since only the web depth varied with length, the weak axis buckling load was considered to be unaffected by the taper. However, the strong axis buckling load varies with the taper ratio. These results are reported by Lee and Al.

Using the analytical solutions for tapered columns, an elastic axial design formula was proposed. The philosophy behind the formula was not to generate a "new" formula if the present AISC column formula could be modified to account for tapered members. This has two advantages ; (1) the designer will be working with the familiar AISC formulas for prismatic columns with a modification factor included and (2) the designer can see the increase in strength of a tapered member over a prismatic member. The most likely way to incorporate tapered members into the prismatic formulas is by modifying the length of the tapered beam. Thus the buckling stress of a pin-ended prismatic column having the same smaller end cross section and length $g\ell$ is equated to the buckling stress (at the small end) of the original pin-ended tapered column, Figure 5 :

$$\frac{\pi^2 E}{(g\ell/r_o)^2} = \sigma_{taper} = \frac{P_{cr}}{A_o} \qquad (1)$$

where r_o is the radius of gyration of the smaller end. For weak axis buckling $g = 1.0$ and for strong axis buckling, it was proposed that

$$g = 1.00 - 0.375\gamma + 0.080\gamma^2 \quad (1.00 - 0.0775\gamma) \qquad (2)$$

For taper ratios between zero and six, g is less than unity.

For slender columns that buckle elastically, Lee et al recommended equation (1) with an appropriate factor of safety. For non-slender columns that buckle inelastically, the "basic column curve" of the Column Research Council was recommended with the modifying factor g :

$$\sigma_{taper} = \left[1.0 - \frac{(g\ell/r_o)^2}{2C_c^2}\right]\sigma_y \; ; \quad \frac{g\ell}{r_o} \leqq C_c \qquad (3)$$

Where

$$C_c = \sqrt{\frac{2\pi^2 E}{\sigma_y}}$$

The function g was derived for pin-ended columns. To include other support conditions an effective tapered length factor was developed from a four membered

rectangular frame, Figure 6. The critical load was determined by using slope-deflection equations adopted to tapered members, and then the critical load was equated to the Euler buckling load for one column, i.e. ;

$$P_{cr} = \frac{\pi^2 E I_o}{(K_\gamma \ell)^2} \tag{4}$$

where $K_\gamma \ell$ is the effective tapered length and is interpreted as the length of an equivalent pin-ended prismatic column having a cross section equal to the smaller end of the tapered column. Some typical results for the effective tapered length factor are shown in Figure 7 and 8 for frames without side-sway and frames with side-sway, respectively. The quantities R_T and R_B are a measure of the restraints at the column top and bottom. To represent a pin-ended column, the top and bottom beams would have zero moments of inertia, thus $R_T = R_B = \infty$. If the top and bottom beams had an infinite moment of inertia, then $R_T = R_B = 0$.

In comparing tapered columns to prismatic columns, the effective length is seen to decrease with increasing taper ratio. Thus it is possible to have effective tapered length factors less than 0.5 when side-sway is prevented and less than 1.0 when side-sway is permitted.

For columns which are not simply supports equations (1) and (3) apply if g is replaced by K_γ :

for $K_\gamma \ell / r_o \geq C_c$

$$\sigma_{taper} = \frac{\pi^2 E}{(K_\gamma \ell / r_o)^2} \tag{5}$$

for $K_\gamma / r_o \leq C_c$

$$\sigma_{taper} = \left[1 - \frac{(K_\gamma \ell / r_o)^2}{2 C_c^2} \right] \sigma_y \tag{6}$$

Figure 9 contains a graph of equations (5) and (6) for different yield stress levels and also includes the AISC factor of safety used for prismatic columns.

The inelastic column curve, equation (6), is not based on any analytical or experimental solution for tapered columns. It resulted from the philosophy of the design of prismatic columns and the desire to modify the prismatic formulas to account for tapered columns. The remainder of this paper will develop the procedure used to determine inelastic tapered column buckling loads and compare these results to the proposed design formula, equation 3.

The weak axis inelastic buckling load will be essentially independent of the taper, since the web has very little effect on the weak axis moment of inertia. Thus for weak axis buckling the column can be considered prismatic. The strong axis inelastic buckling load can be determined from

$$B_x(z) \frac{d^2 v}{dz^2} + Pv = 0 \tag{7}$$

where v is the strong axis deflection and B_x is the bending rigidity, e.g. $B_x(z) = EI_x(z)$ if the column is elastic. When the column starts to yield the bending rigidity becomes a complex function of z and P.

If the tangent modulus concept is used,

$$B_x(z) = \int_{\text{Area}} E_t \, y^2 \, dA \tag{8}$$

where E_t is the tangent modulus. I residual stresses are present and the material is idealized as perfectly elastic-plastic, then equation (8) may be written as,

$$B_x(z) = EI_{c_x}(z) \tag{9}$$

where I_{c_x} is the moment of inertia of the elastic core at a point z along the column. Due to the complexity of equation (7), numerical procedures must be used. The particular procedure used herein is the Finite Element Method. If the column is divided into n elements such that over each element the bending rigidity is constant, then equation (7) can be transformed into the Finite Element formulation (Lee and Morrell) :

$$[K] \begin{Bmatrix} V_i \\ \theta_i \\ V_j \\ \theta_j \end{Bmatrix} - [N] \begin{Bmatrix} V_i \\ \theta_i \\ V_j \\ \theta_j \end{Bmatrix} = \begin{Bmatrix} 0 \\ 0 \\ 0 \\ 0 \end{Bmatrix} \tag{10}$$

where

$$[K] = B_x \begin{bmatrix} 12/\ell^3 & & \underline{\text{SYM}} & \\ -6/\ell^2 & 4/\ell & & \\ -12/\ell^3 & 6/\ell^2 & 12/\ell^3 & \\ -6/\ell^2 & 2/\ell & 6/\ell^2 & 4/\ell \end{bmatrix}$$

and

$$[N] = P \begin{bmatrix} 6/5\ell & & \underline{\text{SYM}} & \\ -1/10 & 2\ell/15 & & \\ -6/5\ell & 1/10 & 6/5\ell & \\ -1/10 & -\ell/30 & 1/10 & 2\ell/15 \end{bmatrix}$$

where v_i and θ_i are the deflection and rotation degrees of freedom at node i. Since yielding will begin at the smaller end in tapered columns and progress towards the larger end, elemental lengths should be considerably smaller in the yielded portion

than in the elastic portion *.

The bending rigidity in each element was determined by using Alvarez and Birnstiel's method. At each node the cross-section is divided up into a grid of "fibers".+ Each fiber m has dimensions ΔX_m and ΔY_m. The axial load is applied in increments. Within each increment the internal axial force is calculated through an iterative method until it equilibrates the applied axial load at that node. When the internal axial force is in equilibrium with the applied axial force at each node, the resulting bending rigidities are averaged and the elemental matrices are calculated and assembled for a given applied axial force. The determinate of the reduced master matrix will indicate if the column has buckled. If the determinate does not change sign from the previous increment, then another increment is applied and the process is repeated until the determinate is zero or nearly zero.

In the process of equilibrating the internal axial force, each increment in axial load is assumed to strain the elastic core remaining after the previous iteration :

$$\Delta\varepsilon_a = \frac{-\Delta P}{EA_c} \qquad (11)$$

where $\Delta\varepsilon_a$ is the increment in axial strain due to the axial load ΔP and A_c is the elastic core area. The total strain is obtained by adding the preceding axial force strain and the residual strain to this increment, $\Delta\varepsilon_a$. Using the total strain, the stress and tangent modulus in each fiber can be computed from the stress-strain curve. Knowing the stress and tangent modulus, the internal axial force can be calculated and compared with the applied force ; and the bending rigidities can be determined. If the internal axial force does not equal the applied force then the process is repeated.

Using the above procedure strong axis buckling curves were obtained for a tapered column having a typical small end cross section. Three different taper ratios and two different residual stress patterns were considered, Figure 4. The results with the shear cut residual stress pattern are presented in Figure 10 and the results with the flame cut residual stress pattern are presented in Figure 11. For the prismatic column ($\gamma = 0$), the results are similar to those obtained by McFalls and Tall. Also shown on these figures are equations (1) and (3), the proposed design formulas. The tapered column solutions lie between the prismatic solutions and the design formula in the inelastic range (C_c - 117). Thus as the taper ratio is increased the design formulas become more accurate in predicting the column's behavior. This can be explained by the fact that the yielding is confined to the smaller end region, i.e., the penetration of yielding measured from the smaller end at incipient buckling is decreased as the taper is steepened.

4. SUMMARY AND CONCLUSIONS

Analytical solutions for linearly tapered I-shape columns have been described. The major emphasis of this paper was to present inelastic column solutions and compare them with the proposed design formulas (for detailed treatment of elastic tapered columns see Lee et al).

---

* Generally the column was divised into 12 elements with four elements at the smaller end having lengths equal to 1/36th of the total column length and the remaining eight elements had lengths of 1/9th the total length (for $\gamma = 4$ the total number of elements was increased to 15).

+ At each node, each flange was divided into 400 "fibers" and the web was divided into 80 "fibers".

Typical residual stress patterns were presented for fabricated sections composed of shear cut plates or flame cut plates. A representative pattern was assumed for each and used in the analytical investigation of inelastic tapered column strength. Column curves were obtained by the solution procedure described herein using the Finite Element Method to find the critical loads. The results indicated that the effect of tapering a column moves the theoretical column curve closer to the design formula, equation (3) or (6).

ACKNOWLEDGMENT

The author is indebted to his colleagues and research collaborators, Professor Robert L. Ketter and Professor Michael L. Morrell, for their significant contributions to the research program of study in which the results presented herein are a part.

5. REFERENCES

1. Lee, G.C. and Ketter, R.L.
RESIDUAL STRESSES IN WELDED TAPERED SHAPES
Civil Engineering Research Report, SUNYAB, Feb. 1972

2. Lee, G.C., Morrell, M.L. and Ketter, R.L.
DESIGN OF TAPERED MEMBERS
Welding Research COuncil Bulletin, No. 173, June 1972

3. Prawel, S.P., Morrell, M.L. and Lee, G.C.,
BENDING AND BUCKLING STRENGTH OF TAPERED STRUCTURAL MEMBERS
to appear in J. Exp. Mech.

4. Alvarez, R.J. and Birnstiel, C.,
INELASTIC ANALYSIS OF MULTI-STORY, MULTI-BAY FRAMES
ASCE J. Struct. Div., Vol. 95, Nov. 1969

5. Lee, G.C. and Morrell, M.L.
FINITE ELEMENT ANALYSIS OF SPACE FRAMES OF THIN-WALLED MEMBERS
Civil Engineering Research Report, SUNYAB, Feb. 1972

6. McFalls, R.K. and Tall, L.
A STUDY OF WELDED COLUMNS MANUFACTURED FROM FLAME-CUT PLATES
Welding Research Supplement, pp. 141-s-153-s, April 1969

TAPERED BEAM GEOMETRY

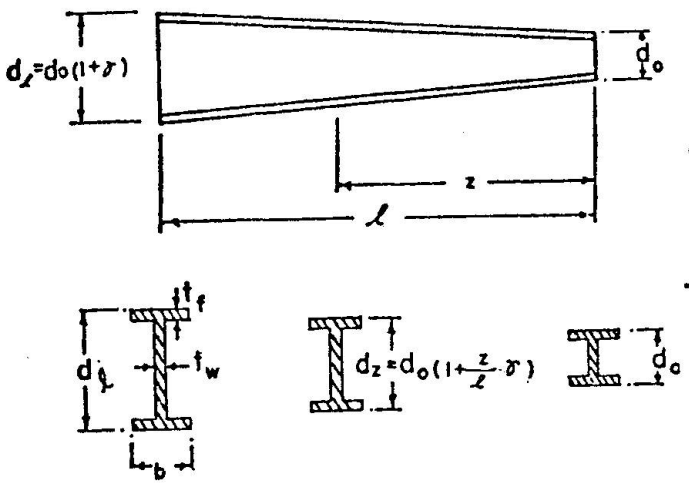

$d_o = 6"$, $d_\ell = 6" \sim 42"$, $t_w = 0.10 \sim 0.25$

$b = 6"$, $t_f = 0.25" \sim 0.75"$

$\ell = 96" \sim 432"$

Fig. 1 -General tapered geometry-

SERIES A : SHEAR CUT EDGES

ℓ	d_o	d_ℓ	No. of beams	No. of panels
100"	6"	12"	2	4
97	6	16	2	4
98	10	36	3	3

25 - SHEAR CUT MEASUREMENTS

SERIES B : SHEAR AND FLAME CUT EDGES

ℓ	d_o	d_ℓ	No. of beams		No. of panels
			S.C.	F.C.	
120"	6"	6"	1	1	4
120	6	12	1	1	4
120	6	18	1	1	4
120	6	24	1	1	4
120	24	24	1	1	4

20 - SHEAR CUT MEASUREMENTS

20 - FLAME CUT MEASUREMENTS

Fig. 2 Summary of residual stress measurements

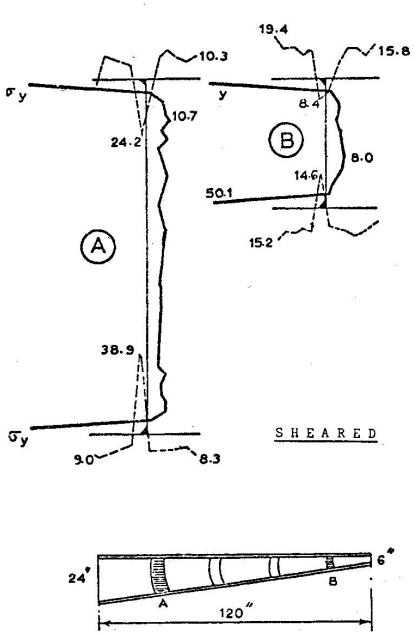

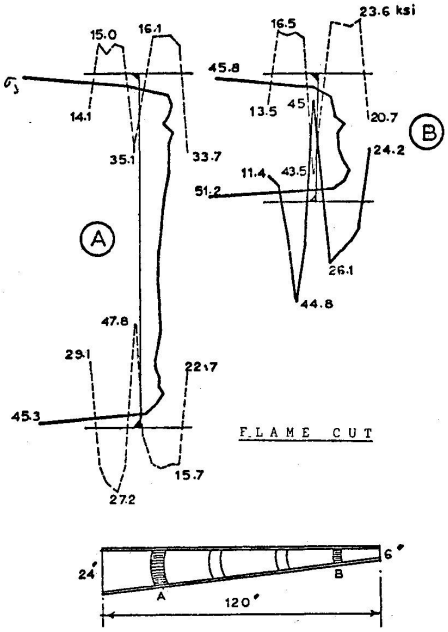

FIGURE 3 : WELDED SECTIONS

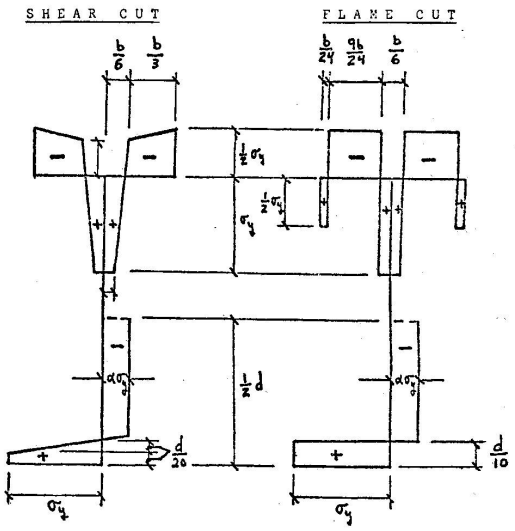

FIGURE 4 : ASSUMED RESIDUAL STRESS PATTERNS

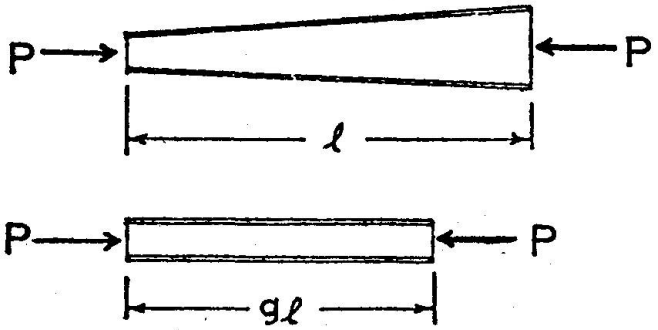

FIGURE 5 : DEFINITION OF THE LENGTH MODIFICATION g FOR COLUMN

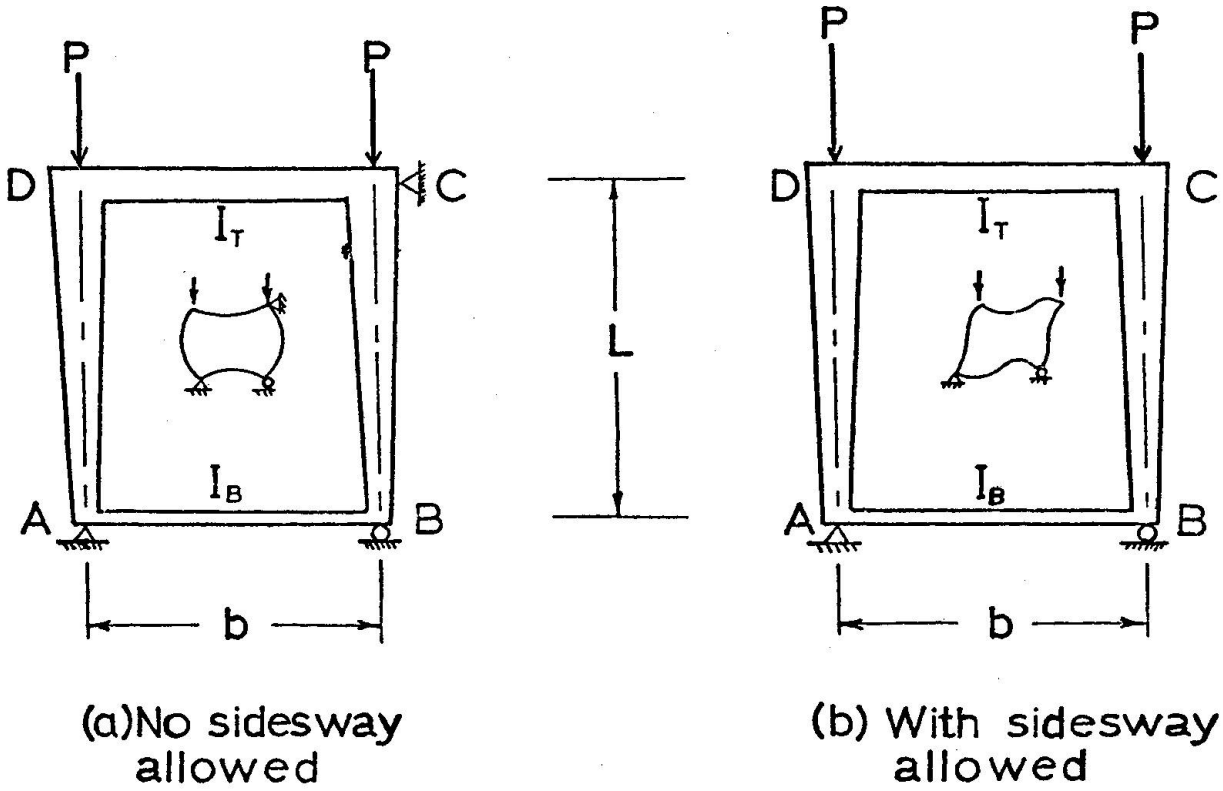

FIGURE 6 : STRUCTURAL MODELS USED FOR DETERMINATION OF THE EFFECTIVE LENGTH FACTORS OF TAPERED COLUMNS IN FRAMES

FIGURE 7

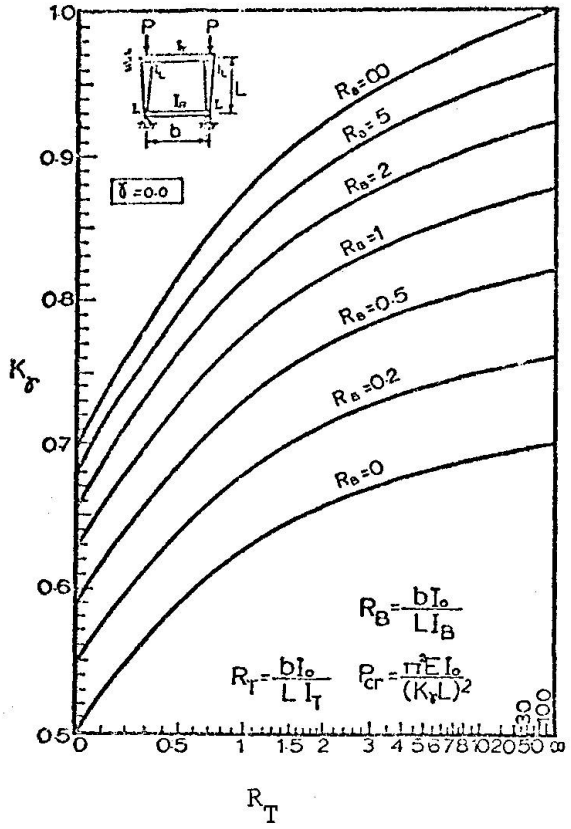

Effective length factors for tapered columns : side-sway prevented $-\gamma = 0$

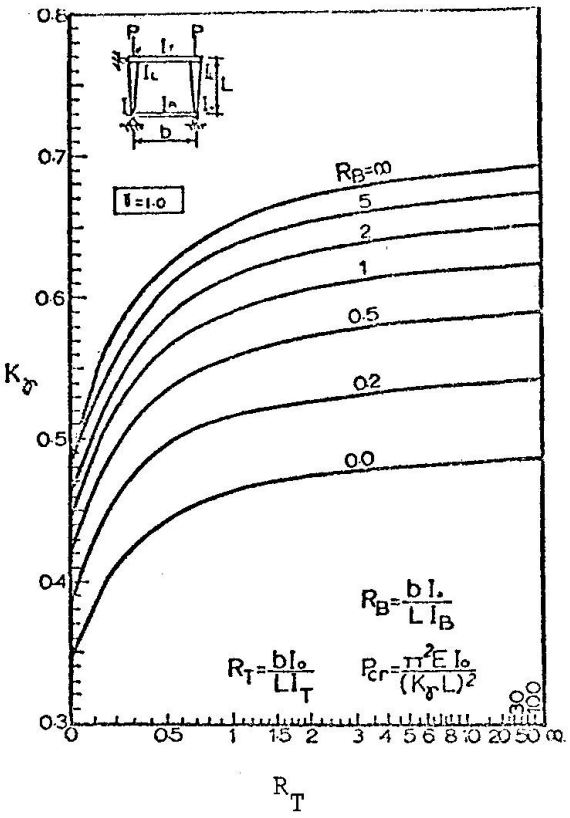

Effective length factors for tapered columns : side-sway presented $-\gamma = 1.0$

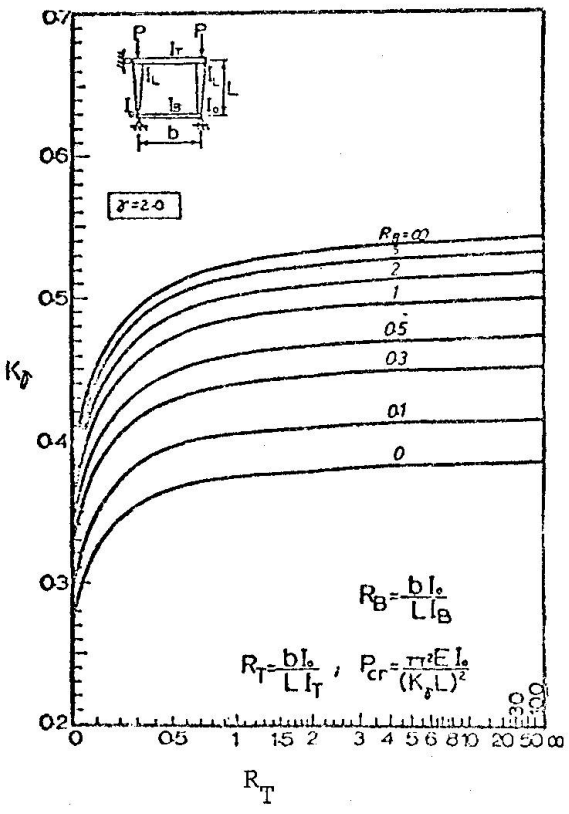

Effective length factors for tapered columns : side-sway prevented $-\gamma = 2.0$

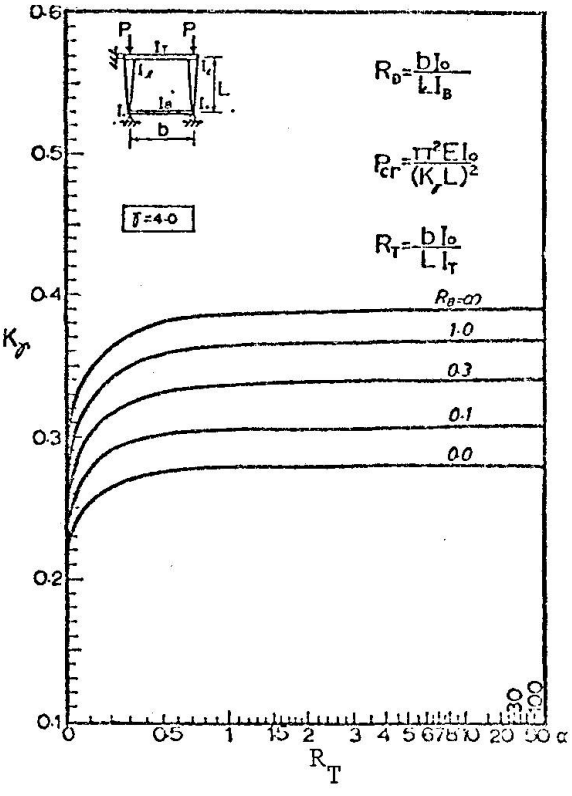

Effective length factors for tapered columns : side-sway prevented $-\gamma = 4.0$

FIGURE 8

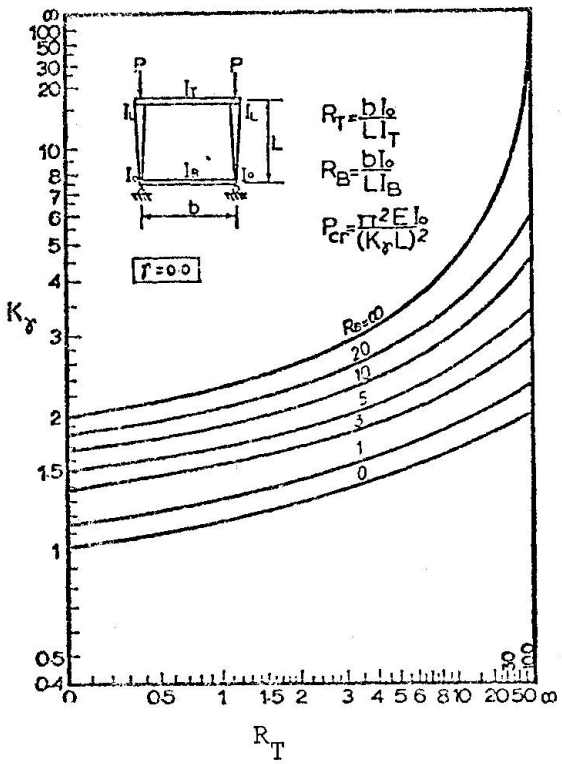

Effective length factors for tapered columns : side-sway permitted — γ = 0

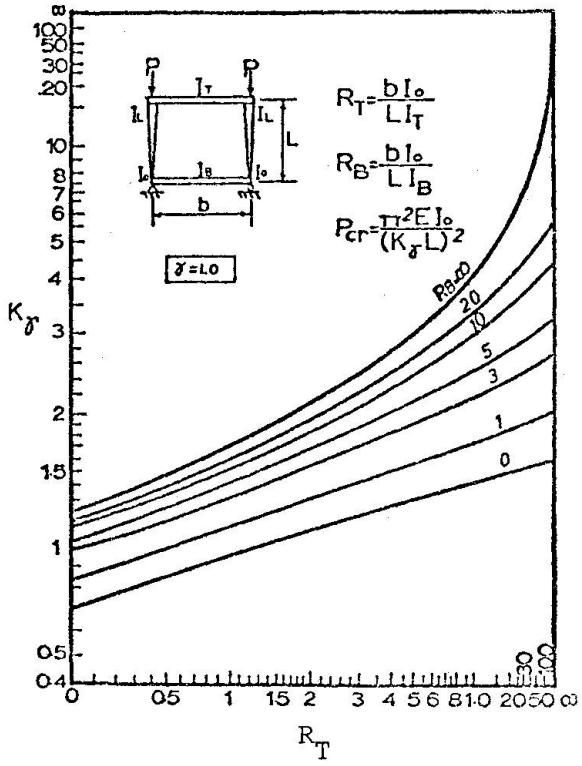

Effective length factors for tapered columns : side-sway permitted — γ = 1.0

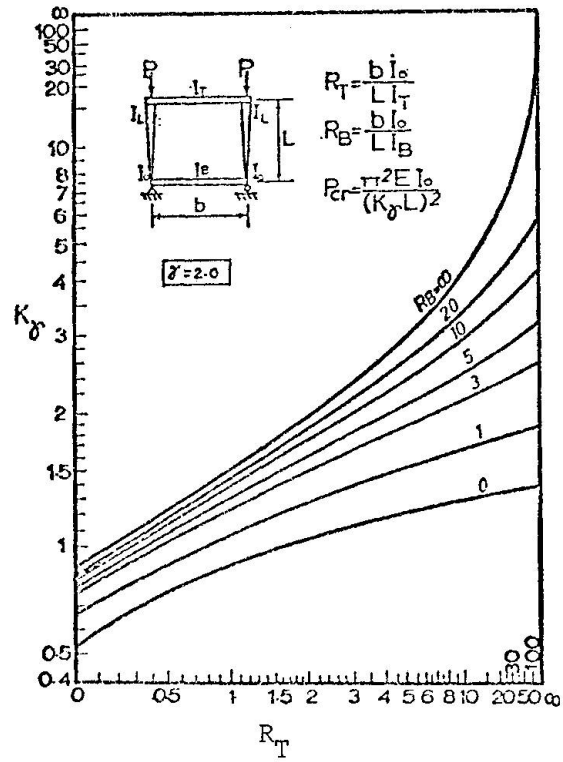

Effective length factors for tapered columns : side-sway permitted — γ = 2.0

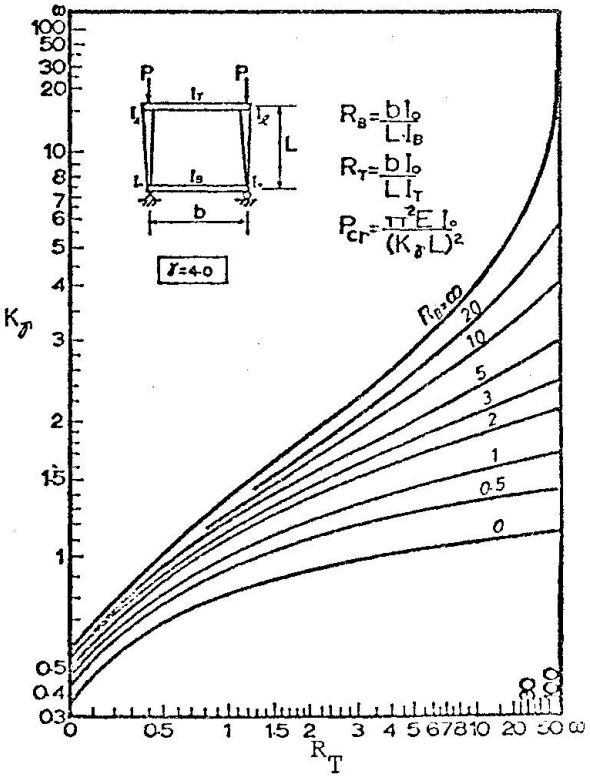

Effective length for tapered columns : side-sway permitted — γ = 4.0

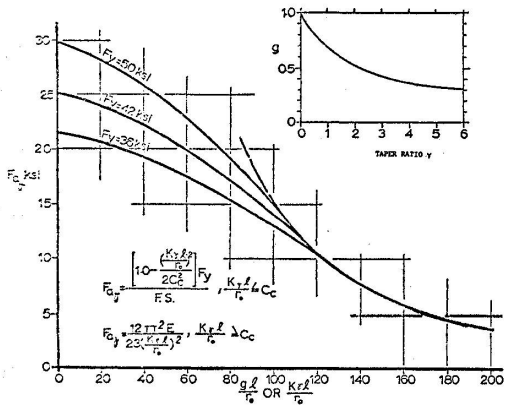

FIGURE 9 : AXIAL DESIGN CURVE FOR TAPERED COLUMNS

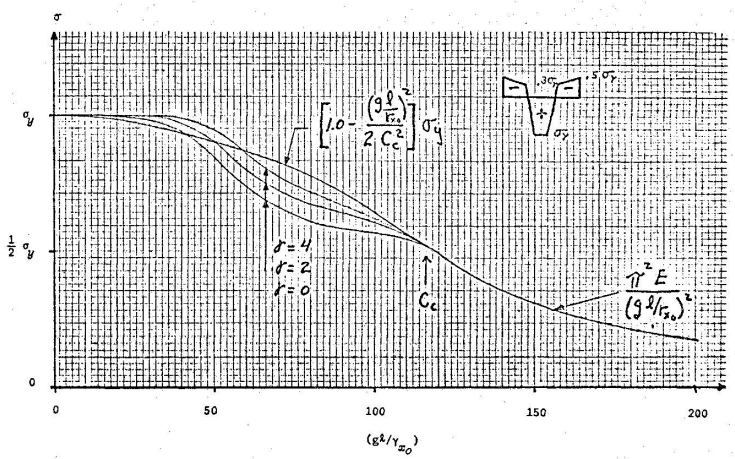

FIGURE 10 : STRONG AXIS — SHEAR CUT EDGES

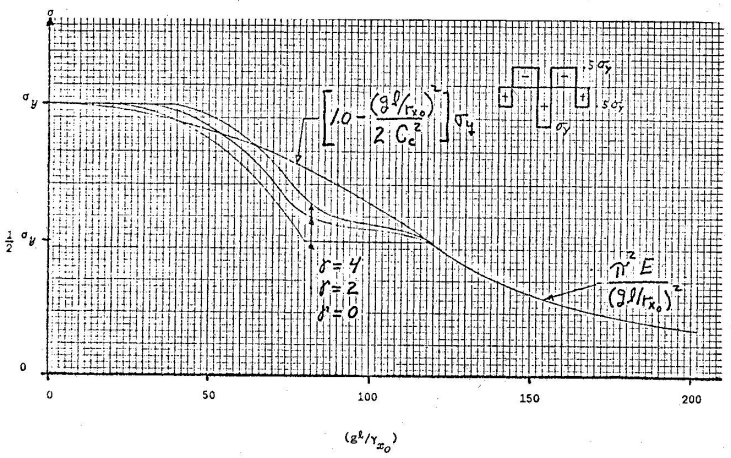

FIGURE 11 : STRONG AXIS — FLAME CUT EDGES

EFFECT OF INITIAL STRESSES ON PLATE BUCKLING AND BUCKLING OF BOX COLUMNS

Henrik Nylander
Professor, Techn.Dr.
Department of Building Statics
and Structural Engineering
Royal Institute of Technology
Stockholm

ABSTRACT

The plate buckling is studied in Appendix 1, presented as a contribution at the IABSE-Congress, Amsterdam 1972.

When dealing with the column buckling of the welded box columns with quadratic cross sections it is assumed that the effective cross section consists of four angles with the flange width b_m (= b_e in Figure 3 in Appendix 1). b_m is the effective width of the compressed plate at the failure load in plate buckling.

The failure criterion at the column buckling is assumed to be that failure occurs when the compressive stress in the two most loaded angle flanges exceeds the value $\sigma_{kb} \cdot b/b_m$, where σ_{kb} is the value of $\sigma_o = N/2bd$ at plate buckling failure.

Results of the calqulations are given in Appendix 2. The diagrams show that the influence of the initial stresses is of great importance.

Bg. 6 AK 23

FAILURE LOAD AND EFFECTIVE WIDTH OF COMPRESSED STEEL PLATES WITH INITIAL STRESSES AND INITIAL DEFLECTIONS

Column buckling is influenced by the local plate buckling. The local plate buckling is dependent on initial stresses due to welding and initial deflections of the plates.

The author has studied the plate buckling in the overcritical range using a model of calqulation, which enables to consider the initial stresses and the initial deflection in a relatively simple manner.

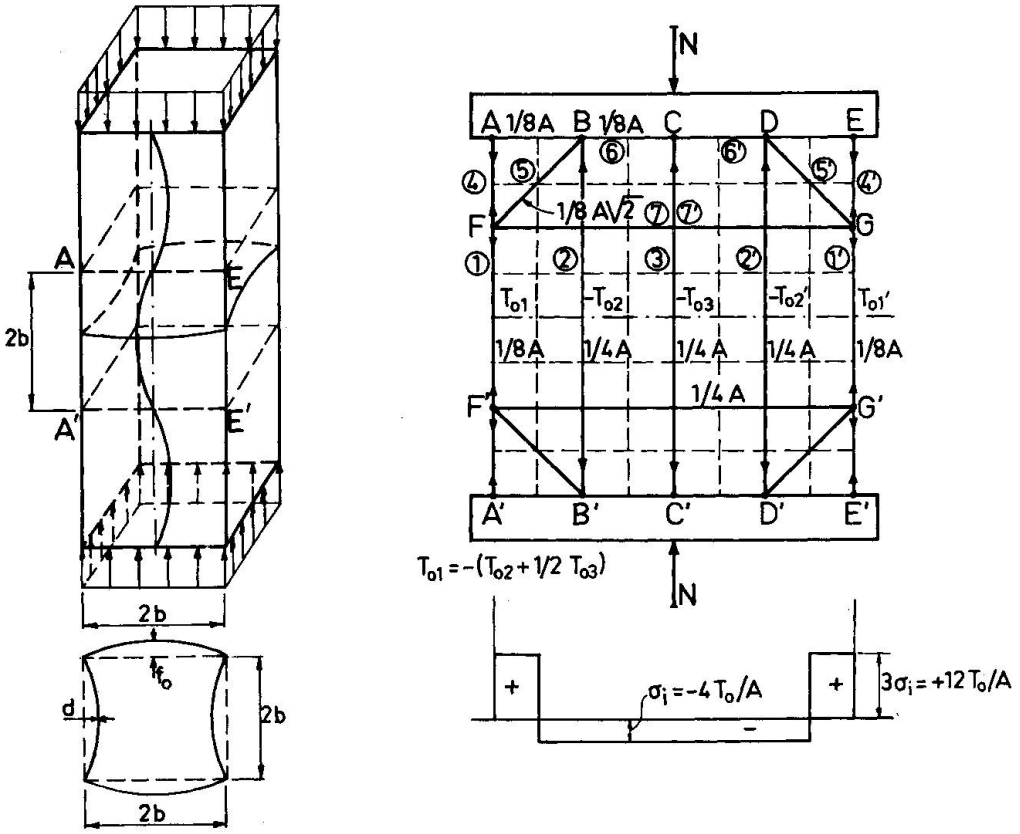

Fig. 1a and 1b Model of Calculation

The investigation is part of a research project regarding the carrying capacity of welded hollow columns, built up by thin plates. The project is carried out at the Department of Building Statics and Structural Engineering at the Royal Institute of Technology, Stockholm and at the Swedish Institute of Steel Construction, Stockholm.

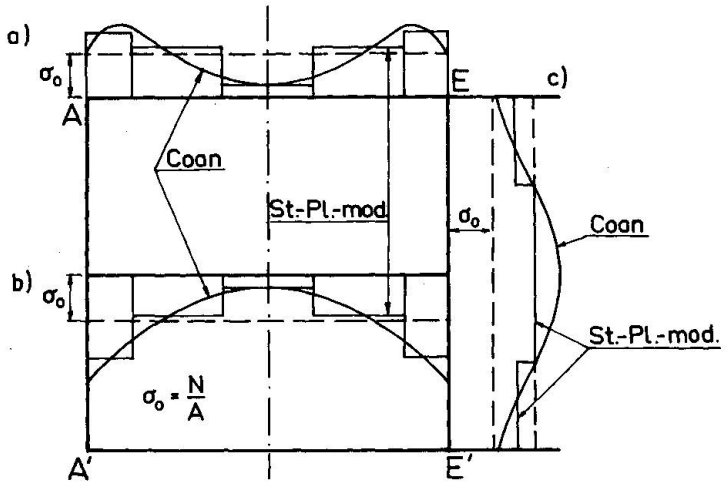

Fig. 1c
Distribution of compressive stresses in the direction of the load N at the edge A-E (a)) at the line of symmetry (b)) and the edge E-E´ (c)). Comparison with solution by Coan $\sigma_o/\sigma_{e\ell}$ = 1,74.

The model of calqulation consists of a plate acting only in plate bending and of the strips 1-7 and 1´- 7´, taking the membrane stresses only. (Fig. 1) The strips are connected to the plate at the points A-G and A´- G´. The areas of the strips are shown in Fig. 1, where $A = 2b \cdot d$ is equal to the area of the cross section of the plate. The normal forces in the strips are caused by 1) the initial stresses, 2) the normal force N in the plane of the plate, which gives forces in the different strips in proportion to their areas and 3) of forces which are caused by the changes of length of the strips as the bending deformation of the strips follows the bending deformation of the plate.

The mathematical treatment is omitted in this connection. It is the author´s intention to publish the theory and the rather comprehensive results in a near future.

A treatment of the problem starting from the fundamental Eq. by von Kármán and Marguerre adjusted to take into account the influence of the initial stresses is in the author´s opinion very difficult. In Fig. 1c a comparison is made with a solution by Coan |1| for a case where $\sigma_i = 0$. The membrane stresses in the direction of the compressive load N at the supports at the middle of the plate and along a free edge are considered. It is seen from the Figure that it is a good agreement between Coan´s results and the results from the calqulations for the model in Fig. 1b both regarding the maximum values and the distributions of stresses.

It is hardly possible to precise adequate criteria of failure for the highly statically indeterminate system in question where the elasto-plastic state of stresses must be considered. The author has instead of trying to give a complex theory started from a relatively detailed study of the stresses in different parts of the elastic plate caused by bending and torsional moments and the normal forces. Then that load has been determined at which total yielding (yield stress over the whole cross section) will occur at the point considered, if the bending and torsional moments as well as the normal forces have the values calqulated

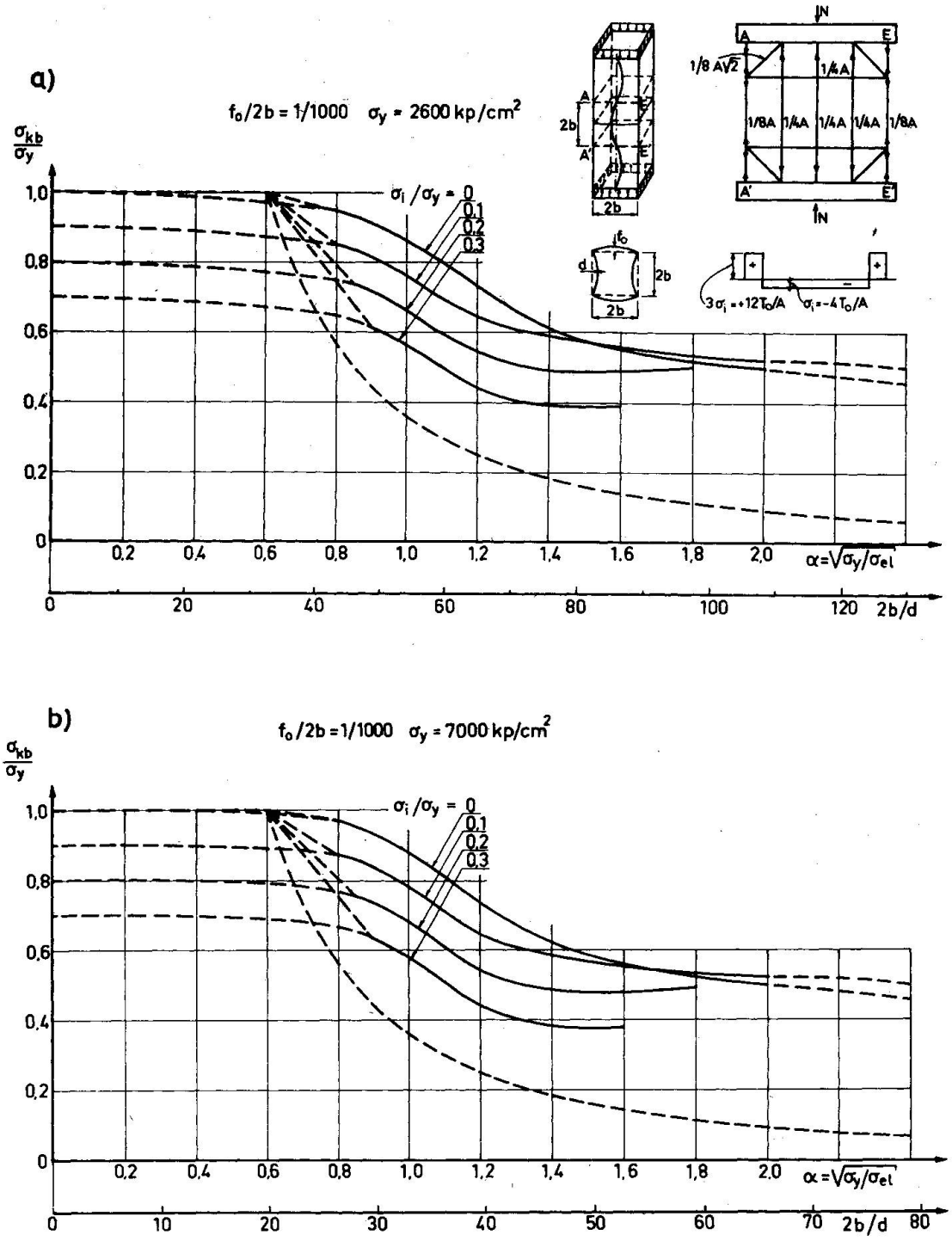

Fig. 2a and 2b Values of $\sigma_{kb} = N/2bd$ at buckling failure divided by σ_y at different σ_i/σ_y as function of $\alpha = \sqrt{\sigma_y/\sigma_{el}}$

a) σ_y = 2 600 kp/cm² b) σ_y = 7 000 kp/cm²

from the theory of elasticity. At the judgement of the failure load the following points have been considered:

1. The midpoint of strip (A-A´, Fig. 1a). Yielding due to normal force (compression) in the direction of the load N.
2. The midpoint of the strip 2 (B-B´, Fig. 1a). Yielding due to bending moment and normal force in the direction of the compressive load N.
3. The centre of the plate (midpoint of strip 3). Yielding due to bending moment and normal force in the direction of the compressive load N.
4. The corner points. Yielding due to torsional moment and normal force in the direction of the load N.

The results are given in Fig. 2 for two values of the yield stress: 2 600 kp/cm^2 and 7 000 kp/cm^2 and for the ratio initial deflection over plate width $f_0/2b$ = 1/1 000. For most of the calqulated points of the diagrams the alternatives 2) and 3) above were most dangerous and the failure loads were for these points calqulated as the average values of the failure loads for the alternatives 2) and 3).

For σ_i/σ_y = 0 and 1,2 < α < 2,0 and for σ_i/σ_y = 0,1 and α > 1,8 alternative 4) was most dangerous. For σ_i/σ_y = 0 and α > 2,0 alternative 1) was most dangerous.

The effective width b_e (see Fig. 3) is of importance for the column buckling. Calqulated values at failure load are given in Fig. 3 for different σ_i/σ_y ($f_0/2b$ = 1/1 000; σ_y = 2 600 kp/cm^2). It is seen from the Figure that the initial stresses highly affect the values of b_e/b.

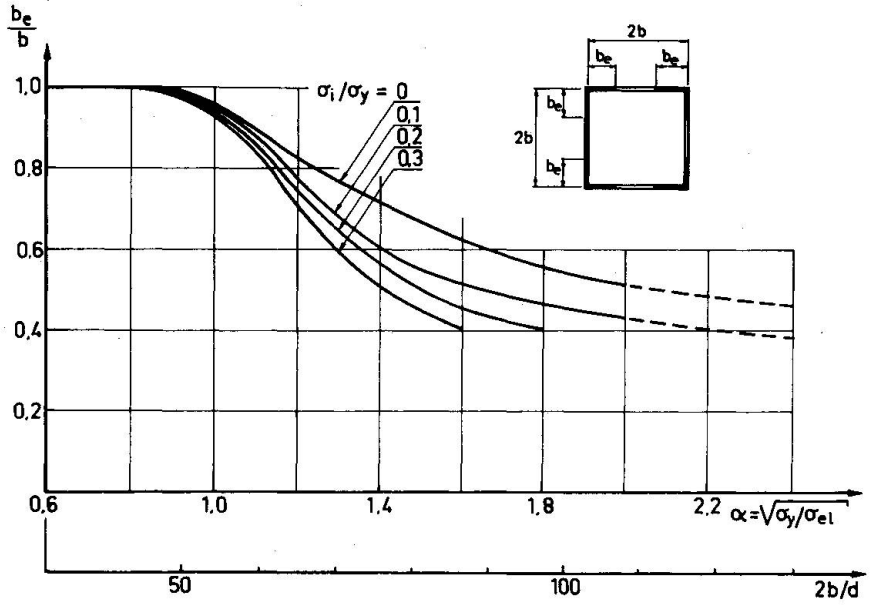

Fig. 3 Ratio b_e/b at the failure load as a function of α.
(σ_y = 2 600 kp/cm^2)

It is seen from Fig. 2 that the initial stresses have a very important negative influence on the critical buckling stresses especially for $0,8 < \alpha < 1,6$. The initial stresses have a negative effect on the effective width b_e (see Fig. 3). Both these effects reduce the column buckling load. The applied distribution of the initial stresses is unfavourable. Calqulations of a case where $\sigma_i = 0$ in the strip 3 have given higher failure loads. It is therefore a need of studying the influence of the fabrication methods on the distribution of initial stresses. Finally the author among investigations will remind of those by Nishino, Ueda, Tall |2|; Dwight, Moxham |3| and Dwight, Ractcliffe |4| of buckling of welded columns of hollow sections, where it was pointed out that the initial stresses have a large unfavourable effect on the failure load.

SUMMARY

The behaviour of compressed steel plates in the overcritical range is studied. A simplified model of calqulation, Fig. 1, which enables to consider initial stresses and deflections is used. The results are intended to serve as a basis for design rules. It is shown that the initial stresses reduce the failure load especially for the dimensions corresponding to $0,8 < \alpha < 1,6$, Fig. 2. Furthermore the effective width is reduced by the initial stresses, Fig. 3. Here omitted results for other distributions of the initial stresses are more favourable.

REFERENCES

|1| Coan, J.M.: Large Deflection Theory for Plates with Small Initial Curvature Loaded in Edge Compression. Journ. of Appl. Mech., June 1951.

|2| Nishino, F.; Ueda, Y. and Tall, L.: Experimental Investigations of the Buckling of Plates with Residual Stresses. Am. Soc. Testing Mats., p. 12, 1967.

|3| Dwight, J.B. and Moxham, K.E.: Welded Steel Plates in Compression. The Struct. Eng., No. 2, 1969.

|4| Dwight, J.B. and Ractcliffe, A.I.: The Strength of Thin Plates in Compression. Thin Walled Structures, Crosby Lockwood, 1969.

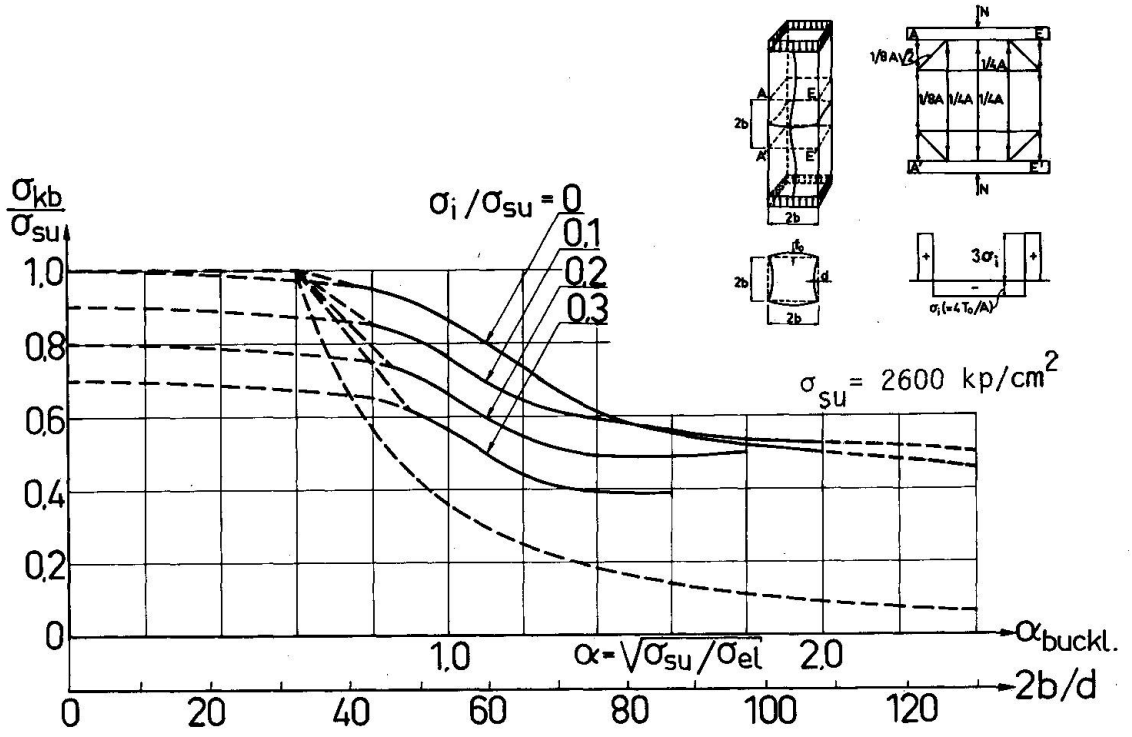

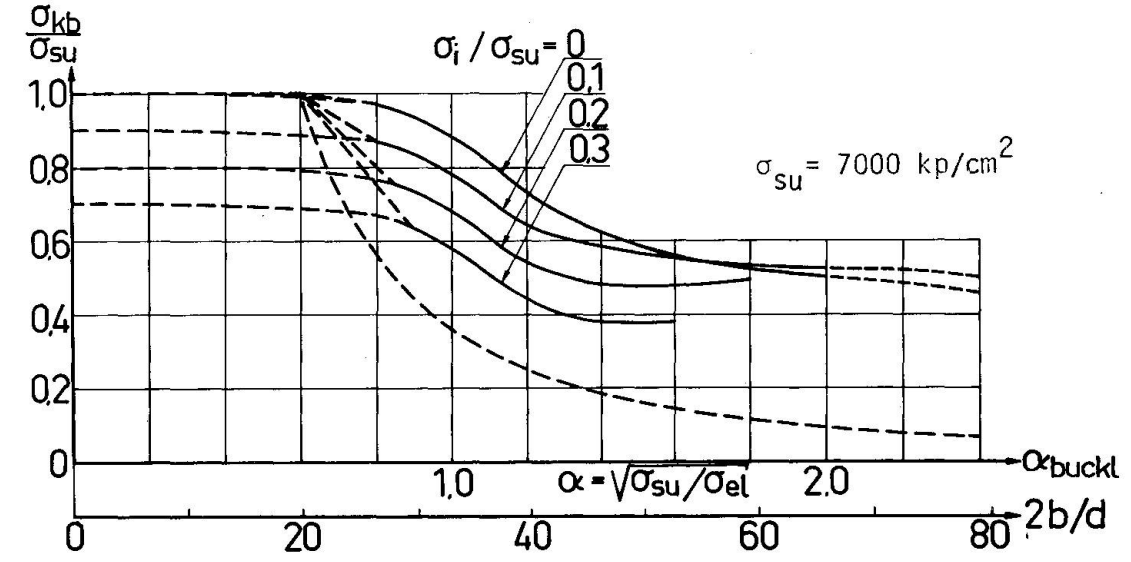

Fig. 1 Critical stress $\sigma_{kb} = N_{kb}/2bd$ at plate buckling, divided by σ_{su} at different σ_i/σ_{su} as a function of $\alpha_{buckl} = \sqrt{\sigma_{su}/\sigma_{el}}$. Initial stress distribution 1. ($\sigma_{su} = \sigma_y$) $f_o/2b = 1/1000$;

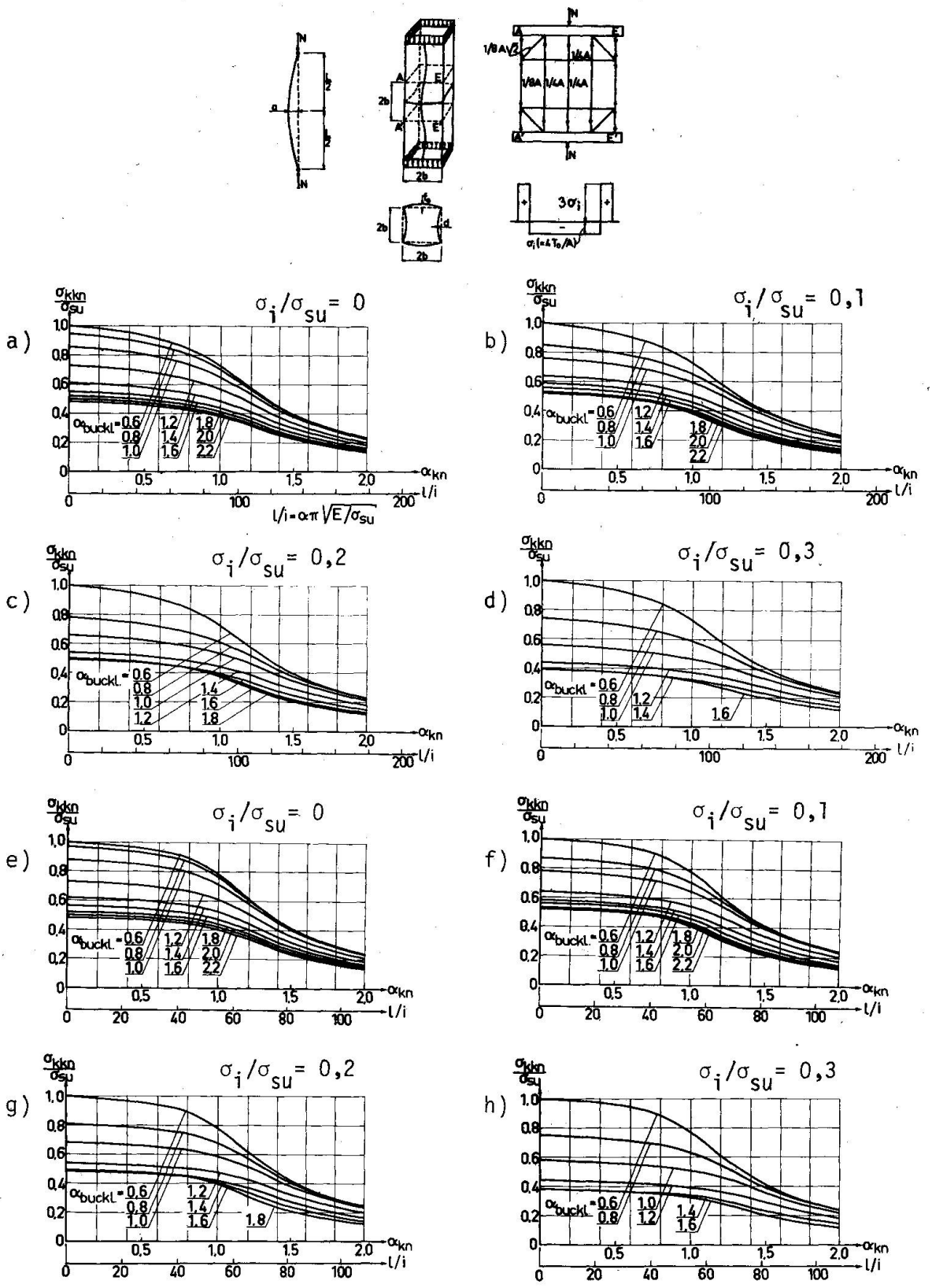

Fig. 2 Critical stress $\sigma_{kkn} = N_{kkn}/2bd$ at column buckling, divided by σ_{su} at different α_{buckl} as a function of $\alpha_{kn} = \sqrt{\sigma_{su}/\sigma_{e\ell}}$. Initial stress distribution 1. ($\sigma_{su} = \sigma_y$) a/ℓ = 1/1000; $f_o/2b$ = 1/1000;
a)-d): σ_{su} = 2600 kp/cm^2; e)-h): σ_{su} = 7000 kp/cm^2.

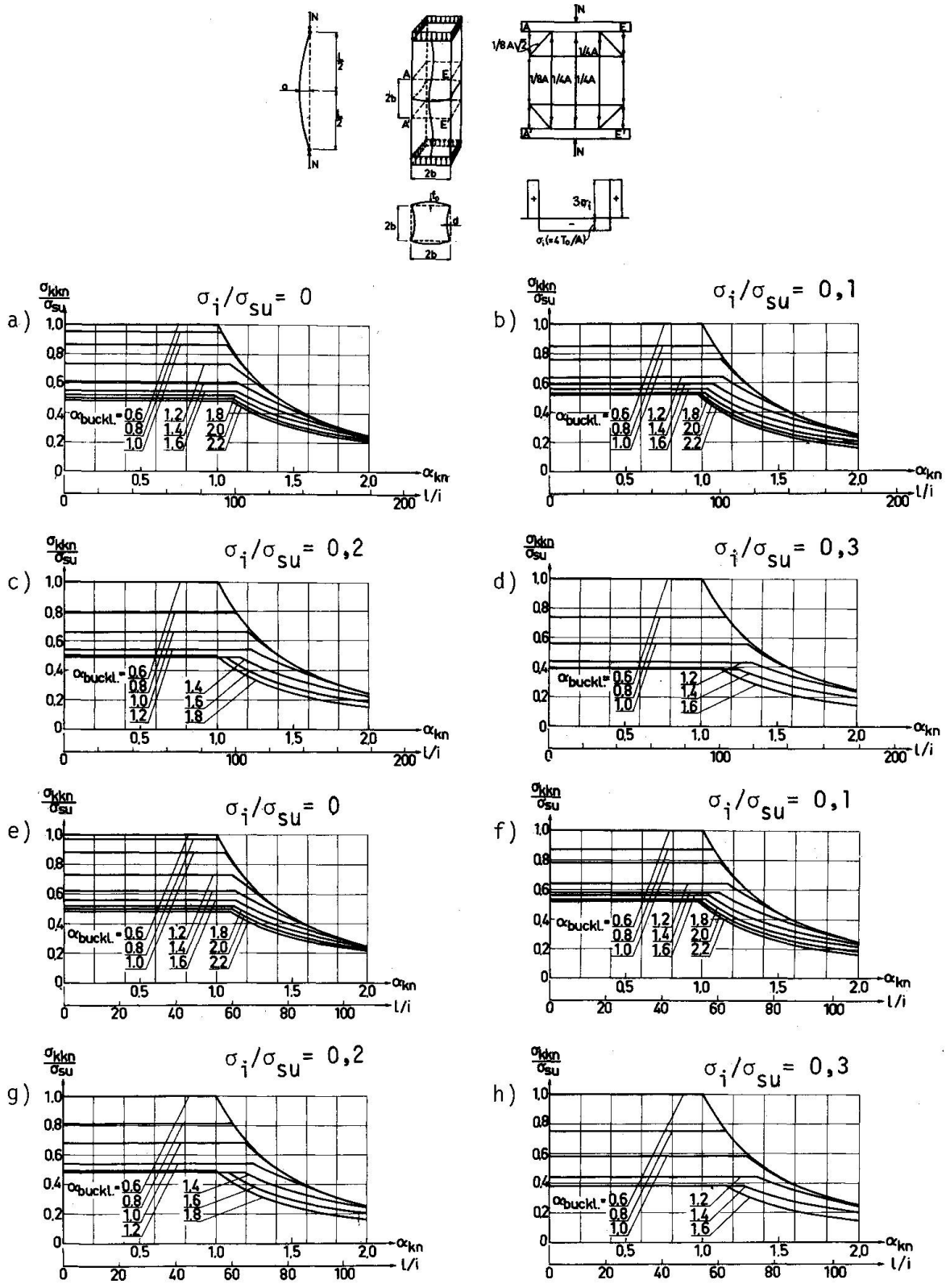

Fig. 3 Critical stress $\sigma_{kkn} = N_{kkn}/2bd$ at column buckling, divided by σ_{su} at different α_{buckl} as a function of $\alpha_{kn} = \sqrt{\sigma_{su}/\sigma_{e\ell}}$. Initial stress distribution 1. ($\sigma_{su} = \sigma_y$); $a/\ell = 0$; $f_o/2b = 1/1000$;
a)-d): σ_{su}= 2600 kp/cm^2; e)-h): σ_{su}= 7000 kp/cm^2.

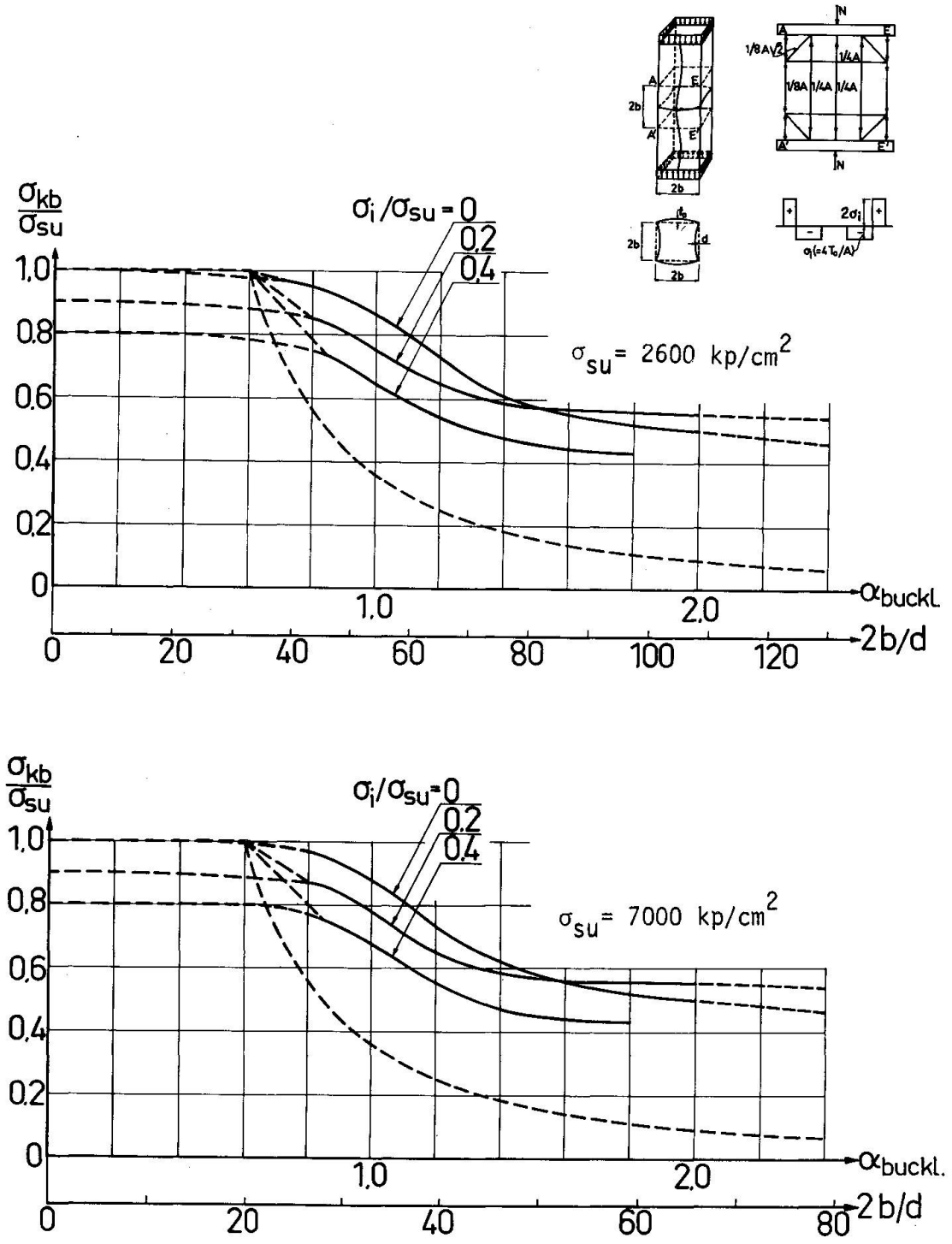

Fig. 4 Critical stress $\sigma_{kb} = N_{kb}/2bd$ at plate buckling failure, divided by σ_{su} at different σ_i/σ_{su} as a function of $\alpha_{buckl} = \sqrt{\sigma_{su}/\sigma_{e\ell}}$. Initial stress distribution 2. ($\sigma_{su} = \sigma_y$). $f_o/2b = 1/1000$.

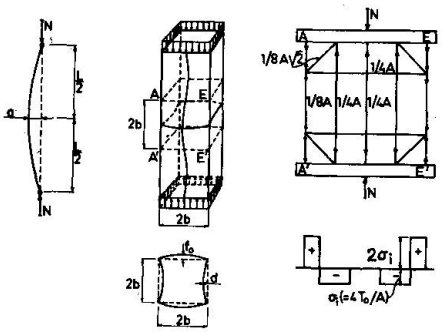

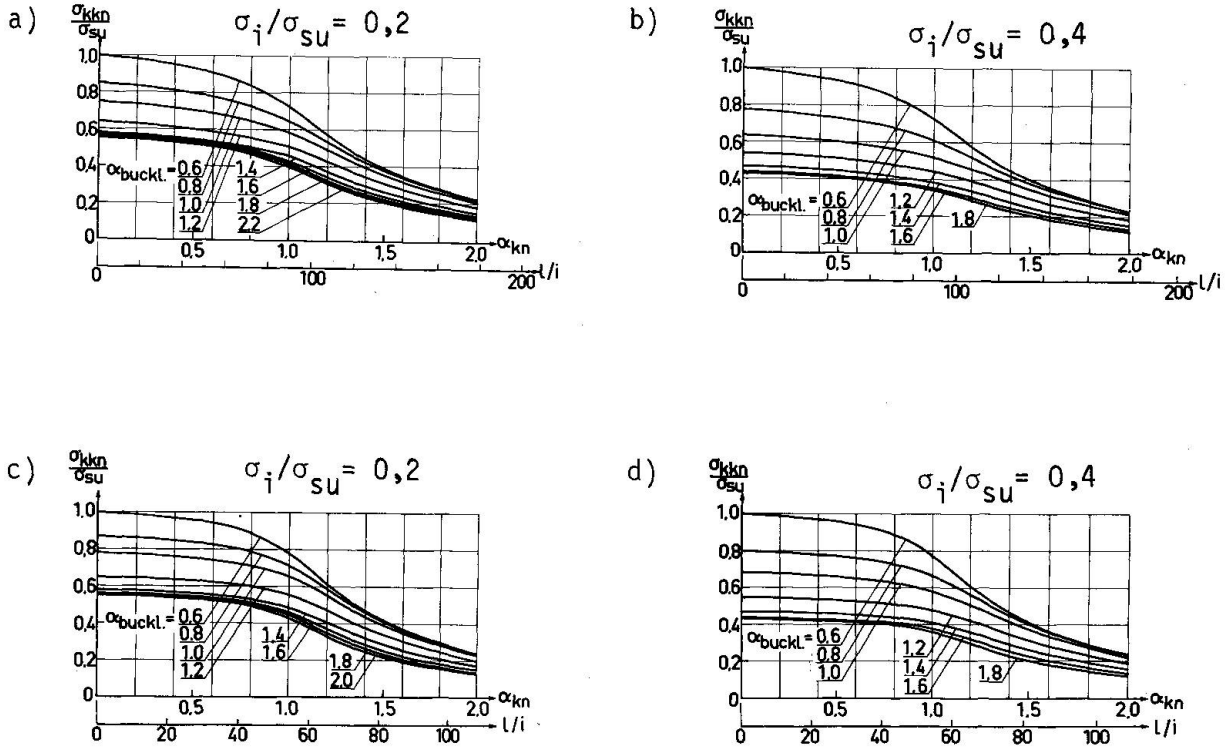

Fig. 5 Critical stress $\sigma_{kkn} = N_{kkn}/2bd$ at column buckling divided by σ_{su} at different α_{buckl} as a function of $\alpha_{kn} = \sqrt{\sigma_{su}/\sigma_{e\ell}}$. ($\sigma_{su} = \sigma_y$).
Initial stress distribution 2. $a/\ell = 1/1000$; $f_o/2b = 1/1000$;
a) - b): $\sigma_{su} = 2600$ kp/cm^2 ; c) - d): $\sigma_{su} = 7000$ kp/cm^2.

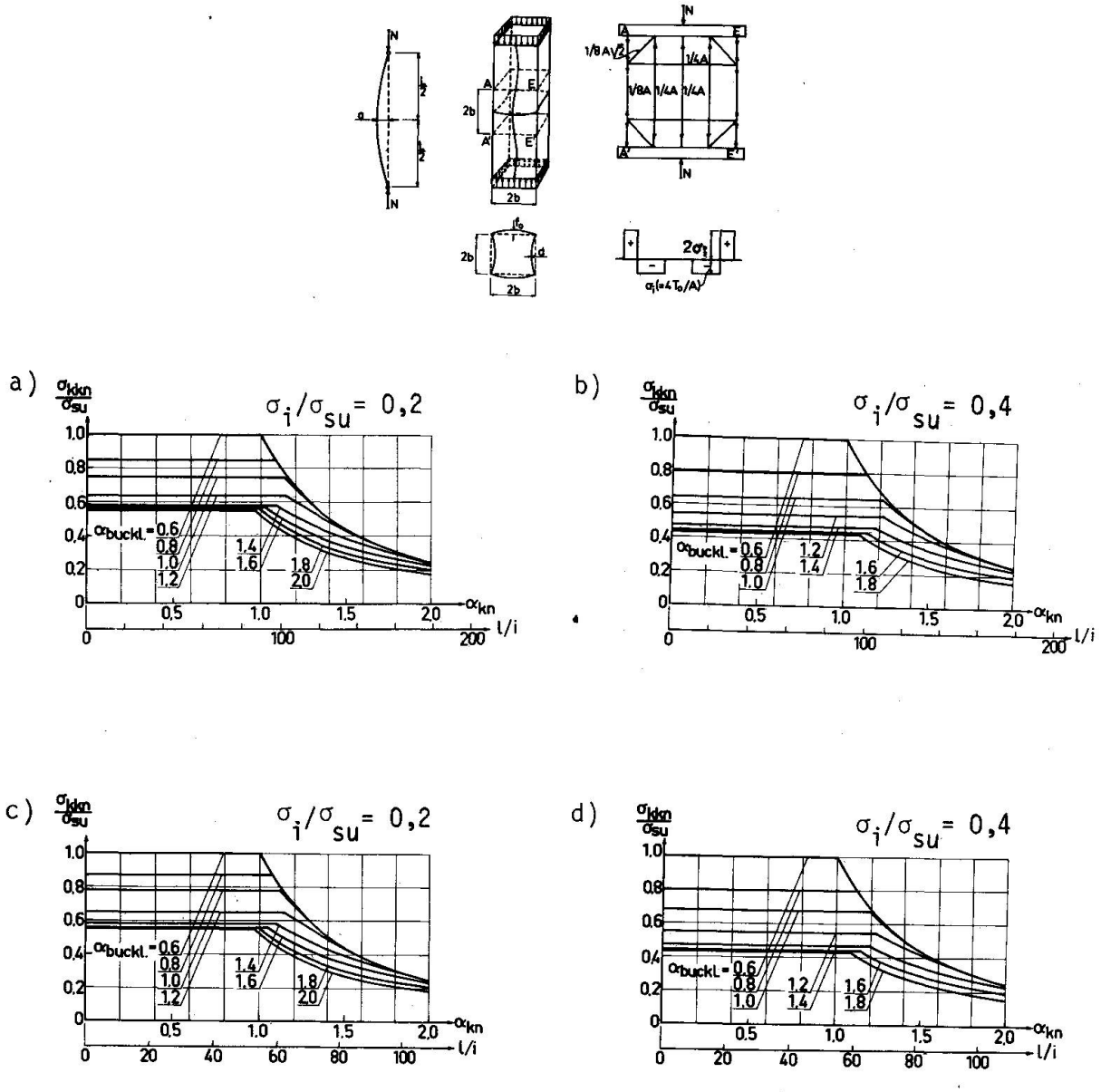

Fig. 6 Critical stress $\sigma_{kkn} = N_{kkn}/2bd$ at column buckling divided by σ_{su} at different α_{buckl} as a function of $\alpha_{kn} = \sqrt{\sigma_{su}/\sigma_{e\ell}}$. ($\sigma_{su} = \sigma_y$).
Initial stress distribution 2. $a/\ell = 0$; $f_o/2b = 1/1000$;
a) - b): $\sigma_{su} = 2600$ kp/cm^2 ; c) - d): $\sigma_{su} = 7000$ kp/cm^2.

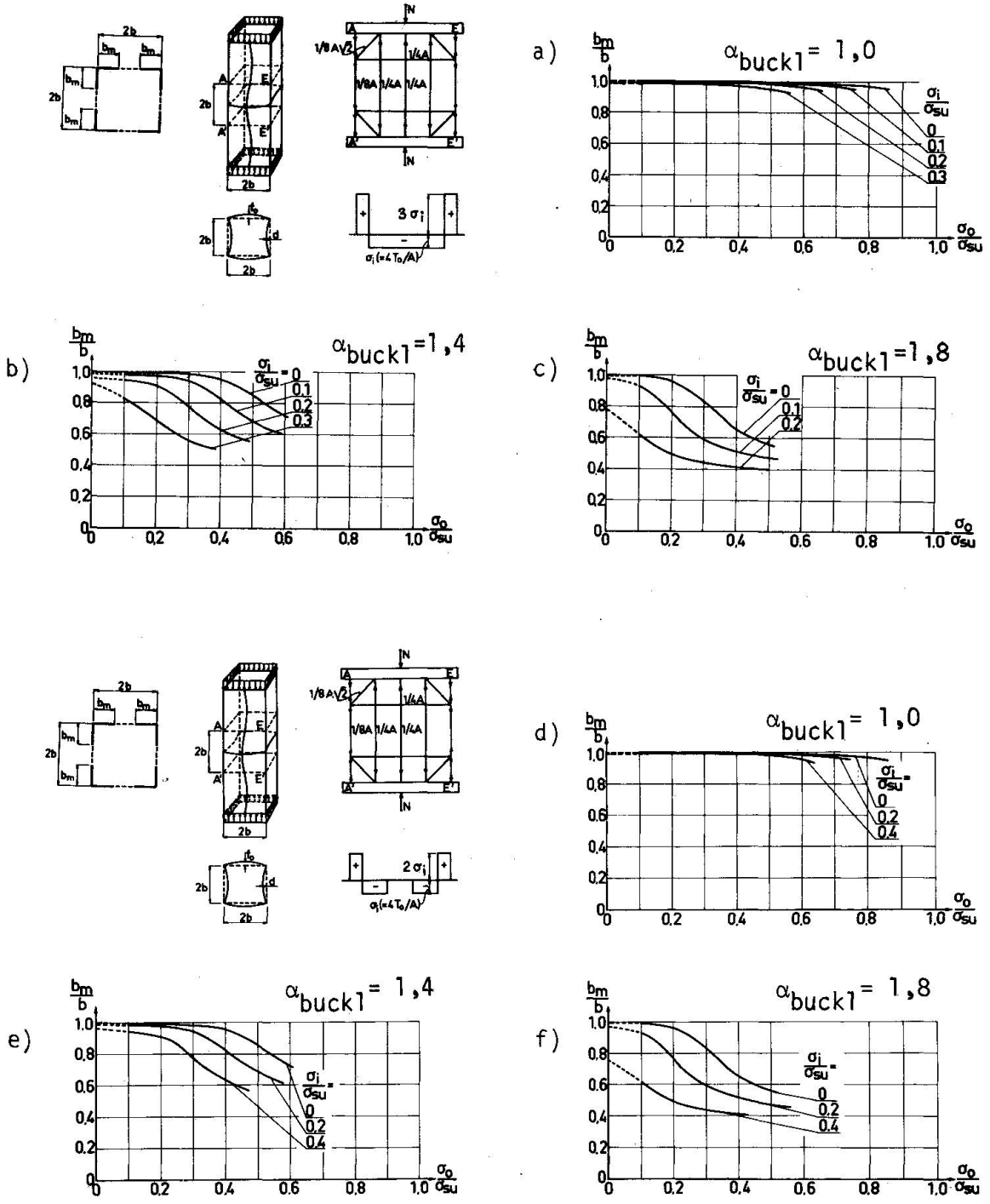

Fig. 7 Effective width b_m divided by b at different σ_i/σ_{su} as a function of $\sigma_o = N/2bd$, divided by σ_{su}. ($\sigma_{su} = \sigma_y$). σ_{su} = 2600 kp/cm^2 ; $f_o/2b = 1/1000$;

a) - c): Initial stress distribution 1

d) - f): Initial stress distribution 2.

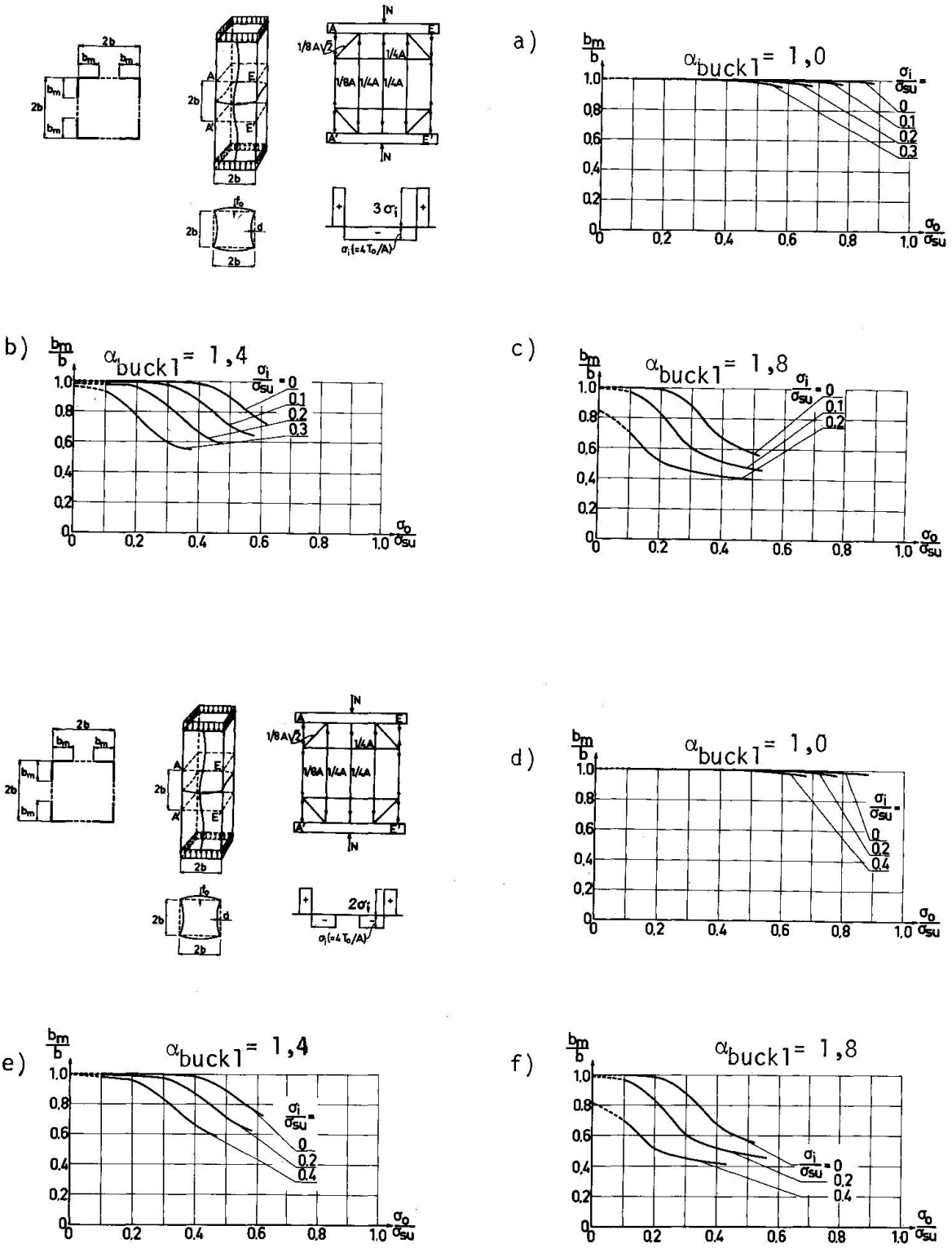

Fig. 8 Effective width b_m divided by b at different σ_i/σ_{su} as a function of $\sigma_o = N/2bd$, divided by σ_{su}. ($\sigma_{su} = \sigma_y$). $\sigma_{su} = 7000$ kp/cm^2 ; $f_o/2b = 1/1000$;

a) - c): Initial stress distribution 1

d) - f): Initial stress distribution 2.

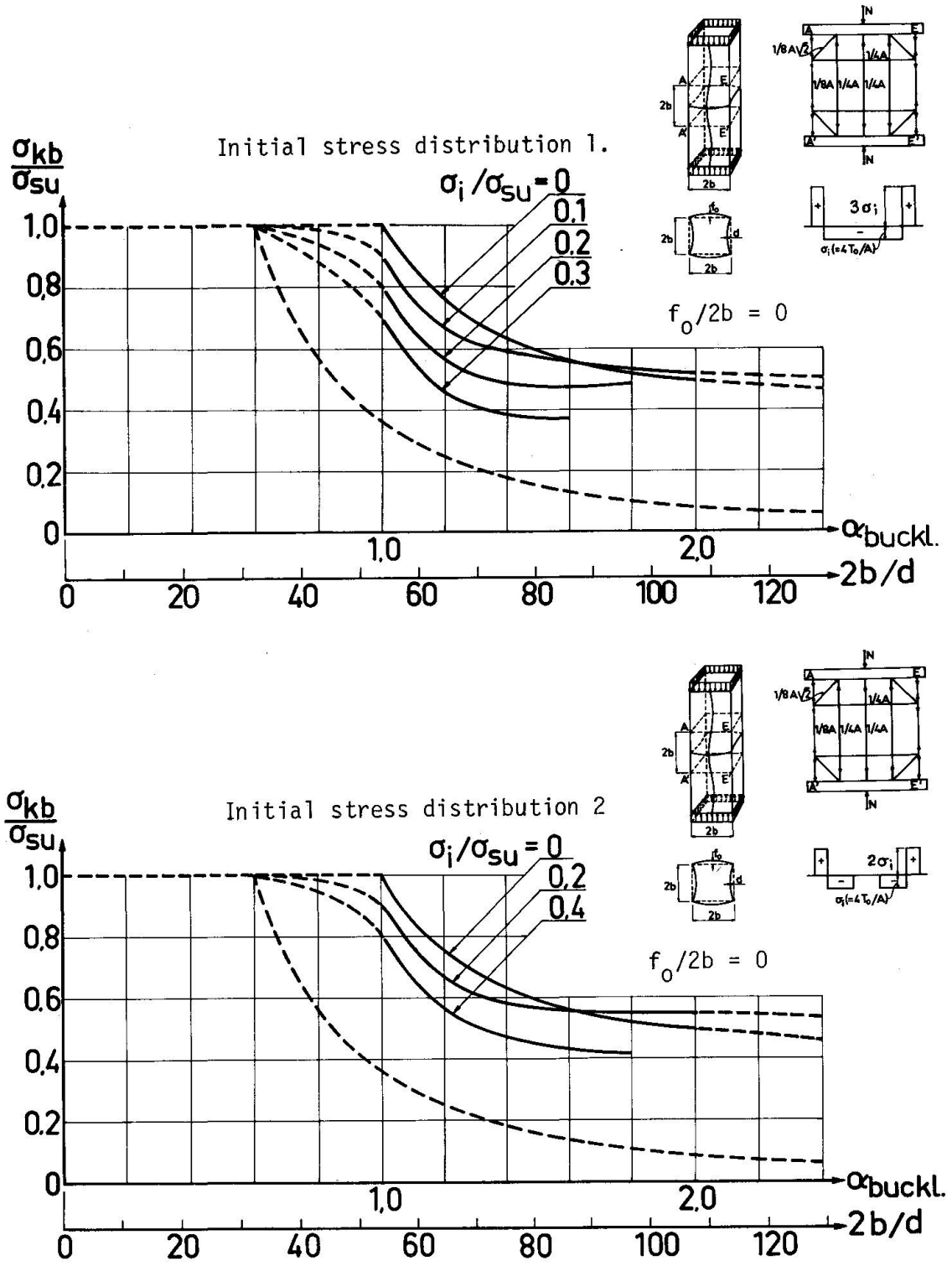

Fig. 9 Critical stress $\sigma_{kb} = N_{kb}/2bd$ at plate buckling divided by σ_{su} at different σ_i/σ_{su} as a function of $\alpha_{buckl} = \sqrt{\sigma_{su}/\sigma_{e\ell}}$. ($\sigma_{su} = \sigma_y$) $f_o/2b = 0$; $\sigma_{su} = 2600$ kp/cm^2 and $\sigma_{su} = 7000$ kp/cm^2.

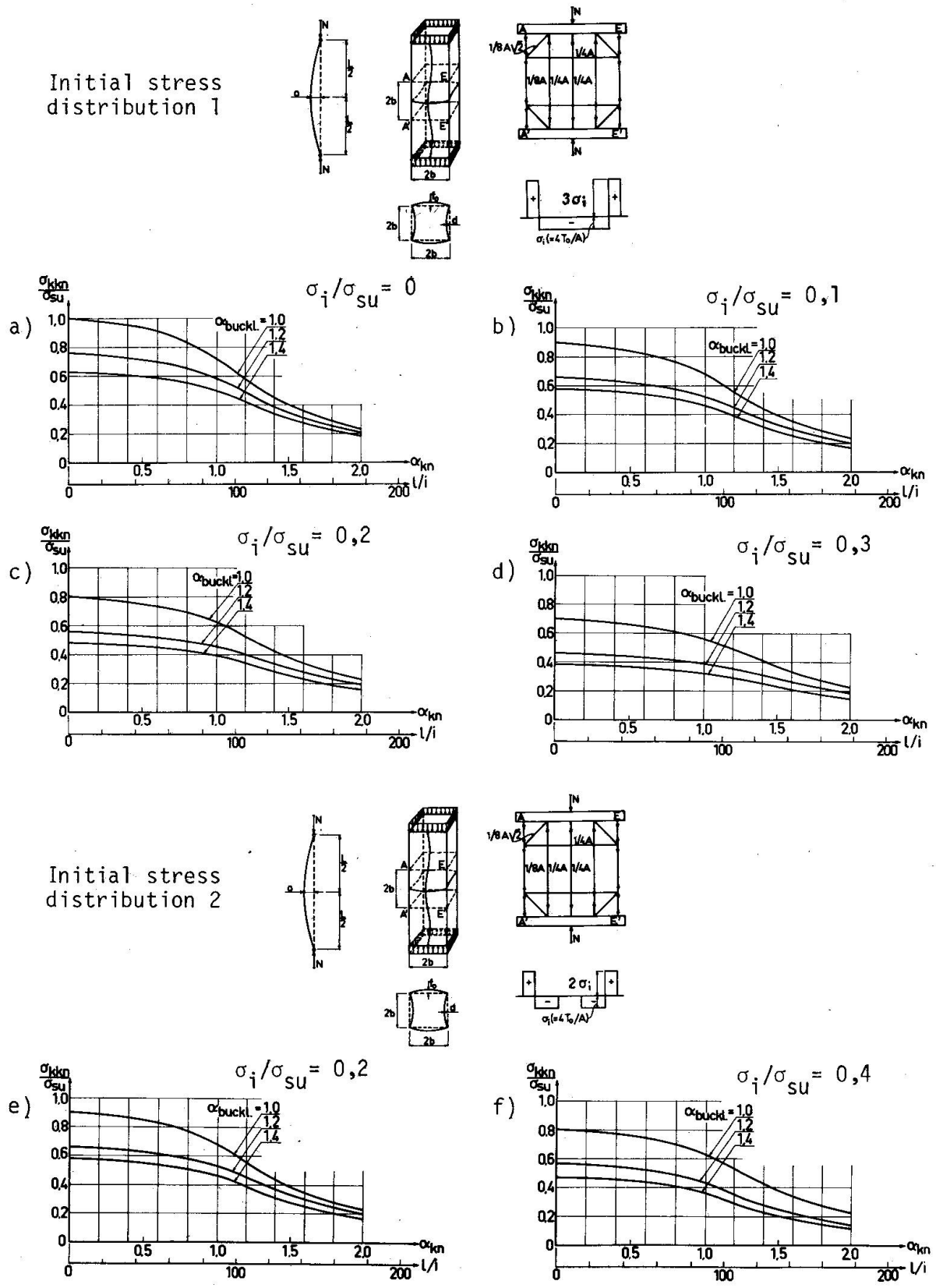

Fig. 10 Critical stress $\sigma_{kkn} = N_{kkn}/2bd$ at column buckling divided by σ_{su} at different α_{buckl} as a function of $\alpha_{kn} = \sqrt{\sigma_{su}/\sigma_e}\,\ell$. ($\sigma_{su} = \sigma_y$); σ_{su} = 2600 kp/cm^2; a/ℓ = 1/1000; $f_o/2b$ = 0.

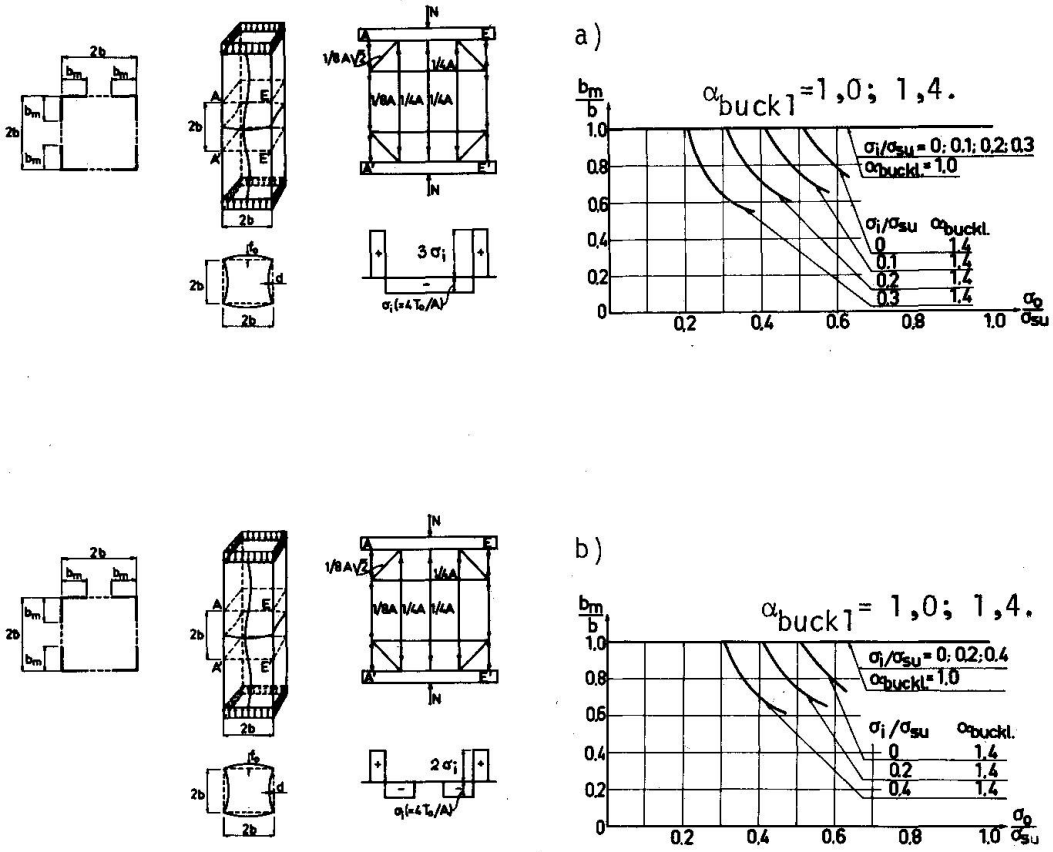

Fig. 11 Effective width b_m, divided by b at different σ_i/σ_{su} as a function of σ_o= N/2bd, divided by σ_{su}. (σ_{su}= σ_y) σ_{su}= 2600 kp/cm^2 and σ_{su}= 7000 kp/cm^2. $f_o/2b$ = 0.

a) Initial stress distribution 1.
b) Initial stress distribution 2.